

LIMESTONE DECAY IN HISTORIC MONUMENTS AND CONSOLIDATION
WITH NANODISPERSIVE CALCIUM HYDROXIDE SOLUTIONS

A THESIS SUBMITTED TO
THE GRADUATE SCHOOL OF NATURAL AND APPLIED SCIENCES
OF
MIDDLE EAST TECHNICAL UNIVERSITY

BY

EVİN CANER

IN PARTIAL FULFILLMENT OF THE REQUIREMENTS
FOR
THE DEGREE OF DOCTOR OF PHILOSOPHY
IN
RESTORATION

MARCH 2011

Approval of the thesis:

**LIMESTONE DECAY IN HISTORIC MONUMENTS AND
CONSOLIDATION WITH NANODISPERSIVE CALCIUM HYDROXIDE
SOLUTIONS**

submitted by **EVİN CANER** in partial fulfillment of the requirements for the degree of **Doctor of Philosophy in Architecture Department in Restoration Middle East Technical University** by,

Prof. Dr. Canan ÖZGEN
Dean, Graduate School of **Natural and Applied Sciences**

Assoc. Prof. Dr. Güven Arif SARGIN
Head of Department, **Architecture**

Prof. Dr. Emine N. CANER SALTİK
Supervisor, **Architecture Department, METU**

Examining Committee Members:

Prof. Dr. Asuman TÜRK MENOĞLU
Geological Engineering Department, METU

Prof. Dr. Emine N. CANER SALTİK
Architecture Department, METU

Prof. Dr. Tamer TOPAL
Geological Engineering Department, METU

Prof. Dr. Yeter GÖKSU
Physics Department, Adıyaman University

Assist. Prof. Dr. Güliz BİLGİN ALTINÖZ
Architecture Department, METU



Date: 18.03.2011

I hereby declare that all information in this document has been obtained and presented in accordance with academic rules and ethical conduct. I also declare that, as required by these rules and conduct I have fully cited and referenced all material and results that are not original to this work.

Name, Last name : Evin CANER

Signature :

ABSTRACT

LIMESTONE DECAY IN HISTORIC MONUMENTS AND CONSOLIDATION WITH NANODISPERSIVE CALCIUM HYDROXIDE SOLUTIONS

CANER, Evin

Ph.D., Department of Architecture, Graduate Program in Restoration

Supervisor: Prof. Dr. Emine N. CANER SALTİK

March 2011, 124 pages

Exposure to atmospheric conditions results of deterioration in historic monuments and their stones. Limestone conservation presents many problems that have to be investigated in detail. In this study, limestone deterioration and development of its conservation treatments were investigated through examination of the statues carved from karstic limestones in Nemrut Dağ Monument. The decay mechanisms that had major roles in their deterioration during two thousand years of exposure to atmospheric conditions and the development of their conservation treatments involved several types of analyses that were carried out in the field and in the laboratory. Exposed surfaces of limestones having karstic veins, interior crack surfaces were examined and compared with relatively undeteriorated interior parts. Similar limestones from the geological formations nearby were artificially deteriorated by salt crystallization and were also examined for comparison. Standard physical and physicochemical tests, petrographical analysis, XRD, SEM-EDX and FTIR were used during those examinations. Swelling nature of clays in limestones and their control were quantified by CEC measurements.

The micro structure of limestone was observed to be composed of micritic calcite with karstic veins of sparitic calcite crystals. Some karstic zones were found to be preferred sites of dissolution and precipitation of calcium carbonate where swelling action of clays and widening of cracks occurred. Iron oxides that moved through those zones, as well as biological activity were also found to contribute to those phenomena. Preparation of high concentrations of nanodispersive calcium hydroxide solutions was achieved for the conservation treatments of the deteriorated limestone. Success of treatments with nanodispersive Ca(OH)_2 solutions targeted to the decay zones were discussed in terms of their ability to control the swelling action of clays, carbonation of nanodispersive solution, and improvement in the physicochemical properties of treated limestone.

KEYWORDS: limestone deterioration, nanodispersive Ca(OH)_2 solution, consolidation, Nemrut Dağ Monument

ÖZ

TARİHİ ANITLARDAKİ KİREÇTAŞLARININ BOZULMASI VE NANO TANELİ KALSİYUM HİDROKSİT ÇÖZELTİLERİYLE SAĞLAMLAŞTIRILMASI

CANER, Evin

Doktora, Mimarlık Bölümü, Restorasyon Programı

Tez Yöneticisi: Prof. Dr. Emine N. CANER- SALTİK

Mart 2011, 124 sayfa

Atmosferik koşullara açık anıtlarda taş bozulmaları da önemli bir sorundur. Bu anıtlarda kullanılan kireçtaşlarının korunmasında çözüm bekleyen birçok sorun bulunmaktadır. Bu çalışmada kireç taşlarının bozulma sorunlarının incelenmesi ve koruma metotlarının geliştirilmesi için Nemrut Dağı Anıtı'nın yapımında kullanılan kireçtaşları çalışılmıştır. Bu anıtta karstik kireçtaşından yapılmış olan ikibin yıllık heykellerin bugün içinde buldukları bozulmuşluk durumlarından sorumlu olan bozulma mekanizmaları ve koruma yöntemleri arazide ve laboratuvarında çeşitli analizlerle incelenmiştir. Bu amaçlarla, karstik kireçtaşlarının dış koşullara açık yüzeyleri, iç çatlak yüzeyleri incelenmiş ve göreceli olarak bozulmamış iç kısımlarla karşılaştırılmıştır. Benzer yapı gösteren ve Nemrut dağının biraz aşağı seviyelerinden alınan taş örnekler laboratuvarında tuz kristallendirme döngüleri ile eskitilmiş ve heykellerdeki bozulmuş örneklerle karşılaştırılmıştır. Taş örneklerin fiziksel ve fizikomekanik özellikleri standart deneylerle, taşın mikroyapısındaki değişimler, minerolojik ve petrografik özellikleri ise ince kesitlerin polarize mikroskopla analizi, XRD, SEM-EDX ve FTIR analizleri ile incelenmiştir.

Kireçtaşlarının çatlaklarındaki killerin şişme özellikleri ve bunların kontrol altına alınması nicel olarak CEC ölçümleri ile yapılmıştır.

Kireçtaşının mikro yapısının mikritik kalsitten, ve sparitik kalsit içeren karstik damarlardan oluştuğu izlenmiştir. Bazı karstik bölgelerde özellikle kalsiyum karbonatın çözünme ve tekrar çökme tepkimelerinin tercih edildiği, killerin bu bölgelerde şişme özellikleri ile çatlaklarının oluşup genişlemesine katkıda bulunduğu tespit edilmiştir. Bu karstik bölgelerdeki bozulmalara demiroksitler ve biyolojik aktivitenin de katıldığı izlenmiştir. Çatlakların oluşmasını ve ilerlemesini kontrol etmek amacıyla yüksek derişimde nano taneli kalsiyum hidroksit çözeltileri hazırlanmıştır. Bozulma bölgelerine özellikle çatlaklara, nano taneli kalsiyum hidroksit çözeltileri ile yapılan koruma işlemlerinin başarıları killerin şişme özelliklerini azaltmaları, nano taneli çözeltinin karbonatlaşma tepkimesinin takibi, ve taşın fizikomekanik özelliklerinin gelişmesinin izlenmesi ile değerlendirilmiştir.

ANAHTAR KELİMELER: kireçtaşı bozulması, nano taneli Ca(OH)_2 çözeltisi, konsolidasyon, Nemrut Dağı Anıtı

ACKNOWLEDGMENTS

I would like to express my gratitude to Prof. Dr. Emine N. Caner-Saltık for her supervision, guidance and encouragement throughout this study.

I am also grateful to Prof. Dr. Tamer Topal and Asist. Prof. Dr. Güliz Bilgin Altınöz for their invaluable contributions to my thesis.

I kindly thank to my friend, Research Assistant B. Alp Güney, for his helps in the experimental part of the work and for the invaluable discussions throughout the study.

I would also like to thank all members of Material Conservation Laboratory-Graduate Program in Restoration-METU for their kind assistance during this study.

This study was partially supported by the Kommagene Nemrut Conservation and Development Program Project. Therefore, I gratefully acknowledge it.

Lastly, my special thanks are to my family, for their invaluable support and encouragement from beginning to the end of the study.

TABLE OF CONTENTS

ABSTRACT	iv
ÖZ.....	vi
ACKNOWLEDGMENTS.....	viii
TABLE OF CONTENTS	ix
CHAPTERS	
1. INTRODUCTION.....	1
1.1. Aim and Scope of the Study.....	1
1.2. Historic Stone Conservation Criteria.....	2
1.3. Mechanisms of Limestone Deterioration	5
1.3.1. Dissolution Reactions of Calcium Carbonate.....	6
1.3.2. Precipitation of Calcium Carbonate	13
1.3.2.1. Impurity Ions	14
1.3.2.2. Ionic Strength	15
1.3.2.3. Effect of CO ₂ Flow Rate, Relative Humidity, Temperature	15
1.3.2.4. Effects of Surfactants and Additives	17
1.3.2.5. Invitro Biomineralization	18
1.4. Clay Minerals in Deterioration.....	19
1.5. Iron Oxides in Deterioration.....	22
1.6. Biological Deposits in Deterioration	23
1.7. Consolidation of Limestones with Nanodispersive Solutions.....	24
2. EXPERIMENTAL METHODS	26
2.1. Visual Analyses of Limestone Weathering Forms at the Historic Site	28
2.2. Sample Collection and Nomenclature	29
2.3. Determination of Physical and Physicomechanical Properties	34
2.3.1. Determination of Basic Physical Properties	35

2.3.2. Determination of Drying Rate	36
2.3.3. Determination of Basic Physicomechanical Properties.....	37
2.4. Microstructural Analyses.....	38
2.4.1. Preparation of Artificial Weathered Limestones by Salt Crystallization	38
2.4.2. Preparation of X-Ray Powder Diffraction (XRD) Samples	39
2.4.3. Preparation of X-Ray Powder Diffraction (XRD) Samples of Clay Constituents	39
2.4.4. Preparation of FTIR Samples	40
2.4.5. Preparation of Scanning Electron Microscope Samples	40
2.4.6. Preparation of Samples for CEC Measurements	40
2.4.6.1. CEC measurements of Clay minerals.....	41
2.4.7. Preparation of Nanodispersive Solutions of Calcium Hydroxide	41
2.4.8. Determination of Calcium Hydroxide Concentration in Nanodispersive Solution by Volumetric Method.....	42
2.4.9. Determination of Carbonation Rate of Nanodispersive Calcium Hydroxide Solution	43
3. EXPERIMENTAL RESULTS	44
3.1. Results of Visual Analyses on Weathering Forms of Limestones at the Historic Site	44
3.2. Physical and Physicomechanical Properties of Limestones	48
3.2.1. Results of Physical and Physicomechanical Properties of decayed limestones and marbles.....	48
3.2.2. Results Physical and Physicomechanical Properties of Artificially Weathered Limestones by Salt Crystallization.....	49
3.2.3. Results of Drying Rate of Artificially Weathered Limestones by Salt Crystallization.....	52
3.3. Thin Section Examination of Limestones and Marbles by Optical Microscopy	53

3.3.1. Thin Section Examination of Quarry Limestones from the lower parts of the Nemrut Dağ and from Quarry at the West Terrace of Nemrut Dağ Monument.....	54
3.3.2. Thin Section Examinations of Weathered Limestones from Nemrut Dağ Monument.....	55
3.4. X-Ray Diffraction Analyses	59
3.4.1. XRD traces of weathered limestones before acid treatment	59
3.4.2. Directly taken XRD traces of crack surfaces and exterior surfaces	62
3.4.3. XRD traces of powdered samples scraped from crack surfaces.....	64
3.4.4. XRD traces of acid treated samples from crack surfaces	67
3.4.4.1. Determination of acid insoluble percentage	67
3.4.4.2. XRD traces of acid insoluble parts of the unweathered Nemrut Dağ limestones	67
3.5. FTIR Analyses of Weathered Zones and Clays	74
3.6. Scanning Electron Microscope-EDX Results	75
3.6. EDX Analyses of Clays and Iron Oxides	79
3.7. Experiments on the Preparation of Nanodispersive Calcium Hydroxide Solution for the Conservation Treatments.....	81
3.8. Treatments of limestones with nanodispersive Ca(OH) ₂ solution	82
3.8.1. Treatment of limestone cracks and deteriorated surfaces with nanodispersive Ca(OH) ₂ solution	82
3.8.2. Treatment of acid insoluble constituents of limestones containing clay minerals	87
3.9. Carbonation of nanodispersive Ca(OH) ₂ solution	88
4. DISCUSSIONS AND CONCLUSIONS.....	92
4.1. Weathering of Limestone	92
4.2. Conservation treatments with nanodispersive calcium hydroxide solutions	96
4.3. Conclusions	97
4.4. Further Studies.....	98
REFERENCES	100

APPENDICES

A. BASIC PHYSICAL PROPERTIES OF LIMESTONE SAMPLES TAKEN FROM NEMRUT DAĞ MONUMENT	117
B. BASIC PHYSICAL AND PHYSICOMECHANICAL PROPERTIES OF ARTIFICIALLY WEATHERED LIMESTONE SAMPLES	120
C. CONCENTRATION OF SUSPENDED NANO CALCIUM HYDROXIDE SOLUTION IN TIME	123

CHAPTER 1

INTRODUCTION

1.1. Aim and Scope of the Study

The aim of this study is to investigate the main deterioration mechanisms of historic limestone and to develop its conservation treatments that are efficient in the control of those deterioration mechanisms.

Limestones of Nemrut Dağ Monument exhibited characteristic decay problems in limestones that have developed in a long time scale. The investigation of their decay mechanisms for the purpose of their conservation was expected to contribute to the conservation of limestones elsewhere. Therefore the studies were carried out with the limestones of Nemrut Dağ Monument.

It was aimed to study initially the weathering forms of limestone at the site by visual observations and then make their representative sampling for the purpose of examining the changes in physical and physicomachanical properties as well as the changes in microstructure of stone.

The microstructural changes of weathered stone at exposed surfaces and crack surfaces and their comparison with the relatively protected interiors were planned to be studied in detail. Results of those analyses were expected to guide the studies on the development of retreatable and compatible conservation treatments for historic limestone.

During this research, the start of the Kommagene Nemrut Project and part of it being the conservation problems of limestone statues was an opportunity for the detailed site investigations of stone deterioration. The project also enabled to establish links with other conservation issues of the site such as information on climatic conditions and geological formations of the site, as well as structural problems of the statues at the site.

In the light of the site and laboratory investigations of stone deterioration, some treatments were expected to be developed in the laboratory. During the study, Kommagene Nemrut Conservation project gave opportunity to make some trial applications of stone treatments at the site and analyses of their performance at the site and in the laboratory.

The current approach in historic stone conservation is to improve the performance of the stone that has suffered from decay, by retreatable and compatible conservation treatments while keeping its aesthetic values and authenticity. Therefore, conservation of limestone was tried to be achieved by reincorporating similar type of structure in the stone, which was calcite. Formation of calcite in the weak and deteriorated limestone was studied by the preparation and application of nanodispersive solutions of calcium hydroxide. It was also necessary to study the conditions that transformed nanodispersive calcium hydroxide solution to calcite. The efficiency and compatibility of those conservation treatments were attempted to be evaluated by using several analytical methods.

1.2. Historic Stone Conservation Criteria

Conservation studies on historic building materials and particularly stone conservation goes back to nineteenth century. However, successful conservation treatments of stone are rather recent. There are quite a number of problems to be overcome in stone conservation. The important issues of stone conservation were

well presented in the Acts of International Congress on the Conservation of Stone and Other Materials held in Paris, in 1993 (Thiel, 1993).

It was stated that methodologies were needed to be improved in diagnostic studies as well as conservation treatments that could be evaluated and monitored with measurable parameters (Tabasso 1993; Sasse 1993; Charola 1993). The proposals and recommendations in the act pointed out the importance of future studies on technical standards and guidelines, exchange of knowledge, specialized training and education of conservation scientist and clarification of authenticity in artistic, functional and historic interpretation of the term (Thiel, 1993).

Advances in science and technology have contributed to advances in conservation science and the process of conducting stone conservation research. Knowledge gained in other disciplines of science and technology has contributed to stone conservation research in quite a number of ways. Conservation scientist is expected to recognize the interdisciplinary aspect of stone conservation and should be able to integrate the recent advances in science and technology to his/her specific topic of conservation concern. Increase in the number of conservation scientists, have been of prime importance for the desired advances in conservation science (Price, 1996). Most developments in the care and treatments of collections and the monuments stem from scientific investigations and their integration with the experience of conservation architects, conservators, art historians, etc. (Tennent, 1994; Price, 1996).

Diagnosis in the monument and material scale is an important step in stone conservation. Unfortunately that step has long been neglected. Stone treatments used to be selected and applied without any diagnostic studies. Almost in all cases they were harmful to the stone or did not have an effect on the control of decay (Clark and Ashurst 1972; Torraco 1976). The diagnostic studies involve the assessment of the deterioration state of the material and the factors affecting it. A close look at the deterioration state of stone is necessary as well as putting the

decay in numbers, e.g. measuring the extent of decay and its rate through looking beneath the surface. Non-destructive analyses such as ultrasonic velocity measurements and quantitative infrared thermography are being improved for those purposes (Caner-Saltık, 2011; Caner-Saltık et al., 2011; Tavukçuoğlu et al., 2011).

Conservation treatments aims to control the decay mechanism and improve performance of decayed stone through its physical, physicomachanical and chemical properties and support its survival without disturbing its visual and aesthetic characteristics. Those can only be achieved through the results of diagnostic studies. Conservation studies include a series of operations related to the control and elimination of decay sources in a larger scale as well as the treatments that are applied to the decayed material.

There is a growing awareness of the principle of minimum intervention, of the need to limit the use of materials that might prove harmful to either the stone or to the environment, and of the fact that prevention is better than cure (Price, 1996).

In the context of stone conservation, reversibility is more idealistic than realistic. Treatment is irreversible, in practice, but decay through neglect is irreversible too. The dilemma highlights the importance of preventive conservation, but there are instances where preventive conservation is not enough. Ultimately it will be necessary to reach a carefully balanced decision for treatments, taking into account all aspects of each individual case (Price, 1996).

Conservation treatments are expected to have the qualifications of retreatability, compatibility, and durability. These days there is nearly a general agreement that strict reversibility must be replaced by the demand for compatibility and retreatability of the procedures. Those qualifications need to be described and assessed by measurable parameters in terms of physical, physicomachanical and chemical compatibility with the original material and it is an obvious requirement for all new techniques. A set of parameters and investigations are suggested by

previous researchers for the assessment of the effectiveness of different treatments and the evaluation of their compatibility with the relatively unchanged stone material by using different analytical techniques and tools preferably nondestructive (Sasse and Snethlage, 1997; De Witte et al., 1985; Tabasso, 1988; Mertz, 2006).

Conservation treatments are usually defined for the common cases and adopted to particular situations. The unsuitability of many stone conservation treatments forced the research efforts to develop new materials and procedures for the preservation of stone. There is need to conduct research on the new methods of conservation treatments and on the assessment of the long term durability of treatments (Tennent, 1994; Sasse and Snethlage, 1997; Price, 1996).

1.3. Mechanisms of Limestone Deterioration

Sedimentary carbonate minerals that contain calcite and to a lesser extent dolomite occupy an important part of earth's crust. Studies on the changes in those formations whether on earth's surface, in shallow water or deep sea sediments are of great importance in a number of ways. An understanding of the factors that control the dissolution and precipitation of carbonate minerals is important for modeling of geochemical cycles and the impact of fossil fuel CO₂ on climate, diagenesis of sediments and sedimentary rocks. That knowledge has practical applications for areas such as behavior of carbonates in petroleum and natural gas reservoirs and preservation of buildings and monuments constructed from limestone and marble (Morse and Arvidson, 2002).

The mechanism of limestone deterioration is mainly the result of four basic groups of reactions; purely physical degradation caused by the action of water, temperature variations and abrasion; physicochemical mechanisms involving the recrystallisation of soluble or semi-soluble salts without associated chemical change; chemical reactions initiated by normal constituents and pollutants of the

atmosphere and ground water; and finally microbiological activity causing direct physical damage to the surface and promoting chemical attack via trace element concentration and waste product manufacture. In geological formations exposed to atmospheric conditions and on the historic buildings constructed of limestones, the results of those weathering phenomena are visually observed as different types of decay forms in the form of flaking and scaling of the surface layers, cracks on the surface and in the stone, powdering, material loss in stone in various forms such as alveolisation, outbursts, granular and fragmental disintegration etc.

The deterioration process of limestone involves contributions from various reactions which lead to dissolution and recrystallization of calcium carbonate. Knowledge on those reactions of calcium carbonate is very useful for understanding of limestone deterioration phenomena.

On the other hand, the understanding of the dissolution and recrystallization reactions of calcium carbonate, the conditions that favor precipitation of calcium carbonate including the physicochemical parameters that affect those reactions will also be helpful to choose the proper experimental methods for the improvement of decayed limestone with its own constituent through precipitation of calcium carbonate in its microstructure.

1.3.1. Dissolution Reactions of Calcium Carbonate

Dissolution and recrystallization of calcium carbonate are common reactions happening during the weathering process of limestone along with other physicochemical phenomena. The main minerals in the crystal structure of limestone are calcite, aragonite and vaterite (Table 1.1).

It is important to know the dissolution and precipitation characteristics of the main mineral constituent calcite in the composition of limestone. Aragonite is less abundant than calcite and vaterite is rarely found in its composition.

Table 1.1 Some properties of related carbonate minerals

Mineral	Crystal form	Density	Free energy of formation Δf in kcal/mole	Solubility in distilled water		Solubility in sea water (ionic strength 0.7)		
				(K: mol ⁻² l ⁻²)		(K: mol ⁻² l ⁻²)		
				pK ^c at 25C	pK at 20C	pK at 5C	pK at 25C	pK at 5C
Calcite (CaCO ₃)	Hexagonal (rhombohedral cleavage)	2.71	-269.78 ^a	8.42 ^b 8.45 ^d	8.48 ^c 8.50 ^e	8.35 ^b	6.22 ^d	6.09 ^d
Aragonite (CaCO ₃)	Orthorhombic	2.93	-269.53 ^a	8.28 ^d	8.21 ^d	6.05 ^d		5.95 ^d
Vaterite (CaCO ₃)	Hexagonal	2.56 ^f						

a. Rossini et al., 1952

b. Jacobson and Langmuir, 1974

c. Christ, Hostetler and Siebert, 1974

d. Berner, 1976

e. Sjöberg, 1976

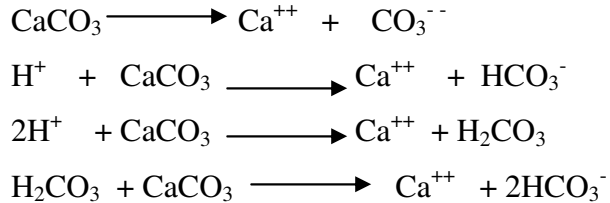
f. Northwood and Lewis, 1968

There have been a large number of studies focused on the dissolution kinetics of carbonate minerals. Calcite being the most common carbonate mineral, has received the most attention (Berner and Morse, 1974; Plummer and Wigley, 1976; Sjöberg, 1976, 1978, 1983; Busenberg and Plummer, 1986; Compton and Unwin, 1990; Lea et al., 2001; Morse and Arvidson, 2002; Cubillas et al., 2004).

The rate of dissolution of any mineral is dependent upon the rate of transport of the reactants and the reaction products between the mineral surface and the bulk solution, the rate of homogeneous reaction at the mineral surface, and possibly on the rates of homogeneous reactions within the solvents (Caner, 1978). It is important to determine the conditions under which calcite dissolution is surface reaction controlled and those that are transport controlled. The pH, partial pressure of carbondioxide, temperature, ionic strength, minor and trace components which

may act as inhibitors or accelerators, are variables that control the degree of undersaturation and rate of dissolution.

Calcium carbonate dissolves according to following reactions;



“Rate controlling mechanisms of calcite dissolution like any reaction in chemical kinetics can be broken down into different steps:

1. diffusion of reactants through solution to the solid surface,
2. adsorption of the reactants on the solid surface,
3. migration of the reactants on the surface to an “active” site (e.g., a dislocation),
4. the chemical reaction between the adsorbed reactant and solid which may involve several intermediate steps where bonds are broken and formed, and hydration of ions occurs,
5. migration of products away from the reaction site,
6. desorption of the products to the solution,
7. diffusion of products away from the surface to the “bulk” solution.” (Morse and Arvidson, 2002)

A central concept in reaction kinetics is that one of these steps will be the slowest and that the reaction can, therefore, not proceed faster than this limiting step. Steps 1 and 7 involve the diffusive transport of reactants and products through the solution to and from the surface. When this process is rate-limiting, the reaction is said to be diffusion (transport) controlled. Steps 2-6 occur on the surface of the solid and when one of them is rate controlling the reaction is said to be surface controlled.” (Morse and Arvidson, 2002)

Preferential dissolution of sites with excess surface energy and consequently well defined edges are characteristic of surface reaction controlled dissolution kinetics (Berner and Morse, 1974; Caner and Seeley, 1979; Simon and Snethlage, 1992).

Researchers have studied the dissolution and precipitation characteristics of calcite at solutions having different pH. Studies indicated that calcium carbonate, at pH values greater than 4, showed surface reaction controlled dissolution and precipitation (Caner and Seeley, 1979). Those surface reaction controlled dissolution and precipitation reactions proceeded with the mechanisms described below.

Precipitation and dissolution of ionic solids have been considered to proceed by the attachment or detachment of ions at kinks in molecular steps on the crystalline surface (Fig. 1.1) (Berner and Morse, 1974).

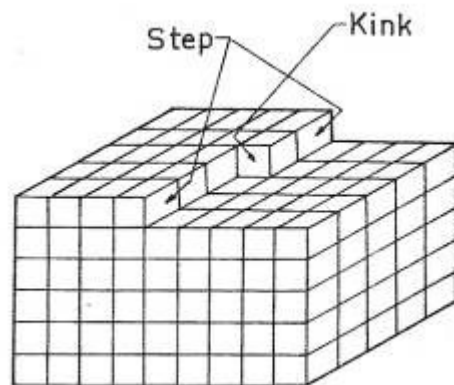


Figure 1.1 Model of Crystal Surface. Each unit cube corresponds to a molecule, atom, ion pair etc. (Berner and Morse, 1974)

The schematic representation of a crystal surface is shown in Fig. 1.2. This model is known as Kossel model (Angwal, 1983).

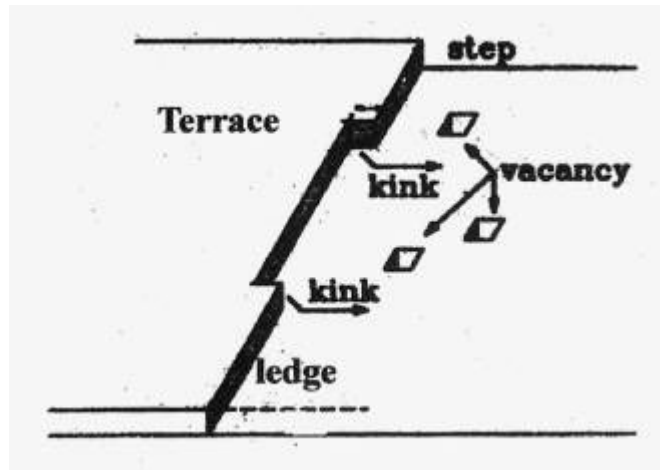


Figure 1.2 Surface of a crystal according to Kossel. The types of dislocations are shown. (After Koutsoukos, 2001, p.79)

The dissolution proceeds by the detachment on the crystal units in the following steps (Koutsoukos, 2001):

- detachment from an active site (e.g. kink)
- partial hydration on the detached unit
- hydration of the vacant site
- diffusion of the partially hydrated unit along the edge of a step
- diffusion of the unit along the step and completion of hydration
- the unit is transferred to the bulk solution through the diffusion boundary layer on the crystal system

The kink is a favorable site for detachment because of greater degree of exposure to the solution on the part of ions located at the kink. Once a kink is removed, a new kink forms adjacent to the old one.

Kinks, being points of excess surface energy, are preferred sites for impurity ions and molecules. If they are bound strongly at the kink site, they block kink mobilization and inhibit dissolution. These adsorbed impurities are called

inhibitors. All crystals have imperfections which include steps, kinks, terraces, ledges and holes or vacancies. The number of kinks on a unit crystal surface is limited, thus the concentrations of inhibitors required to block these kink sites are usually very low.

Impurities or foreign compounds often interact with the calcitic surface by adsorption. As a consequence, the active sites (kinks) are blocked and dissolution of crystal reduced or stopped.

Schematically, the blocking of the active sites by adsorption is given below (Fig.1.3).

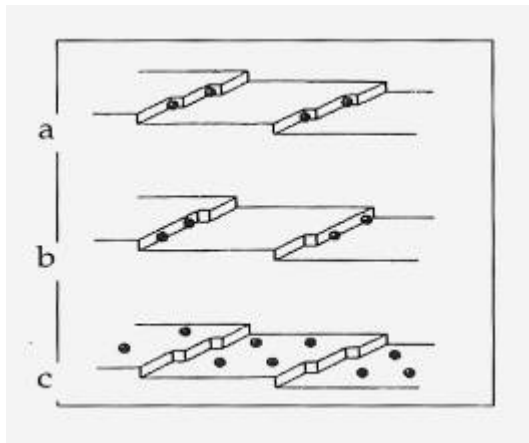


Figure 1.3 Impurities on a crystal surface

- a. blocking kinks
- b. blocking ledges (edges)
- c. blocking terraces (steps)

(After Koutsoukos, 2001, p.83)

The existence of those kinks, ledges and steps were later on observed on calcite surfaces by atomic force microscopy and proved the correctness of previous assumption on the process (Hausner et al., 2007).

A number of studies have reported the effects of several chemical compounds on dissolution and crystal growth of calcium carbonate (Nestaas and Terjesen, 1969; Dove, 1993; Kanellopoulou et al., 2001; De Lieu, 2002, Kamiah et al., 2004).

For example addition of 0.01 M of sodium pyrophosphate in the solution resulted in complete stop of the dissolution process of calcite. That result showed that ionized phosphate groups had to have a retarding effect on the dissolution through adsorption at the active growth sites of the calcitic surface (Kanellopoulou et al., 2001). In another study, it was reported that lanthanum ion inhibited both dissolution and crystal growth of calcite and the inhibition by lanthanum ion caused the deposition of insoluble lanthanum carbonate on calcite surface (Kamiya et al., 2004). A research showed that compounds containing ionized carboxylic and phosphate groups, in solutions at pH: 8.25, were adsorbed on calcite and retarded the dissolution process (Koutsoukos et al., 2001).

Dissolved organic compounds were known to inhibit the rate of dissolution of calcium carbonate as well as its precipitation (Morse, 1974; Morse and Arvidson, 2002). The inhibition mechanism was supposed to proceed by blocking kinks on the crystal surface (Berner and Morse, 1974; Morse and Arvidson, 2002). The blocking action might not last long and it was likely to be interrupted by processes like hydrogen adsorption (Berner and Morse, 1974) which helped to free the active site from organic molecules and include it in the solution. The result was surface reaction controlled dissolution of limestone revealed by the well defined edges of calcite crystals (Caner and Seeley, 1979).

Precipitation of calcium carbonate was also influenced by dissolved organic compounds (Kitano and Hood, 1965). The rate and degree of pH was affected in a different manner by the presence of organic compounds which affected the rate of precipitation and the crystal form produced (Kitano and Hood, 1965).

The kinetics of the dissolution and precipitation of calcite may also be influenced by the presence of clay minerals suspended in solution or in contact with exposed surfaces of calcium carbonate. Properties of clay minerals like ion exchange and adsorption may change variables like concentration, ionic strength, pH etc., which in turn will influence the kinetics of dissolution and precipitation (Caner and Seeley, 1978; Wendler, 1997; Simon and Herm, 1996).

1.3.2. Precipitation of Calcium Carbonate

In nature, there are several factors that affect the formation of the polymorphs of calcium carbonate, namely calcite, aragonite and vaterite. Impurity ions, ionic strength, pH, temperature, surfactants etc. are important factors controlling the kinetics of dissolution and precipitation affecting the formation of those polymorphs of calcium carbonate.

Calcite is the most abundant polymorph of calcium carbonate, aragonite being the next. Vaterite, calcium carbonate monohydrate and calcium carbonate hexahydrate are its other polymorphs (Manoli and Dalas, 2001). Aragonite and vaterite are thermodynamically unstable in comparison to calcite (Cölfen, 2003). Vaterite is quite scarce in nature in geological formations.

However, in the biological systems, aragonite and vaterite can nucleate and grow in stable form. Their crystal lattices maintain stability with the existence of bioorganic macromolecules (Cölfen, 2003, Spanos and Koutsoukos, 1998).

Factors that affect precipitation of calcium carbonate such as impurity ions, ionic strength, surfactants and additives, CO₂ flow rate, pH, temperature and precipitation as invitro biomineralization are briefly summarized below.

1.3.2.1. Impurity Ions

Some ions were found to influence the nucleation or growth of calcite. Mg^{2+} ion inhibited the growth of calcite and caused the precipitation of CaCO_3 as aragonite (Bischoff and Fyfe 1968, Lippmann 1973). The phenomenon was ascribed to the inability of calcitic nuclei to grow when surrounded by adsorbed magnesium ions still hydrated on the outside. The purposely added calcite nuclei are ineffective when enough magnesium is present in solution to cause the precipitation of aragonite. However, when minute amounts of aragonite seeds had been added to a solution free of magnesium which would yield calcite without seeding, aragonite was formed as the only phase. This showed that the rate of crystallization for aragonite was greater than that of calcite, although the opposite was true for the nucleation rates at ordinary temperature. Seeding with calcite did not avert the formation of aragonite in solutions with magnesium. Lippman has found that a ratio Mg/Ca bigger than one was sufficient for complete suppression of calcite at room temperature when $\text{MgSO}_4 \cdot 7\text{H}_2\text{O}$ was added to the solution (Lippmann 1973, p 111).

Bischoff and Fyfe (1968) indicated the inhibiting influence of SO_4^{2-} in calcite precipitation, similar to that of Mg^{2+} by experiments with Na_2SO_4 . However, calcite was quite able to nucleate and grow at considerable sulphate levels (e.g. $\text{SO}_4^{2-}/\text{Ca}^{2+}$ molar ratio 2.1) at room temperature while other polymorphs of CaCO_3 could also precipitate at 100°C (Lippmann, 1973, page 112). SO_4^{2-} ion at lower concentrations was not expected to act as a retarding agent (Lippmann 1973).

Magnesium is the geologically most important inhibitor, especially in view of the fact that most aragonite occurring on the earth has formed in the sea. In normal seawater retarding influence of SO_4^{2-} may be considered unimportant in comparison to the inhibiting power of Mg^{2+} (Lippmann 1973).

Fe^{2+} and Ni^{2+} were tested by Fyfe and Bischoff (1965). They exerted inhibiting influence on the precipitation of calcite similar to that of Mg^{2+} .

1.3.2.2. Ionic Strength

Some ions are not related to CaCO_3 nor form sparingly soluble salts with the component ions Ca^{2+} and CO_3^{2-} act as accelerators throughout. Bischoff and Fyfe (1968) indicated that the reaction rate increases with the ionic strength of such cosolutes. A similar influence is known to occur in many chemical reactions, and it is not clear so far which step in the transformation aragonite-calcite could be particularly affected by ionic strength (Lippmann 1973).

1.3.2.3. Effect of CO_2 Flow Rate, Relative Humidity, Temperature

Precipitation of CaCO_3 depends on many factors including CO_2 concentration, relative humidity and temperature. During the precipitation of calcium carbonate, Ca(OH)_2 reacts with CO_2 and forms calcite crystals, CaCO_3 . Even though carbonation process is defined as a single chemical reaction, there are several steps that take place:

- (i) “The CO_2 diffuses through the paste, being influenced by the microstructure and by the water content;
- (ii) the CO_2 is dissolved in the pore water,
- (iii) the chemical equilibrium of CO_2 in water takes place;
- (iv) the Ca(OH)_2 is dissolved in the water, being influenced by the specific surface area and by the amount of water, specially the complexity of the surface of the walls of the pores
- (v) the precipitation of CaCO_3 takes place
- (vi) the H_2O as product of the reaction is desorbed (Arandigoyen et al., 2006).”

Studies revealed that the increase of CO_2 concentration during precipitation, increase the rate of carbonation (Moorehead, 1986; Cultrone et al., 2005). Dheilly et al. reported that a lime paste underwent a rapid and complete reaction in a

carbonic atmosphere, while in a low CO₂ atmosphere carbonation took twice as long.

CO₂ gas flow rate during carbonation also affected the particle size of calcium carbonate that precipitates. The particle size decreases with increasing flow rate of CO₂ (Wei et al., 1997).

Relative humidity is another crucial factor in the precipitation of CaCO₃. Carbonation is more rapid at a relative humidity of %50-70 and decreases at higher and lower relative humidities (Fattuhi 1988,; Walton et al., 1997; Fernandez Bertos et al., 2004).

The solubility of CO₂ in water decreases as temperature increases and the rate of chemical reactions generally increase with increasing temperature. Therefore the optimum carbonation rate is found at about 20°C (Grandet, 1975). Dheilily et al. indicated that in an atmosphere with a high relative humidity and temperature at around 10°C, carbonation reaches approximately 93% after 10 days.

On the other hand, since the carbonation reaction is exothermic, the heat of reaction promotes the formation of meta-stable forms of CaCO₃. Low temperatures (0-10°C) favour the formation of stable polymorph of CaCO₃ like calcite. Studies showed that more calcite is formed if very cold carbonic acid is used for carbonation (Fernandez Bertos et al. 2004).

Temperature has an influence on the morphology of the precipitated calcium carbonate particles as well as on their size. It was observed that increasing temperature resulted in decrease of particle size (Yu et al., 2004, Cheng et al., 2004)

1.3.2.4. Effects of Surfactants and Additives

Dissolution and precipitation reactions of CaCO_3 are controlled by surface reaction mechanisms in a wide pH range (14-4). That's why surfactants are expected to be successful to control the dissolution and precipitation of calcium carbonate.

The surfactant used by Xiang et al. (2004) was terpinol for producing nano sized calcium carbonate particles. The addition of 0.1-1vol% terpinol to the calcium hydroxide solution, decreased the size of the precipitated calcium carbonate particles, however, addition of higher amounts of terpinol resulted in the precipitation of larger sized particles with irregular shapes.

Calcium lignosulphonate was also used for producing small sized calcium carbonate particles (Kirchgessner and Lorrain, 1987, Wei et al., 1997). The results indicated that the Calcium lignosulphonate should be kept below the optimum level of 1,5wt% in calcium hydroxide solution According to Wei et al., (1997) using 2wt% Calcium lignosulphonate produced same particle sizes (1-2um) as using DispexA40 and DispexA40V. Cheng et al. (2004) used poly acrylic acid which had a significant effect on crystal morphology by influencing the nucleation and growth of CaCO_3 particles. The initial pH levels of the solution do not affect the morphology of the particles precipitated but their size. The size of calcium carbonate particles decreased with increasing pH (Cheng et al., 2004).

Yu et al. (2004) indicated that the poly acrylic acid had the most influence on the morphology of CaCO_3 at 25°C. Octadecyl dihydrogen phosphate was used by Cheng et al. (2004) for controlling the particle size of the CaCO_3 . It reduced the particle size to approximately 75nm. Yu et al. (2004) used polyethylene glycol, CTAB (cetyltrimethylammonium bromide) and polyvinylalcohol. Polyethylene glycol showed no obvious influence on the morphology and particle size of the CaCO_3 at 25°C but using polyethylene glycol at 80°C resulted in irregular shapes and no change in particle size. It was recorded that CTAB had no obvious effect on the morphology of CaCO_3 at 25°C but greater effect on the morphology at 80°C.

According to the experiments of Xiang et al. (2002) EDTA helped to accelerate the carbonation rate and formation of fine calcium carbonate particles. With the addition of zinc chloride, an obvious decrease in particle size was observed and spherical CaCO_3 particles were formed (Xiang, et al. 2002). The addition of magnesium chloride resulted in micron sized spindle and spherical shaped particles (Xiang, et al. 2002).

1.3.2.5. Invitro Biomineralization

Two main bioinspired methods were used to precipitate calcium carbonate, first one was the templating by structured organics and second one was, solution precipitation with growth modifiers such as ions, proteins and synthetic polymers (Raz et al., 2000, Falini, et al., 2002, Feng et al., 2007). Studies revealed that biominerals contained about 0.1-5wt% protein and polysaccharide, which resulted in difference of appearance, structure and other physical and chemical properties between natural minerals and biominerals. In that manner, protein was believed to play a critical role in the process of CaCO_3 formation in the biological system. Amino acids, the main components of proteins, were important factors in controlling CaCO_3 polymorphs.

Manoli et al. (2001) have studied the effect of glutamic acid on the growth of calcium carbonate crystal and its particle size. The studies revealed that the presence of glutamic acid in the supersaturated solutions, stabilized vaterite polymorph and there was no effect on the mechanism or the particle size of the crystal grown.

The kinetics of vaterite crystallization on calcite in the presence of alanine, glycine, lysine, as well as on lysine, glutamic acid, polyglycine, polytyrosine and polymethionine (Manoli et al., 2001, Manoli et al., 2002).

Tong et al. (2004) have investigated the effect of L-aspartic acid on the crystal phase, shape, size and aggregation of CaCO₃.

Xie et al. (2005) used four amino acids that have different kinds of groups such as –SH, –OH, –COOH and NH₂ as effective modifiers to mediate the crystallization of CaCO₃. These amino acids were L-Cystine, L-Tyrasine, DL-Aspartic acid and L-Lysine. The experimental results indicated that amino acids could direct the nucleation and crystallization; control the crystal size and shape of the crystals.

Tiano et al. (2006) used some natural and synthetic polypeptides to control the crystal growth within the pores. Their research indicated that poly aspartic acid could control the size and habit of crystals grown in calcareous stone.

1.4. Clay Minerals in Deterioration

Detrimental effects of clay minerals on the durability of the limestones and sandstones were pointed out by several researchers (Dunn and Hudec, 1966; Jimenez-Gonzales and Scherer, 2004; Rodriguez-Navarro et al., 1998; Veniale et al., 2001; Wüst and McLane, 2000; Williams and Robinson, 1989). The detrimental effects of clay minerals during the wetting and drying events caused several microstructural changes in the stone and contributed to the development of visual weathering forms such as polygonal cracking, scaling and contour scaling.

Clay minerals were shown to be the reliable indicators of physicochemical parameters and the geological environment responsible for weathering, diagenesis and all other stages of soil and rock formation in the zones of weathering (Uskov, 1978). They are the main products of authigenic mineral formation in the weathering processes. Examination of clay minerals for defining their crystallochemical properties such as their parameters of the elementary cell belonging to individual clay types, degree of swelling, mixed layering, iron content help to define and reconstruct the weathering environment and the process of

weathering (Uskov, 1978). Giresse and Wiewiora (2001) have found that in deep-water environment, abundant deposition of iron microparticles controlled by bottom-currents played an ultimate role in the development of montmorillonite. Along with dissolution of kaolinite, crystallochemical modifications of existing smectites and the formation of Fe³⁺-rich montmorillonites were detected in that deep water environment (Giresse and Wiewiora, 2001). Sabrouti and Sokkary (1982) have found that organic acids released through the decomposition of organic matter have facilitated the transformation of kaolite and illite to montmorillonite in the bottom sediments of Lake Edkua, a coastal lagoon in Eastern Mediterranean.

Swellings of clays generate damaging stresses in stone during wetting and drying cycles. Those are mainly intracrystalline swelling and interparticle or osmotic swelling (Rodriguez-Navarro et al., 1998). Intracrystalline swelling is generated by expandable or swelling clays such as smectite or mixed layer smectites. Osmotic swelling or interparticle swelling is experienced by all clay minerals (expandable and nonexpandable clays) during wetting and drying cycles of stone (Carroll, 1970a; Rodriguez-Navarro et al., 1998).

Damages due to swelling action of clays have been the subject of many studies. Those damages were found to be important especially in road construction works and in the foundations of low rise buildings that gave rise to structural cracks. Researchers had to find practical tests to survey large areas of soil grounds for their swelling characteristics and determine the areas with those problems and the areas without those problems (Ergüler and Ulusay, 2003; Yükselen and Kaya, 2008). Cation exchange capacity of clays is defined as the amount of exchangeable cations, expressed as milliequivalents per 100 grams of material at pH 7 under experimental conditions (Table 1.2) (Grim, 1968; Carrol, 1970a).

Table 1.2 Cation Exchange Capacity of Clays (After Grim, 1968, p.189)

Mineral	Cation Exchange Capacity (meq/100g)
Kaolinite	3-15
Illite	10-40
Chlorite	4-47
Montmorillonite group	36-100

In some studies, cation exchange capacity (CEC) determinations of clays by methylene blue and water content determinations of clays at 24 and 72 hours of soaking in water were found to be well correlated with the swelling percent and swelling potential of clays (Yükselen and Kaya, 2008; Ramasamy and Anandalakshmi, 2008; Ergüler and Ulusay, 2003; Claudia, 2000). They have suggested the use of those practical methods for surveying large areas of soil grounds to evaluate swelling percent and swelling pressures to spot the problem areas for road and building construction works.

It is important to indicate that, in some other studies, CEC determination by using methylene blue solution was not found to be so reliable since the adsorption capacity was found to decrease with increasing pH. Adsorbed methylene blue by clay minerals increased with decreasing temperature and increasing initial dye concentration (Gürses et al., 2006).

Al-Rawas et al., (2005) have studied the stabilization of expansive soil by using lime, cement, combinations of lime and cement, Sarooj (artificial pozzolan) and heat treatment. The swell percent was defined as the percentage increase in height in relation to the original height of soil sample due to the increase in moisture content. The swell pressure was measured using the constant volume method. The specimen was given free access to water while the volume was kept constant by continuous addition of loads at each vertical expansion of the tested specimen. The swell pressure was calculated as the load required to prevent swelling divided by the area of the specimen.

The expansive soil under study contained 20% clay with CEC: 70meq/100g. Additions of 3% and 6% lime to soil decreased the swell pressure from 249 kPa to 158 and 0 kPa respectively. By the addition of 6% lime, both the swell percent and swell pressure of soil was reduced to zero. The results showed the effectiveness of lime addition with water to control the swelling behaviour of clay minerals. The swelling behaviour was thought to be controlled through a number of reactions such as cation exchange, flocculation, carbonation and pozzolanic reactions. The cation exchange takes place between the cations associated with the surfaces of the clay particles and calcium cation of the lime, leading flocculation and change in engineering properties of clayey soil (Al-Rawas et al., 2005).

1.5. Iron Oxides in Deterioration

Several types of iron oxides are commonly found in soils as well as in deterioration zones of historic stones together with clay constituents. Iron oxides are often found to be the minor constituent of the original building stones such as limestones and sandstones. Changes in mineral phases of iron compounds in weathering zones of stone may be of importance in the decay mechanisms. There are few studies about the contribution of iron oxides to the weathering of historic stones. Some recent research on the atmospheric corrosion of iron artifacts and definition of stable and reactive faces of those iron compounds such as maghemite ($\gamma\text{-Fe}_2\text{O}_3$), magnetite (Fe_3O_4), haematite ($\alpha\text{-Fe}_2\text{O}_3$), ferrihydrites, goethite ($\alpha\text{-FeOOH}$), akaganeite ($\beta\text{-FeOOH}$), lepidocrocite ($\gamma\text{-FeOOH}$) may be of some use in understanding their possible role in stone decay (Saheb et al., 2007; Monnier, 2008; Dillmann, 2008; Hanesh, 2009). Iron oxides change phases during wetting and drying cycles of atmospheric weathering, ferrihydrites and goethite being among the frequently found products in soil and corrosion layers of archeological iron objects (Bellot-Gurlet et al., 2009). Some recent experimental studies with ferrihydrites point out their nano particle size characteristics, their high surface area and reactivity, therefore make them suitable to clean water of many metallic and anionic contaminants through their absorption characteristics (Bhatnagara, et al., 2009;

Hausner et al., 2009). On the other hand, it was experimentally proved that applied magnetic field have encouraged the nucleation and precipitation of calcium carbonate in hard water, calcite crystals being in greater number with smaller sizes and irregular shapes although the mechanisms were not well understood (Wang et al., 1997; Alimi et al., 2007). Those studies suggest some roles of iron oxides in precipitation reactions of calcium carbonate. Magnetic characteristics of some iron oxides can make them attractive sites of calcium carbonate precipitation in weathering zones of limestones such as cracks. On the other hand, phase changes in iron oxides depending on the physicochemical characteristics of the weathering medium may also affect the weathering process of limestone.

1.6. Biological Deposits in Deterioration

Detailed analysis of biological growth in terms of their types and morphology is beyond the scope of this study. However, some research related to the change in microstructure of limestones due to biological growth was reviewed.

Dupuy et al (1976) point out those blue - green algae generally favored the presence of clay minerals. Kaolinite was much preferred to the more strongly adsorbent ones like attapulgite or bentonite (Fogg, 1973). The blue-green algae by itself formed a micro environment with the help of its sheath material forming a site for the dissolution and precipitation reactions of calcium carbonate. The sheath of algae may play an important role by selectively absorbing some ions from the aqueous environment, providing sites of concentrated ions which result in nucleation and crystallization, and contribute to diagenesis of the rock material (Gebelein and Hoffman, 1973).

Biological growth on limestone surfaces sets free lichen acids and causes the formation of biominerals such as calcium oxalates (Zagari et al., 2000). The production of lichen acids help dissolution of calcium carbonate by chelating

calcium ions rather than by any acidic effect which results in the decomposition of calcium carbonate with the evolution of carbon dioxide (Hale, 1974).

1.7. Consolidation of Limestones with Nanodispersive Solutions

An exposed stone either in an archaeological site or on a monument is subjected to weathering by physical, chemical and biological processes. In time, those weathering processes cause considerable changes in microstructure of stone, such as increase in porosity, decrease in mechanical properties, quite a number of changes in chemical composition etc. starting from exterior surfaces towards interiors of the stone. Those changes are also visible by change in color, detachments as scales and flakes, crack formation material loss as powdering, granular disintegration, fragmental disintegration, karstic dissolution, outbursts etc. (Fitzner et al., 1995).

Conservation and preservation methods used for historical limestones today are not satisfactory. New methods should be improved. In order to decide on the proper methods to be used, stone deterioration should be well defined.

A study of the deterioration state is required before any treatment of stone. Conservation treatments should be applied only after identification of the deterioration state and its progress to assess their use in the control of decay (Lewin, 1966; Torraca, 1982).

Physical, chemical and mechanical compatibility with the original stone is a requirement for the conservation treatments of historic stones (Teutonico et al., 1997; Sasse and Snethlage, 1997; Wendler, 1997). During the consolidation treatments of the weak stone, compatibility can best be achieved by producing a similar structure to the original stone. It is a new approach in conservation science aiming at the formation of a structure similar to the original structure of the historic material to ensure compatibility and durability.

Treatments by nanodispersive solutions to produce calcite network has been promising in the recent studies (Giorgi et al., 2000; Ambrossi et al., 2001, Tiano et al., 2006; Dei and Salvadori, 2006). Consolidation treatments of deteriorated limestone to produce calcite network were done by using nanodispersive solutions and using in vitro biomineralization.

During the treatments, the crystallization of calcium carbonate has to occur in the pores and capillaries of decayed limestone. It can be achieved by treatments with nanodispersive solutions of calcium hydroxide and/or calcium carbonate. The important point for the satisfaction of this method is the average size of the applied calcium hydroxide particles to the stone especially when the matrix of the stone exhibits low porosity (Smith et al., 2000; Cölfen, 2003; Tiano et al., 2006).

Several nanodispersive solutions of Ca(OH)_2 prepared using water and ethanol and propyl alcohol as solvent. They were not able to achieve concentrations of nanodispersive solutions that kept its stability for a long time (Smith et al., 2000; Cölfen, 2003; Tiano et al., 2006; Lopez-Arce et al., 2010). Proper carbonation of nanodispersive Ca(OH)_2 solution in the pore structure of limestone was another difficulty to be overcome.

CHAPTER 2

EXPERIMENTAL METHODS

In this study, experiments were done to examine typical deterioration mechanisms in historic limestones and try to develop conservation treatments for the control of those mechanisms.

Studies have started with visual observations of weathering forms of limestones and their distribution at the historic sites. Representative sampling from those weathering forms were done. It was aimed to study the changes in the microstructure of the weathered stone at exposed surfaces and crack surfaces and their comparison with the relatively protected interiors. The distribution of the minor constituents of limestone such as clay minerals and iron oxides in relation to changes in the decayed microstructure of limestone was also studied. In addition, changes in physical and physico-mechanical properties of limestone by weathering were studied by standard test methods.

The microstructure of exposed surfaces, crack surfaces and interiors were studied by mineralogical and petrographical analyses of thin sections with optical microscopy, analyses of powdered samples by X-ray powder diffractometry. The morphological changes and changes in elemental composition were studied by direct observations of decayed surfaces and cross sections with a scanning electron microscope coupled with energy dispersive of X-rays (EDX) unit. The distribution of minor constituent such as clay minerals and iron oxides were observed by elemental maps of SEM-EDX.

Types of clay minerals were analyzed by XRD and FTIR. Swelling characteristics of clay minerals were examined by cation exchange capacity (CEC) determinations. Acid insoluble constituents of the exterior surfaces, cracks surfaces and interiors were also analyzed by XRD, FTIR, and SEM-EDX

Damage of biological depositions on the surfaces and their penetration to the interiors were also evaluated during those analyses.

Treatments with nanodispersive solutions needed to be developed by studying the i) preparation of the nanodispersive calcium hydroxide solution and ii) its efficient penetration and carbonation in the microstructure of the decayed limestone.

Interaction of the treatments with nanodispersive calcium hydroxide solutions with the microstructure of decayed limestone including minor constituents such as clay minerals and iron oxides and the changes in physical and physicommechanical properties of stone due to those treatments, were also studied and evaluated with the analytical methods mentioned above.

Nemrut Dağ Monument is located on the important crossing points of the upper Euphrates valley, inside the district borders of Kahta, Adıyaman. It was constructed by King Antiochos I (69-36 BC).

At the center of the monument, there is conical tumulus with a 30-35 degree slant. Three terraces surround it in east, west and north directions. While the organizations of east and west terraces show similarity, the construction of the north terrace is completely different. On the east and west terraces, five great limestone sculptures representing five goddess with King Antiochus I among them are displayed, with their backs turned to the Tumulus. They are flanked by two pairs of guardian animals, a lion and an eagle in both terraces. The order of the deities on the terraces from left to right is: King Antiochus I, Commagene/Tyche, Zeus/Oromasdes, Apollon/Mithras-Helios-Hermes and Herakles/Artagnes-Ares.

Behind the row of sculptures the ancient Greek inscriptions (nomos) with the will of King Antiochos I are recovered. Besides the colossal sculptures on the terraces, altars and stele pedestals are found. On the east terrace, there is also a square platform, defined as an altar (Şahin-Güçhan, 2011).

2.1. Visual Analyses of Limestone Weathering Forms at the Historic Site

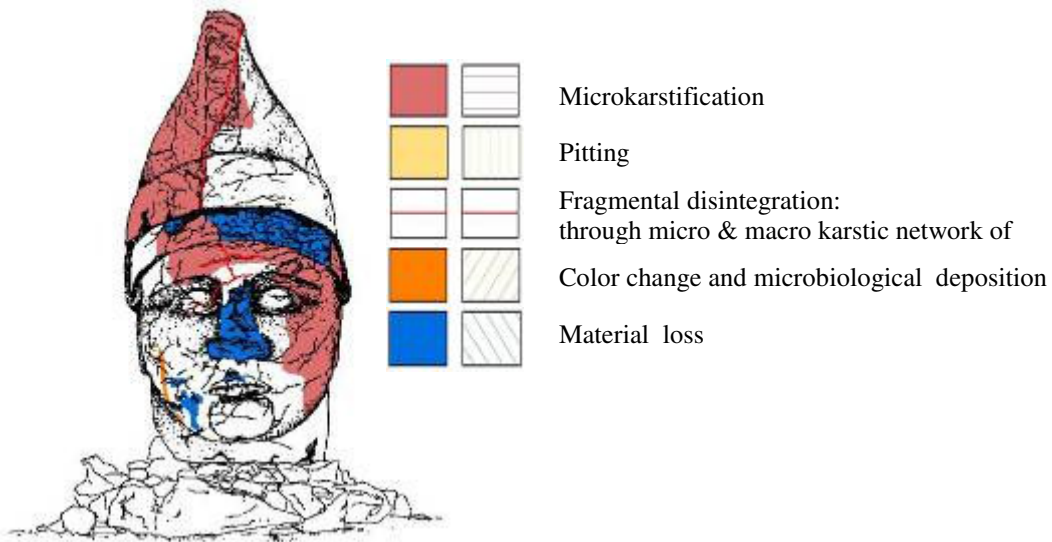


Figure 2.1 Various deterioration forms mapped on a measured drawing of Antiochus (East Terrace) (KNCDP, 2011).

Examination of visual decay forms on Nemrut Dağ Monument limestones were done at the site. Visual decay forms were mapped on the measured drawings of statues and their bodies in the East and West terraces of the site in the context of Kommagene Nemrut Conservation and Development Program Project (KNCDP, 2011).

The weathering forms observed at the site was color change and biological deposition, pitting, micro and macro karsification and fragmental disintegration through micro and macro karstic network of limestone and cracks (Caner et al. 2010). Representative samples were taken from the most abundant deterioration forms for examination.

2.2. Sample Collection and Nomenclature

Micro samples found next to the statues and the ones found detached were collected as representative weathered samples from the Nemrut Dağ Monument and relatively unweathered macro samples from the geological formations nearby the monument that showed similar deterioration forms were also collected. The deteriorated samples from ancient quarry of Pessinus, a quarry at Pessinus archaeological site in the township near Ankara, showing visual decay forms as the scales and granular disintegration to sugary marble grains were collected and used for the trial experiments with nanodispersive calcium hydroxide solutions. Intergranular cracks around the calcite grains in decayed marbles were easily observed in thin sections. Therefore first trials of treatments with nanodispersive solutions were carried out with deteriorated marbles of Pessinus Ancient Quarry. The penetration of nanodispersive solution through intergranular cracks was followed.

Samples were coded with the letters indicating the site, the location in the monument and the number that was related to detailed description of the sample at the site. Example; NE1 indicating the first sample taken from the East Terrace of the Nemrut Dağ Monument. Its specific place is described in detail in Table 2.1.

During the examination of the powdered samples and cross section samples additional codes were given indicating its part on the sample such as exposed surface 'S', crack surface 'C' and relatively undeteriorated interiors 'I', e.g. NE1S indicating exposed surface of the samples' from the East Terrace of the Nemrut Dağ Monument.

The locations of the collected samples were shown on the 1/50 plans of the East and West Terraces of the Nemrut Dağ Monument (Fig. 2.2-2.3). Sample codes and explanations were listed in Table 2.1.

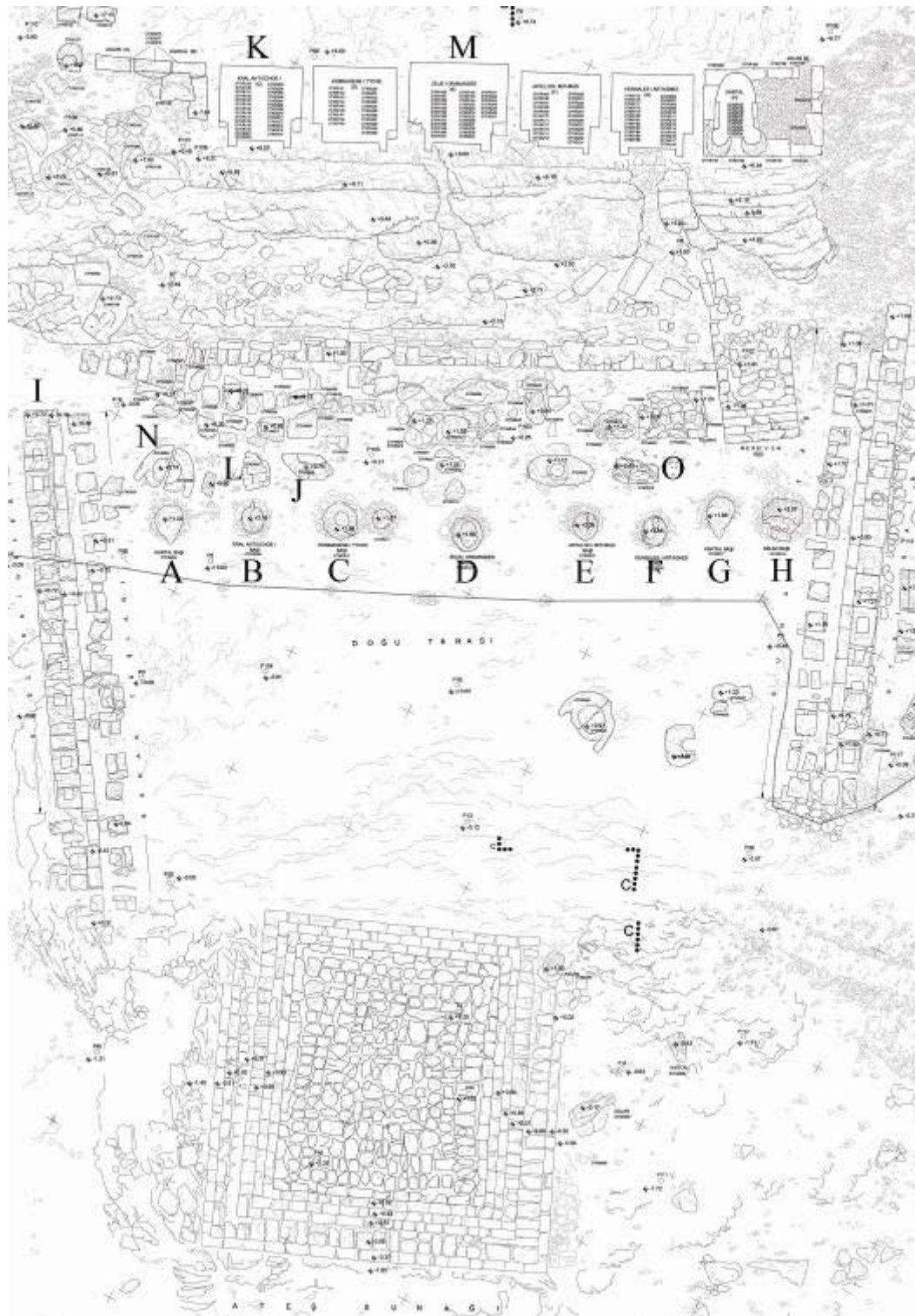


Figure 2.2 Locations of the collected samples on East Terrace plan of Nemrut Dağ Monument (1/50) (KNCDP, 2011).

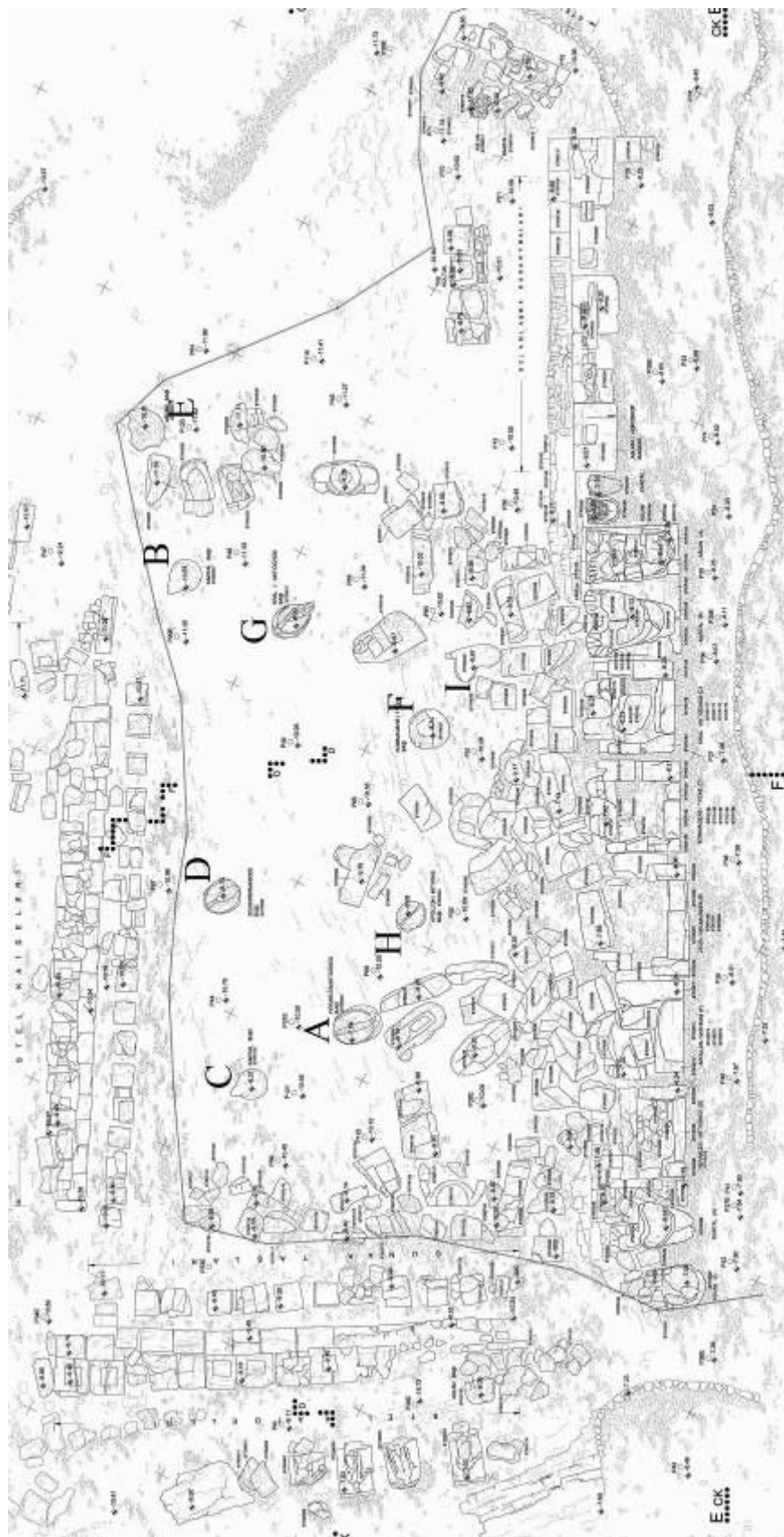


Figure 2.3 Locations of the collected samples on West Terrace plan of Nemrut Dağ Monument (1/50) (KNCDP, 2011).

Table 2.1 List of studied samples

Sample code	Description
	
NE1	East terrace, a break out near the base of the stele at the south (I)
NE2	East terrace, a break out near the head of Apollo (E)
NE3	East terrace, a break out near the base behind Kommagene's head (J)
NE4	East terrace, a break out near the head of Kommagene (C)
NE5	East terrace, a break out near the base of Antiochos (K)
NE6	East terrace, a break out near the head of Heracles (F)
NE7	East terrace, a break out near the Eagle at the north side (G)
NE8	East terrace, a break out near the head of Apollo (E)
NE9	East terrace, a break out near the front of Antiochos' head (B)
NE10	East terrace, a break out near the top of Antiochos' head (B)
NE11	East terrace, a break out near the Eagle at the south side (A)
NE12	East terrace, a break out near the head of Lion (H)
NE13	East terrace, a break out near the head of Kommagene (C)
NE14	East terrace, a break out near the top of Zeus's head (D)
NE15	East terrace, a break out near the base behind Anthiocus' head (L)

Table 2.1 List of studied samples (continued)

NE16	East terrace, a break out near the base behind Kommagene's head (J)
NE17	East terrace, a break out near the base of Zeus (M)
NE18	East terrace, a break out near the base behind the Eagle at the south side (N)
NE19	East terrace, a break out near the base behind Heracles' head (O)
NE20	East terrace, a break out near the Eagle at the north side (H)
NE21	East terrace, a break out near the base behind Antiochos' head (L)
	
NW1	West terrace, a break out near the Heracles' head (A)
NW2	West terrace, a break out near the head of Eagle at the west side (B)
NW3	West terrace, a break out near the head of Eagle at the east side (C)
NW4	West terrace, a break out near the head of Zeus (D)
NW5	West terrace, a break out near the head of Lion (E)
NW6	West terrace, a break out near the head of Kommagene (F)
NW7	West terrace, a break out near the head of Antiochos (G)
NW8	West terrace, a break out near the head of Apollo (H)

Table 2.1 List of studied samples (continued)

NW9	West terrace, a break out near the base behind Kommagene's head (I)
NW10	West terrace, a break out near the base behind Kommagene's head (I)
NW11	West terrace, a break out near the head of Heracles (A)
	
NWQ1	West quarry,
NWQ2	West quarry, piece from a region with lichen growings
NWQ3	West quarry, piece from a region showing similar deterioration with the statues
NWQ4	West quarry, piece from a region with pitting
NWQ5	West quarry, piece from a region with pitting
NWQ6	West quarry, piece from a region with lichen growings
NWQ7	West quarry, piece from a region with grey lichen growings

2.3. Determination of Physical and Physicomechanical Properties

Changes in physical and physico-mechanical properties of limestone by weathering were studied by standard test methods as described below.

2.3.1. Determination of Basic Physical Properties

Limestone and marble samples representing the decay types and relatively unweathered limestone and marbles cubes taken from the quarries nearby and cut to ~ 4.5 cm cubes were analyzed for their basic physical properties such as bulk density, porosity and drying rate.

Samples were oven dried at around 60°C until constant weight (M_{dry} g). They were then immersed in distilled water at room temperature of about 20°C and left immersed for 24 hours. Afterwards they were put under vacuum at 0.132 atm (100 torr) pressure for about 20 minutes in order to have better saturation (M_{arch} g). Samples were wiped with a wet paper and weighed again (M_{sat} g).

Those measurements have allowed the calculation of the physical properties defined below.

Porosity is the empty spaces or voids in a solid mass, expressed as percent volume of the solid mass.

Apparent Volume is the total volume of a sample which includes the pore space.

Real Volume is found by subtracting the pore space accessible to water from the apparent volume.

Bulk (apparent) Density is the ratio of the mass to the apparent volume of the sample.

Real Density is the ratio of the mass to the real volume of the sample.

Calculations were carried out by using following equations (RILEM, 1980).

$$\text{Real Volume} = M_{dry} - M_{arch}$$

$$\text{Real Density} = (M_{dry} / (M_{dry} - M_{arch})) \times 100$$

$$\text{Apparent Volume} = M_{sat} - M_{arch}$$

$$\text{Bulk Density (g/cm}^3\text{)} = (M_{\text{dry}}) / (M_{\text{sat}} - M_{\text{arch}})$$

$$\% \text{Porosity} = (1 - (\text{Bulk Density} / \text{Real Density})) \times 100$$

2.3.2. Determination of Drying Rate

Limestone samples with ~ 4,5 cm cubic shapes that were saturated with water, were left for drying in laboratory around 20°C and 30% relative humidity. The weight loss of the samples was followed by weight measurements (M_{wet}) at certain time intervals such as 15-30-60 minutes, 1-2-4-8-24 hours and 2-3-4-5-6 days subsequently. All weight measurements were recorded with the sensitivity of .0001 grams.

The drying rate was expressed as the density of water vapor flow rate (g) evaporated from the surface of the samples and it was calculated as a function of average moisture content for each time span versus surface area of the sample by using the following formula (RILEM, 1980);

$$(g) = M / A * t$$

where;

(g) : density of flow rate (kg/m².s)

M : moisture content of the sample (kg) at the time t

A : total surface area of the cubic test specimen (m²)

t : time span (second)

M (moisture content of the sample) is calculated by the use of dry, wet and saturated weights of samples:

$$M = (M_{\text{wet}} - M_{\text{dry}}) / (M_{\text{sat}} - M_{\text{dry}})$$

where;

M_{sat} : saturated weight (kg)

M_{dry} : dry weight (kg)

M_{wet} : wet weight (kg) at a certain time

The results were expressed in diagrams as the percentage of the weight loss versus time, and density of water vapor flow rate versus time.

2.3.3. Determination of Basic Physicomechanical Properties

Modulus of elasticity was the only mechanical property obtained for the limestones. It was calculated by using ultrasonic velocity measurements of the limestones and their bulk density using the equation given below (Timoshenco 1970; ASTM 2845-90; RILEM 1980).

$$E_{\text{mod}} = D^* V^2 (1 + \nu_{\text{dyn}}) (1 - 2\nu_{\text{dyn}}) (1 - \nu_{\text{dyn}})$$

where;

E_{mod} : modulus of elasticity (N/m^2)

D: bulk density of the specimen (kg/m^3)

v : wave velocity (m/sec)

ν_{dyn} : Poisson's ratio

In this equation, Poisson's ratio differs from 0.1 to 0.5. It is taken 0.33 for marble.

The instrument used for the ultrasonic velocity measurements was a pulse generating test equipment, PUNDIT plus with its probes, transmitter and receiver of 220 kHz for all samples. The ultrasonic velocity of the waves is calculated by using the following formula.

$$V : l/t$$

where;

V : velocity (m/s)

l : the distance traversed by the wave (mm)

t : travel time (s)

2.4. Microstructural Analyses

The changes in the microstructure of weathered limestone were studied by several methods using the micro samples collected from the sites. Progress of weathering was examined in the laboratory by artificially weathering the limestones cut to 5 cm cubes using salt crystallization cycles.

The microstructure of weathered limestones at exposed surfaces, crack surfaces and interiors were studied by mineralogical and petrographical analyses of thin sections with optical microscopy, analyses of powdered samples by X-ray powder diffractometry. The morphological changes and changes in elemental composition were studied by direct observations of decayed surfaces and cross sections with a scanning electron microscope coupled with energy dispersive of x-rays (EDX) unit. The types, distribution and the behavior of minor constituent such as clay minerals and iron oxides were also studied by several analytical methods described below.

2.4.1. Preparation of Artificial Weathered Limestones by Salt Crystallization

Progress of stone deterioration was examined in the laboratory by salt crystallization tests. This test was first proposed by Brard in 1828 as a means of assessing the frost resistance of stone. Since that time, sodium sulphate crystallization test has been used for general assessment of durability rather than of frost resistance alone. The crystallization test that simulates natural decay mechanism has a good correlation between the results of the tests and the overall weathering behavior of limestones (Price, 1978). Unlike most other techniques the sodium sulphate crystallization test is a comparative test to obtain comparative data for monitoring and discovering the weak zones of limestone.

Limestones from geological formations in the vicinity of Nemrut Dağ that looked quite similar to the ones used on the Nemrut monuments were collected and were used for artificially durability tests. They were cut to cubes of 5 cm size and subjected to salt crystallization cycles in the laboratory. The limestone cubes were soaked in 14% $\text{Na}_2\text{SO}_4 \cdot 10\text{H}_2\text{O}$ solution for 2 hours and dried at 60°C for at least 16 hours and that cycle was repeated. At each 5th cycle of salt crystallization, .8 limestone samples were removed from the test and were examined.

Durability assessment of those limestone cubes has been made by following their weight loss, porosity, bulk density and ultrasonic velocity changes.

2.4.2. Preparation of X-Ray Powder Diffraction (XRD) Samples

XRD analyses were performed on powdered samples. Before the analyses samples were scraped off from the stones' exposed surfaces and crack surfaces. They were ground in agate mortar. Ground powder samples were analyzed by XRD using a Bruker D8 Advance Diffractometer with Sol-X detector.

2.4.3. Preparation of X-Ray Powder Diffraction (XRD) Samples of Clay Constituents

For the preparation of oriented samples of the clay constituents, certain samples were treated with 2% HCl to dissolve the carbonate minerals. The acid insoluble part was filtered through Whatman No.40 filter paper, washed until free of chloride ions then the residues were dispersed in distilled water and poured on cover glasses and left to dry at room temperature.

XRD traces of oriented samples of clay minerals were taken in the dry state and after wetting with ethylene glycol. Wetting the samples with ethylene glycol was done by exposing them to the vapor of the reagent (ethylene glycol) for at least 8 hours at 60°C (Grim, 1968; Carroll, 1970b; Moore and Reynolds, 1997).

The instrument used was Bruker D8 Advance Diffractometer with Sol-X detector. Analyses were done using CuK α radiation, adjusted to 40 kV and 40 mA. The XRD traces were recorded for the 2 θ values from about 3° to 70°. Mineral phases were identified in XRD traces.

2.4.4. Preparation of FTIR Samples

Limestone samples and clay minerals in the acid insoluble residues were powdered with an agate mortar and FTIR measurements were performed directly on the powdered samples using ATR attachment of a Bruker Alpha T FTIR unit. Some samples were powdered and mixed with KBr and pellets were made with a hydraulic press, FTIR measurements were done by using pellets.

2.4.5. Preparation of Scanning Electron Microscope Samples

Small pieces of limestone and marbles samples' exposed surfaces, crack surfaces and relatively unweathered interiors were examined by SEM using Tescan Vega II XMU with large chamber coupled with Oxford Inca EDX system. Samples to be examined were cut by a low speed saw (Buehler Isomet). Then the surfaces to be examined were coated with conducting carbon layer with a carbon coater instrument.

2.4.6. Preparation of Samples for CEC Measurements

CEC measurements were done in acid insoluble residues of deteriorated limestones such as exposed surfaces and crack surfaces. Their clay constituents were examined for their CEC.

2.4.6.1. CEC measurements of Clay minerals

The individual CEC measurements were in clay constituents of acid insoluble parts obtained from weathered exposed surface zones and weathered crack zones of limestones.

About 1 gr of acid insoluble sample was powdered in an agate mortar and put in 100ml of 25mg/L methylene blue solution. Magnetic stirring was done to the solution for about 2 hours. After that, the solution was centrifuged and absorbance was measured 663 nm by using an OPTIMA UV-vis spectrometer. Difference in methylene blue absorption of solution at 663 nm, before and after mixing with the sample was used to calculate CEC (meq/100g) and MBV (methylene blue value:g/100g) of the clay sample (Ramasamy and Anandalakshmi, 2008). Clay samples that were treated with nanodispersive calcium hydroxide solution had to be washed free of unabsorbed calcium hydroxide before they were treated with methylene blue solution, in order to eliminate its interference with the methylene blue solution (Ramasamy and Anandalakshmi, 2008).

2.4.7. Preparation of Nanodispersive Solutions of Calcium Hydroxide

Preparation of nanodispersive solutions was an important step of conservation treatments. In the light of previous research on the subject, experiments were done to improve proper nanodispersive solution of calcium hydroxide for conservation treatment of limestone. For that purpose, Analar grade chemical compounds such as calcium hydroxide and calcium oxide were used. Water, propanol and ethanol were tried to be used as solvents. Application of ultrasonic vibration and vigorous magnetic stirring was necessary to achieve high concentration of nanodispersive calcium hydroxide in the solution. Those trials were done systematically by testing the solutions each time for the concentration of nanodispersive solution and its stability in time (see section 3.9 for the preparation of a nanodispersive solution with high concentration).

Carbonation of nanodispersive solutions were also studied for their carbonation rate under the high concentrations of carbon dioxide (5-20%) and at high relative humidity conditions. Results of those experimental procedures were given in next chapter.

Carbonation of nanodispersive solution was also studied for the formation of well shaped calcite crystals and their attachment to limestone surface by adding 0.025 g sodium stearate in the nanodispersive calcium hydroxide solution (Ukrainczyk et al, 2009; Tran et al., 2010)

2.4.8. Determination of Calcium Hydroxide Concentration in Nanodispersive Solution by Volumetric Method

This test method was based on the complex formation titration using standard EDTA solution. The solution was prepared by dissolving disodium ethylenediaminetetraacetate salt in distilled water. In the titration 0.01 M EDTA solution was used. It was standardized with reference calcium solution prepared from reagent grade pure Ca(OH)₂. It is known that EDTA (Y⁴⁻) makes one to one stable complex with metal ions.



Where, Y⁴⁻ shows anion of EDTA that forms complex with calcium ion.

10 ml of nanodispersive solution sample was treated with 3.0 ml of 5% hydrochloric acid in 100 ml volumetric flask. After the dissolution of calcium compounds, volume was made 100 ml with distilled water. Then 20 ml of this solution was taken and diluted to 100 ml, pH of the solution was adjusted to 12-13 using few milliliters of 10% NaOH and few milliliters Calcon indicator was added. Calcon indicator was prepared by dissolving 0.02 gr Calcon indicator in 100 ml ethanol. The final solution obtained was titrated with 0.01M EDTA solution, until the pink color became permanently blue (Black, 1965).

2.4.9. Determination of Carbonation Rate of Nanodispersive Calcium Hydroxide Solution

The procedure described in 2.4.8 was used for the determination of carbonation rate of nanodispersive calcium hydroxide solution without acid treatment.

CHAPTER 3

EXPERIMENTAL RESULTS

Results of the individual experiments are given here starting with the visual analyses of weathering forms at the historic site. Their combined interpretations and the discussions are given in the next chapter.

3.1. Results of Visual Analyses on Weathering Forms of Limestones at the Historic Site

Abundant decay forms at the site were color change and biological depositions, material loss by fragmental disintegration through the karstic zones and/or the cracks, as well as the detachments with fragmental disintegration. Other decay forms that were often seen were pitting and dissolution of limestone through the karstic veins (Fig. 3.1- Fig.3.6).

The decay forms that needed urgent conservation treatments were the detachments where the fragmental disintegration occurred and material loss areas where detachments with fragmental disintegration have restarted (Fig. 3.1).



Figure 3.1 View of fragmental disintegration and material loss on one of the Nemrut limestone statues (East terrace, back view of the head of Eagle).

Fragmental disintegration through cracks usually started at the surfaces where the cracks were filled with biological depositions (Fig.3.2).

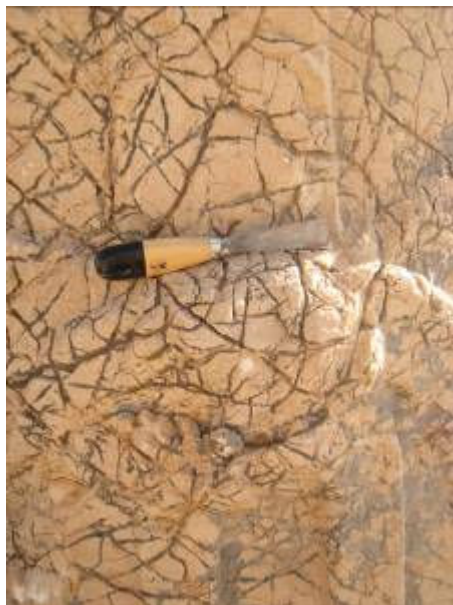


Figure 3.2 View of fragmental disintegration through cracks filled with biological deposition on one of the Nemrut Dağ Monument statues (West terrace, a detail on the head of Herakles).

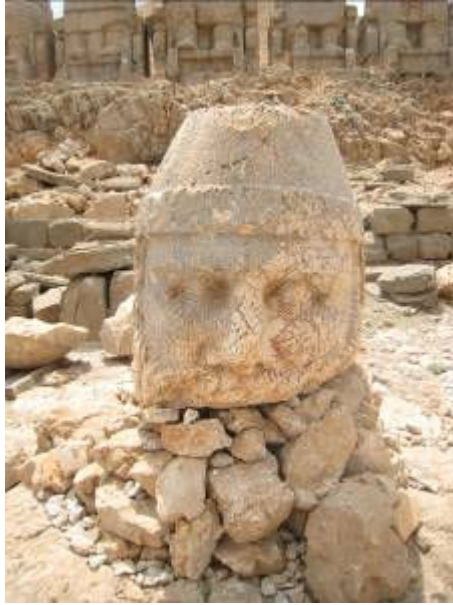


Figure 3.3 Grey color change and biological depositions on the head of Zeus at the East terrace of Nemrut Dağ Monument.



Figure 3.4 Material losses by fragmental disintegration on the head of Antiochos at the east terrace of Nemrut Dağ Monument



Figure 3.5 Material losses by pitting on the head of Kommagene at the east terrace of Nemrut Dağ Monument



Figure 3.6 Material losses by dissolution of limestone through karstic veins on the head of Kommagene at the west terrace of Nemrut Dağ Monument

3.2. Physical and Physicomechanical Properties of Limestones

Physical and physicomechanical properties such as bulk density, total porosity, ultrasonic pulse velocity and modulus of elasticity values of weathered limestone samples were determined. The change in physical and physicomechanical properties of limestone were determined in fresh limestone cubes subjected to different cycles of salt crystallization. Drying rates of limestone cubes at 0, 90, 145 cycles of salt crystallization were also presented.

3.2.1. Results of Physical and Physicomechanical Properties of decayed limestones and marbles

Small pieces of fragmental disintegration collected in the vicinity of the statues and their basement blocks were taken to represent the weathered samples. Their bulk densities were in the range 2.54 - 2.70 g/cm³, average bulk density being 2.68 g/cm³. The total porosities of weathered samples were in the range of 0.27 - 5.86 %, average total porosity being 0.80% (Fig. 3.7).

Average ultrasonic velocity values of the samples were about 1870 m/s. Those results are quite similar with the results of fresh samples taken from the lower parts of Nemrut Dağ that were artificially weathered with 50 cycles of salt crystallization (Table. 3.1).

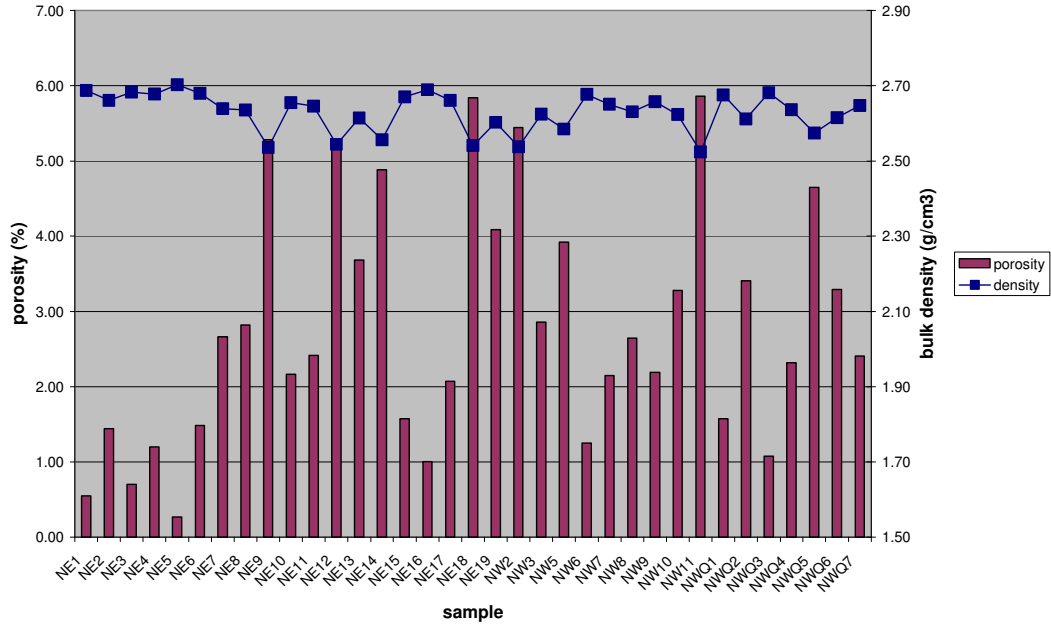


Figure 3.7 Bulk density and total porosity values of the samples taken from the Nemrut Dağ Monument

3.2.2. Results Physical and Physicomechanical Properties of Artificially Weathered Limestones by Salt Crystallization

Table 3.1 Average bulk density, porosity and ultrasonic velocity values of the samples before and after 50 salt crystallization cycles.

	Before salt crystallization cycles	After 50salt crystallization cycles
Bulk density (g/cm ³)	2.69	2.68
Porosity (%)	0.50	0.80
Ultrasonic Velocity (m/s)	3200-5000	1400-2600
Modulus of Elasticity (MPa)	16869	8158

The average bulk densities of the samples after the salt crystallization tests were slightly changed. The porosity was increased from 0.50% to 0.80% at the end of the 50 test cycles. On the other hand, the notable decrease in average ultrasonic

velocity values indicated the microstructural changes of the limestone samples (Table.3.1).

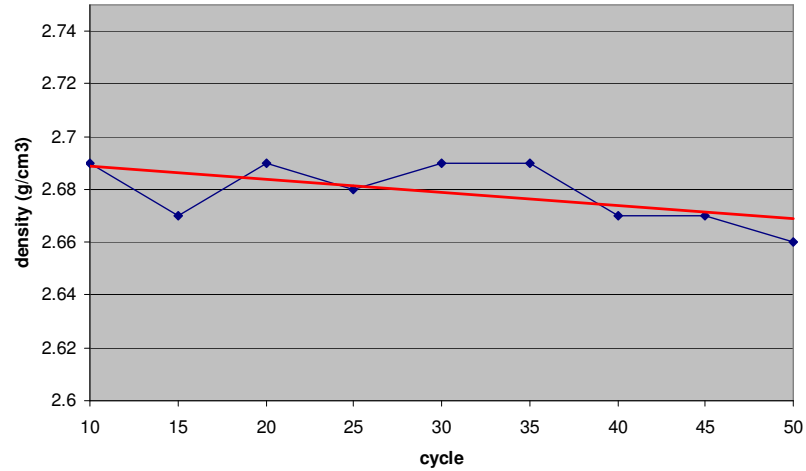


Figure 3.8 The change in bulk density of the samples with respect to salt crystallization cycles

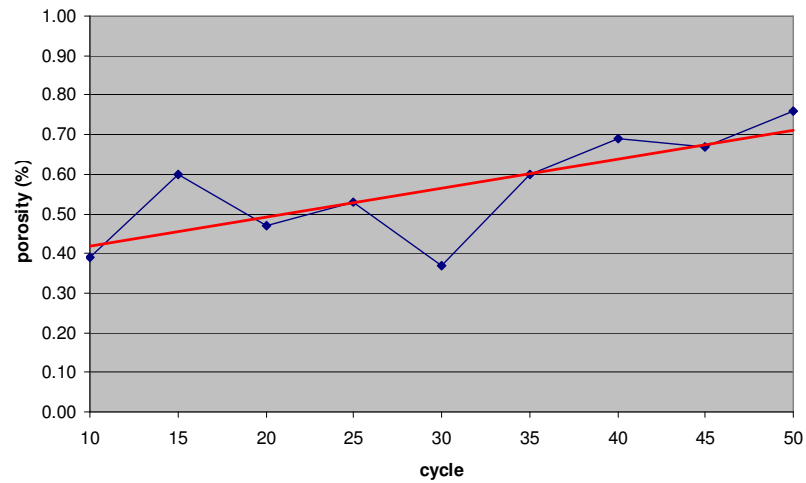


Figure 3.9 The change in porosity of the samples with respect to salt crystallization cycles

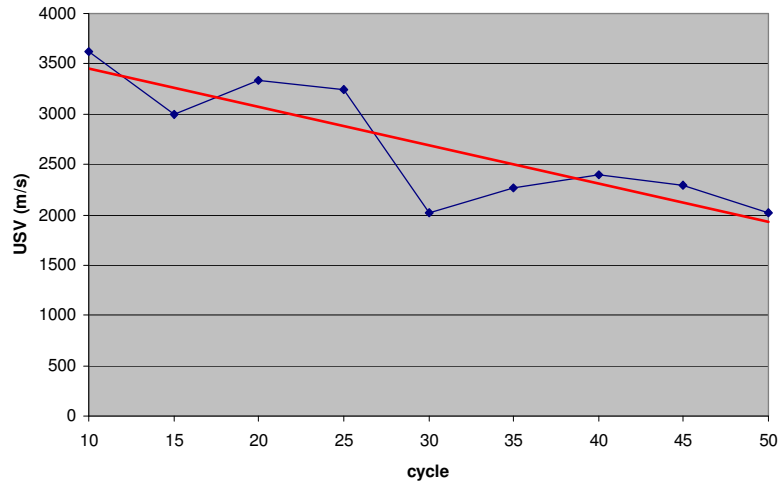


Figure 3.10 The change in ultrasonic velocity values of the samples with respect to salt crystallization cycles

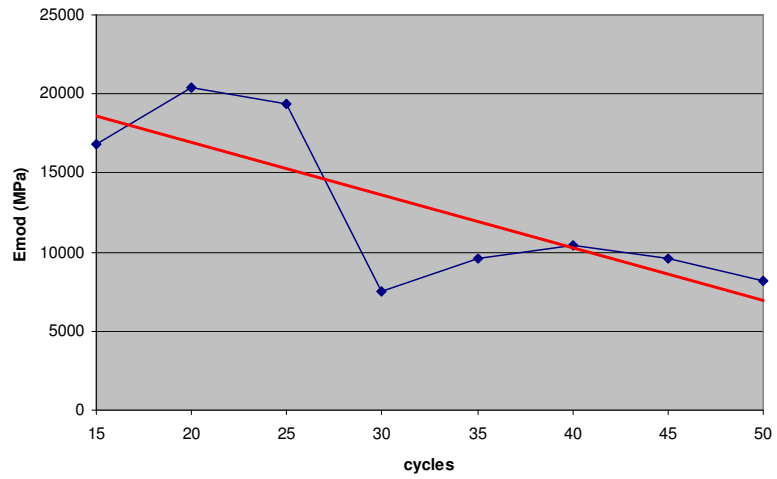


Figure 3.11 The change in modulus of elasticity values of the samples with respect to salt crystallization cycles.

3.2.3. Results of Drying Rate of Artificially Weathered Limestones by Salt Crystallization

Drying rate of artificially weathered limestone cubes that were subjected to 0, 90, 145 salt crystallization cycles indicated that drying rate has decreased with salt crystallization cycles. ‘Weight loss vs. day’ graphs showed that most weathered cubes from 145th cycle completed their drying last (Fig. 3.12). The cubes at 0th and 90th were the first and second ones to complete their drying respectively. Late drying indicated the presence of finer porosity. As a result, artificial weathering by salt crystallization has increased both macro porosity and micro porosity (Fig. 3.13).

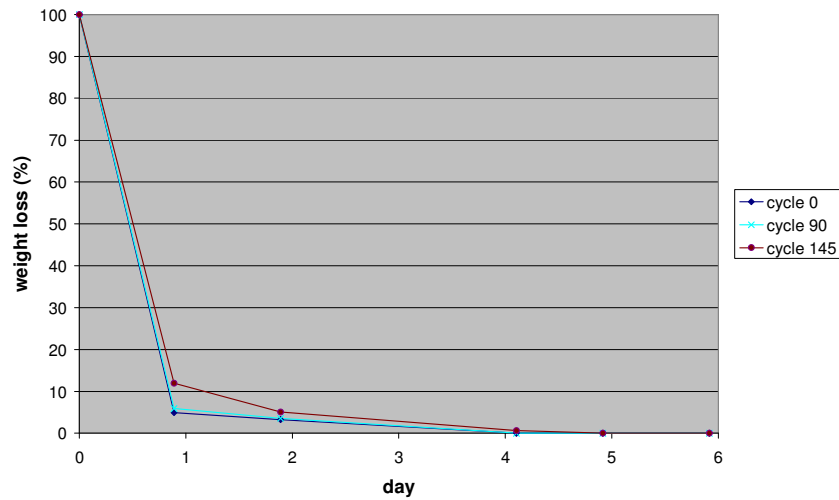


Figure 3.12 Percent weight loss during drying of artificially weathered limestone cubes that were subjected to 0, 90, 145 salt crystallization cycles.

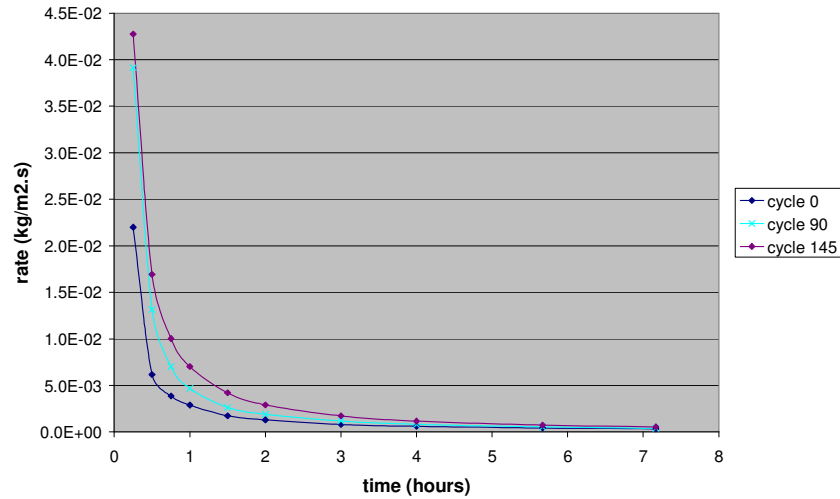


Figure 3.13 Drying rate of artificially weathered limestone cubes that were subjected to 0, 90, 145 salt crystallization cycles.

3.3. Thin Section Examination of Limestones and Marbles by Optical Microscopy

Limestone samples from the Nemrut Dağ Monument were examined for their mineralogical and petrographical characteristics to provide additional data for diagnostic studies on the mechanisms of deterioration and studies on the effects of treatments with nanodispersive calcium hydroxide solutions.

In this section mineralogical and petrographical analyses of the quarry limestones and the relatively unweathered samples as well as weathered limestone samples were presented.

3.3.1. Thin Section Examination of Quarry Limestones from the lower parts of the Nemrut Dağ and from Quarry at the West Terrace of Nemrut Dağ Monument

The limestones from the lower parts of the Nemrut Dağ and from Quarry at the West Terrace of Nemrut Dağ Monument had biosparitic and micritic calcite crystals and had some natural cracks and karstic veins (Figs.3.14-3.18). Karstic veins were filled with bigger calcite crystals. Some fossils were also observed in the micritic matrix. The shells of the fossils were filled with spherulitic calcite crystals.



(a)



(b)

Figure 3.14 Thin section views of Nemrut quarry limestone showing cracks and opaque minerals. (a) scale bar: 250 μ ,(b) scale bar: 250 μ



Figure 3.15 Thin section view of Nemrut quarry limestone showing crack zones, scale bar: 500 μ

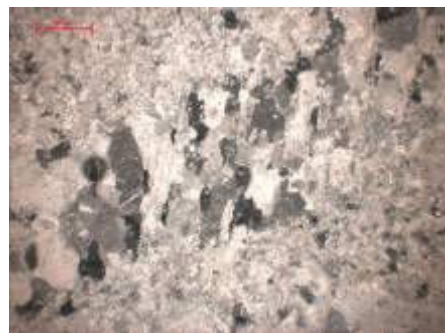


Figure 3.16 View of a Karstic vein in Nemrut quarry limestone, scale bar: 100 μ



Figure 3.17 View of a crack with karstic vein having iron oxides and calcite crystals, cross nicols, scale bar: 100 μ

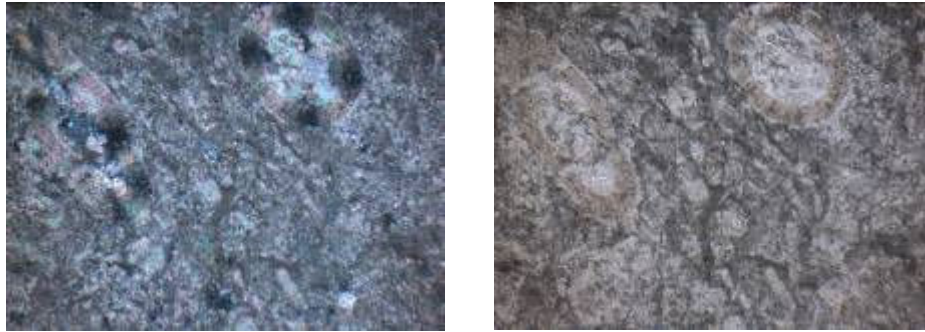


Figure 3.18 Views of a Nemrut quarry sample having fossils in its matrix, left: cross nicols 10X, right: single nicol 10X.

Some cracks with karstic veins were filled with iron oxides and opaque minerals (Fig. 3.17).

3.3.2. Thin Section Examinations of Weathered Limestones from Nemrut Dağ Monument

The thin section analysis of deteriorated limestone pieces, mostly the breakouts from fragmental disintegration at the east and west terraces have revealed their several microstructural characteristics such as micritic limestone matrix, macropores, distribution of karstic veins, their texture, opaque minerals such as iron oxides and clay minerals together with their distribution and microcracks.

The deteriorated samples from East and West terrace had micritic and microsparitic particles and they were bonded with sparitic calcite. Karstic veins were usually filled with sparry calcite crystals. Some karstic veins showed dissolution near the exposed surface. Some opaque minerals most probably were hydrated iron oxides. Some observed fossils were filled with sparry calcite crystals (Figs. 3.19-3.26).

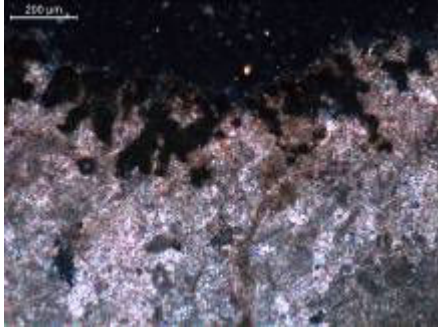


Figure 3.19 Thin section views of deteriorated limestone from east terrace, cross section through exterior surface showing biological growth and cracks growing towards interiors. Scale bar: 200 μ.

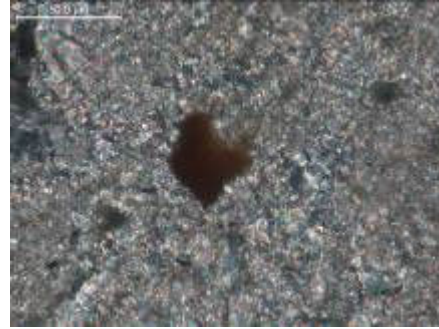


Figure 3.20 Thin section views of deteriorated limestone from west terrace cross section showing opaque minerals, scale bar: 50 μ.

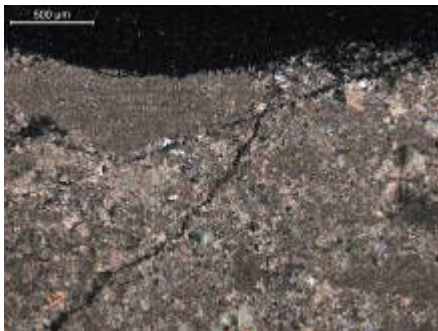


Figure 3.21 Thin section view of deteriorated limestone from east terrace cross section through exterior surface showing biological deposition and cracks. Scale bar: 500 μ.

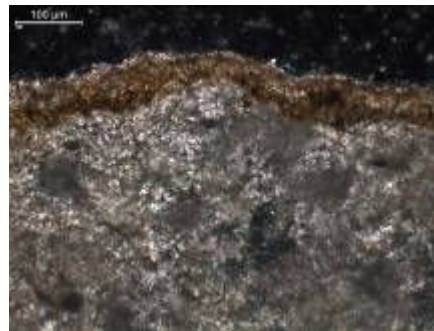


Figure 3.22 Thin section view showing the clay deposition on the exterior surface of a weathered limestone from east terrace cross section. Scale bar: 50 μ.



Figure 3.23 View of a karstic vein and green biological activity on the exterior surface of a deteriorated sample from the West Terrace. (20X cross nicols)

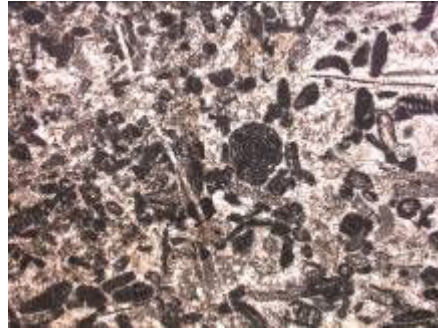


Figure 3.24 Thin section view of a deteriorated sample from the West Terrace showing some fossils in the micritic calcite matrix. (10X single nicol)



Figure 3.25 View of a crack and biological activity on the exterior surface of a deteriorated sample from the West Terrace. (20X cross nicols)

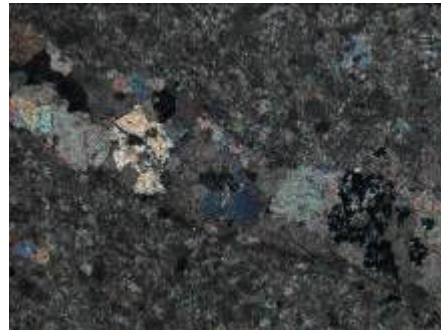


Figure 3.26 View of a karstic vein on the relatively interior part of a deteriorated sample from the East Terrace. (5X cross nicols)

3.4. X-Ray Diffraction Analyses

XRD traces of Nemrut limestones were taken to determine major and minor minerals in their composition as well as the mineral composition of the exposed surfaces and crack surfaces, relatively unweathered interior parts of limestones, insoluble minerals in their composition.

Minor constituents as clay minerals and iron oxides in the limestone composition and in the weathering zones were tried to be separated by treating limestone with 2% HCl and by magnetic separation of some iron oxides.

Firstly, XRD results of weathered limestone samples before acid treatment were given. They include XRD traces of samples powdered from relatively interiors of limestone, directly taken XRD traces of the crack surfaces and exterior surfaces and XRD traces of powdered samples scraped from the crack surfaces.

XRD traces of powdered samples scraped from the crack surfaces were taken in oriented form before glycolation, after glycolation and in heated states.

Secondly, XRD traces of acid treated samples from crack surfaces were given in oriented, glycolated and heated forms.

Lastly XRD traces of surface soil around the statues were given.

3.4.1. XRD traces of weathered limestones before acid treatment

XRD traces of the weathered limestone pieces separated by fragmental disintegration in East and West Terraces showed that calcite was the main mineral constituent of all limestones. No secondary minerals were detected in most of those XRD patterns due to very high percentage of calcite (Figs 3.27, 3.28). However,

some breakouts from west terrace have shown the presence of quartz and biominerals whewellite and weddellite in minor amounts (Fig 3.27).

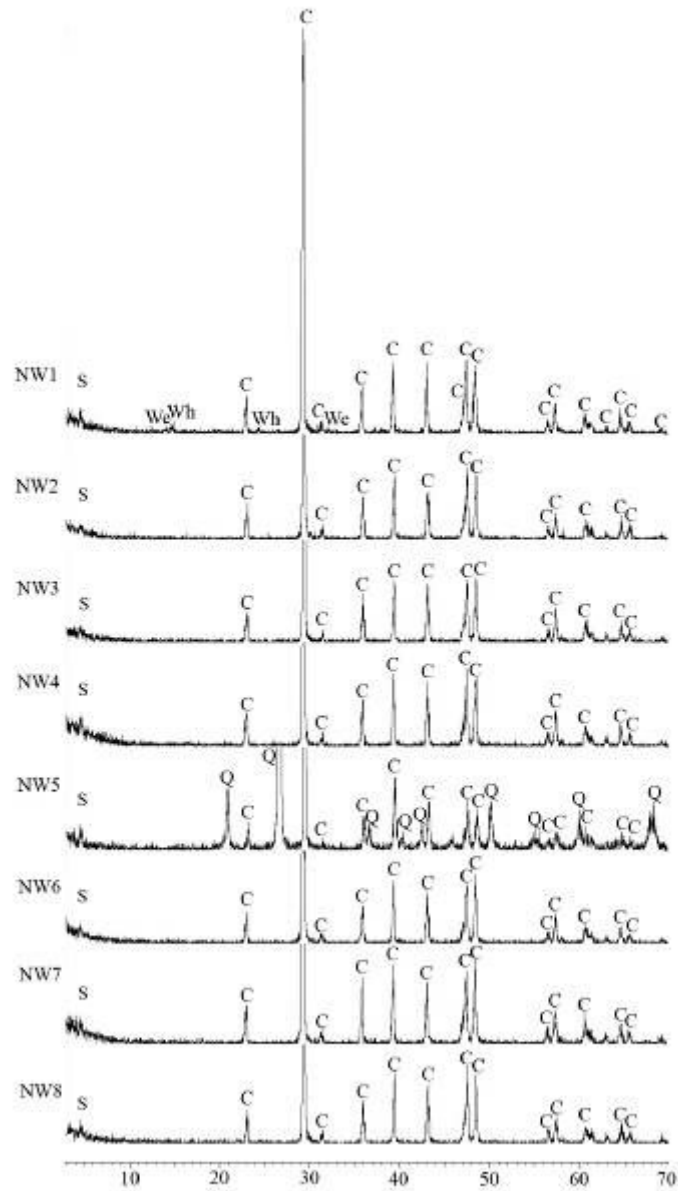


Figure 3.27 XRD traces of limestone samples from the statues on the West Terrace. C: Calcite, S: Smectite, We: Weddellite, Wh: Whewellite, Q: Quartz

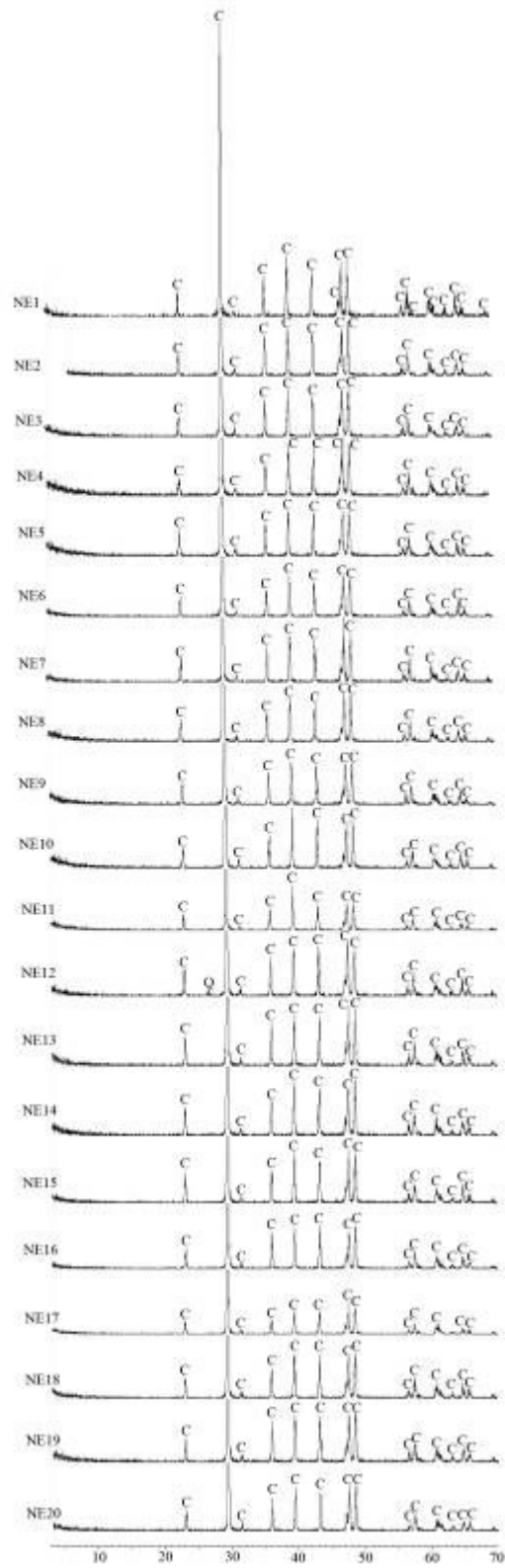


Figure 3.28 XRD traces (CuK α) of limestone samples from the statues on the East Terrace. C: Calcite, Q: Quartz.

3.4.2. Directly taken XRD traces of crack surfaces and exterior surfaces

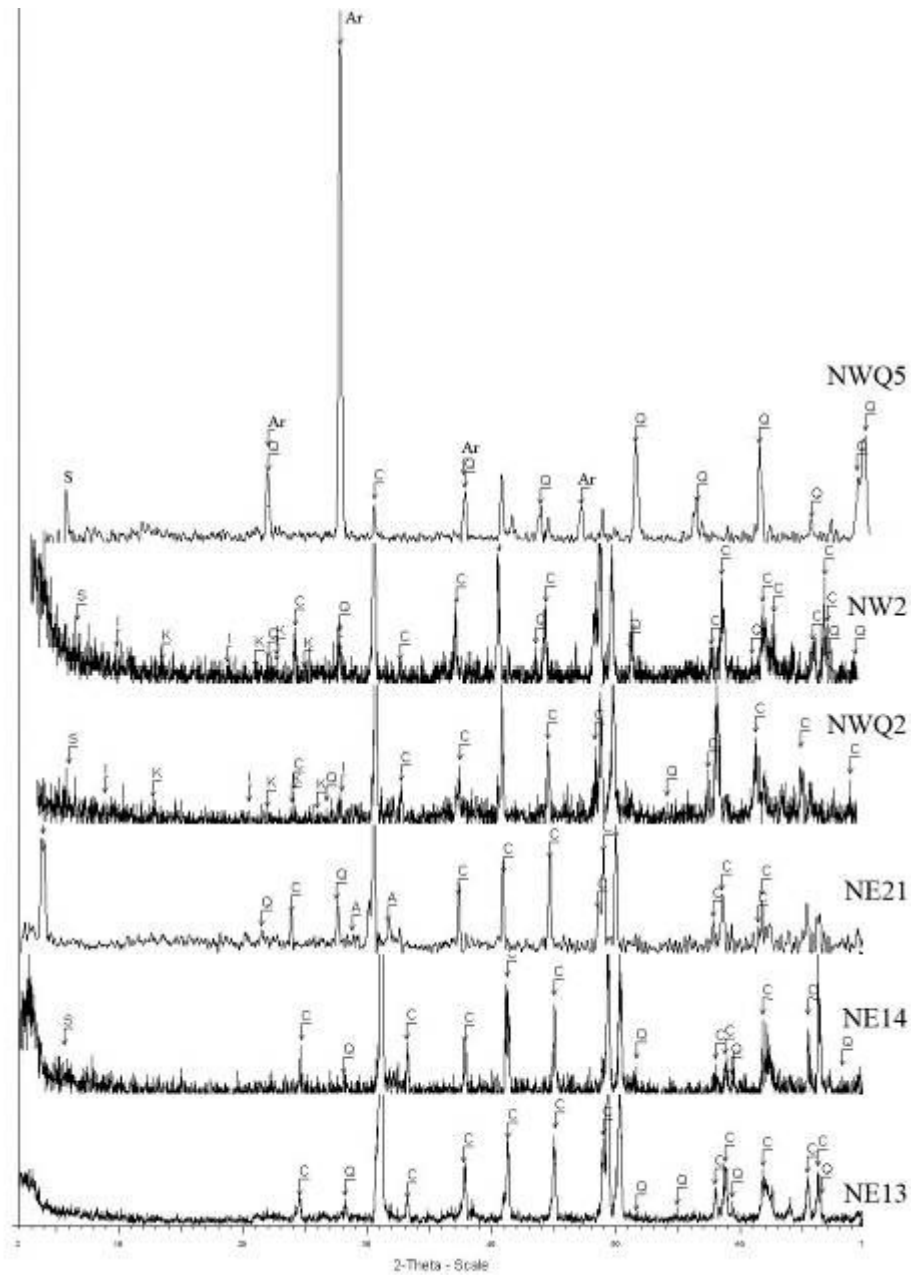


Figure 3.29 Directly taken XRD traces (CuK α) from crack surfaces. C: Calcite, Q: Quartz, A: Aragonite, K: Kaolinite, I: Illite, A: Albite, S: Smectite group.

Directly taken XRD traces from crack surfaces have revealed some information on the presence of aragonite as recrystallization product in the crack surface together with calcite and quartz. The presence of clay minerals, kaolinite, illite and smectite were also detected in those crack surfaces (Fig.3.29).

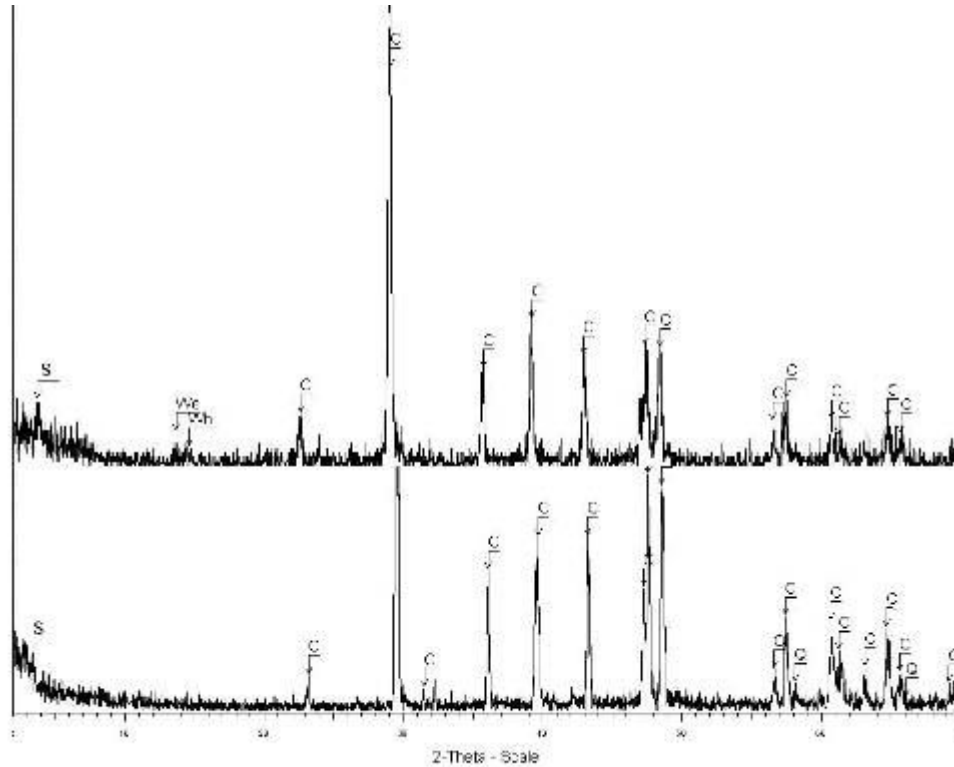


Figure 3.30 Directly taken XRD traces (CuK α) of exterior surfaces. C: Calcite, Q: Quartz, S: Smectite group, Wh: Whewellite, We: Weddellite.

Directly taken XRD traces from exposed surfaces of limestones have shown the presence of biominerals weddellite and whewellite and some smectite group clay mineral together with the main component calcite (Fig. 3.30).

3.4.3. XRD traces of powdered samples scraped from crack surfaces

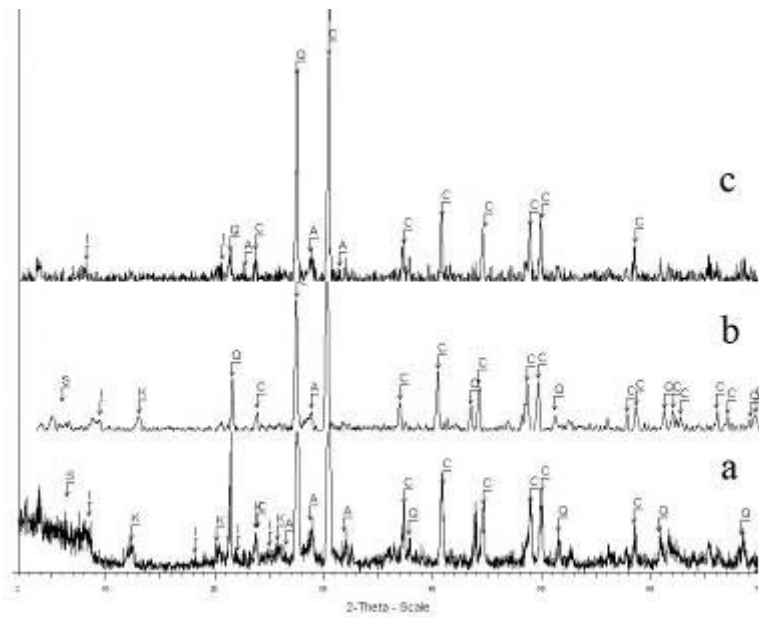


Figure 3.31 XRD traces (CuK α) of crack surface of sample NE16, (a: oriented, b: glycolated, c: heated to 350°C). C: Calcite, Q: Quartz, K: Kaolinite, I: Illite, A: Albite, S: Smectite group.

XRD traces of oriented samples scraped from crack surfaces of limestone breakouts have shown the presence of clay minerals of kaolinite, illite and smectite group together with the main mineral component of limestones that was calcite with some minor quartz and feldspar (albite) (Fig.3.31-3.34).

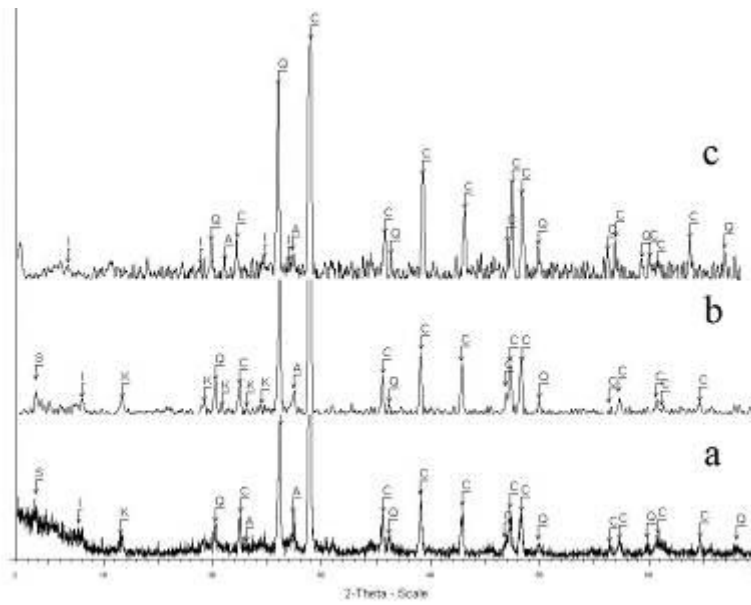


Figure 3.32 XRD traces (CuK α) of crack surface of sample NE21 , (a: oriented, b: glycolated, c: heated to 350°C). C: Calcite, Q: Quartz, K: Kaolinite, I: Illite, A: Albite, S: Smectite group.

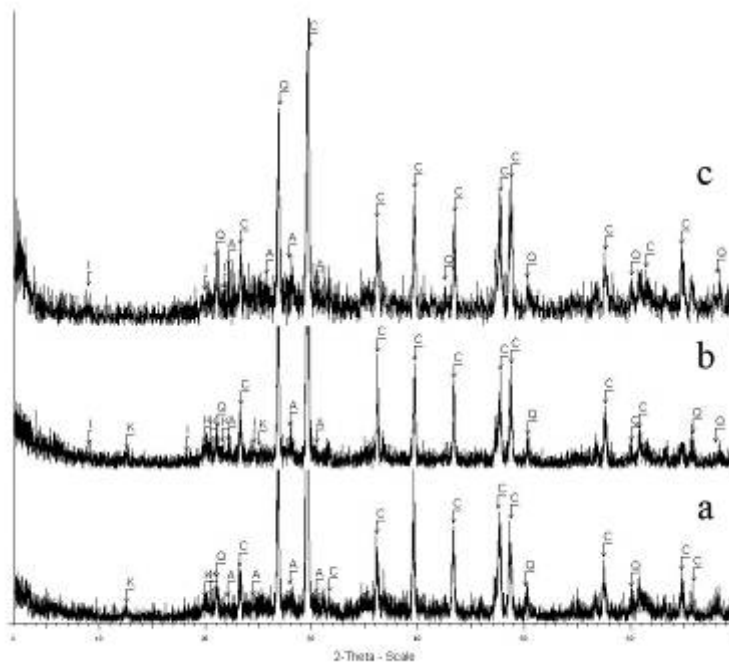


Figure 3.33 XRD traces (CuK α) of crack surface of sample NW5 , (a: oriented, b: glycolated, c: heated to 350°C). C: Calcite, Q: Quartz, K: Kaolinite, I: Illite, A: Albite, S: Smectite group.

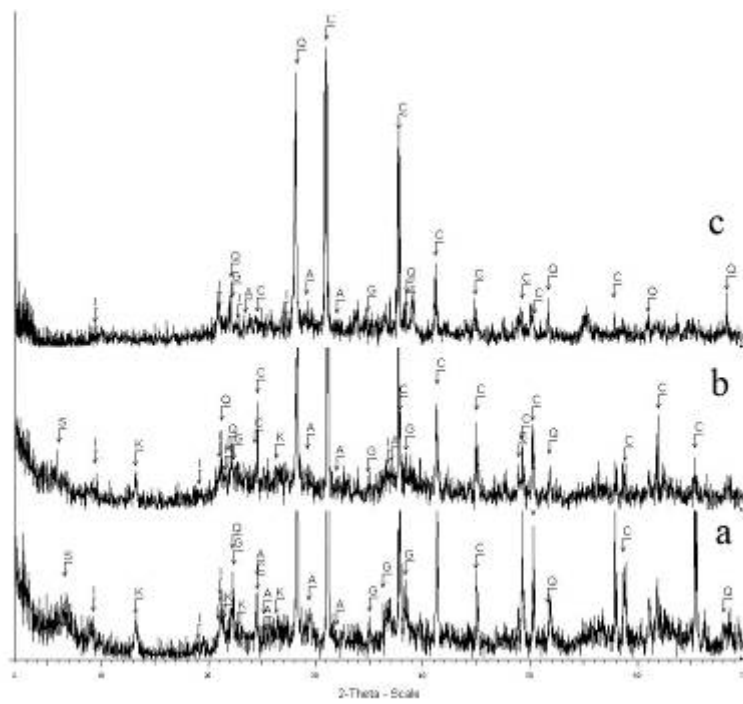


Figure 3.34 XRD traces ($\text{CuK}\alpha$) of crack surface of sample NWQ6 , (a: oriented, b: glycolated, c: heated to 350°C). C: Calcite, Q: Quartz, K: Kaolinite, I: Illite, A: Albite, S: Smectite group.

3.4.4. XRD traces of acid treated samples from crack surfaces

There were some minor minerals in the structure of Nemrut limestone other than calcite. For better determination of those minor minerals, some limestone samples taken from the lower parts of Nemrut Dağ were treated with 5% HCl to dissolve the major component calcite.

3.4.4.1. Determination of acid insoluble percentage

The percentages of those minor minerals were calculated weighing the sample before and after 5% HCl treatment and washing free of HCl. It was found that limestones had ~4% acid insoluble part by weight (Table 3.2).

Table 3.2 Percentage of acid insoluble parts of the unweathered Nemrut Dağ Monument Limestones.

Sample	Initial Mass of the sample (g)	Acid insoluble part of sample(g)	Percentage of acid insoluble part (%)
N1	271.62	8.75	3.22
N2	340.10	12.55	3.69
N3	263.43	10.88	4.13

3.4.4.2. XRD traces of acid insoluble parts of the unweathered Nemrut Dağ limestones

XRD traces of acid insoluble parts of those unweathered Nemrut Dağ limestones have shown the presence of kaolinite, illite and smectite group clay minerals with some quartz and albite (Figs. 3.35-3.36).

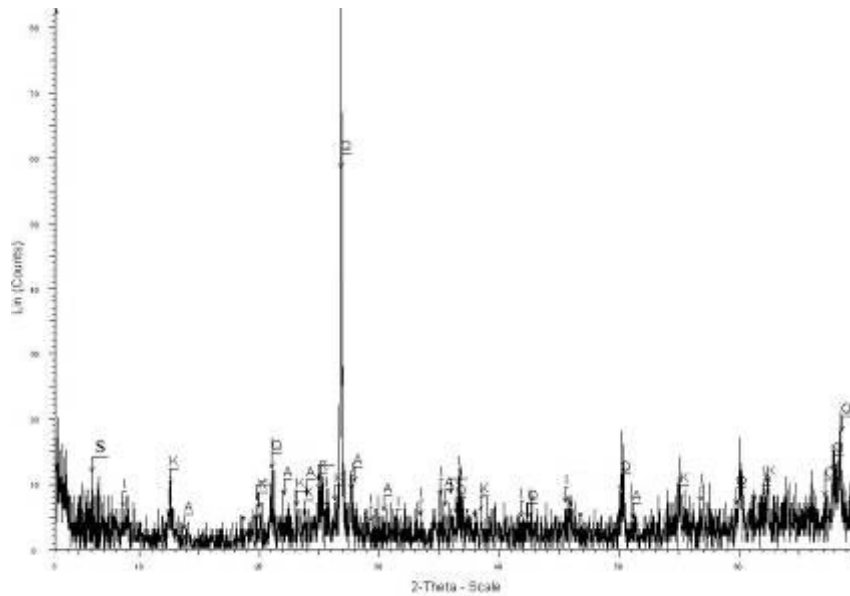


Figure 3.35 XRD traces (CuK α) of acid insoluble part of Nemrut Dağ Limestone, oriented state, Q: Quartz, K: Kaolinite, I: Illite, A: Albite, S: Smectite group.

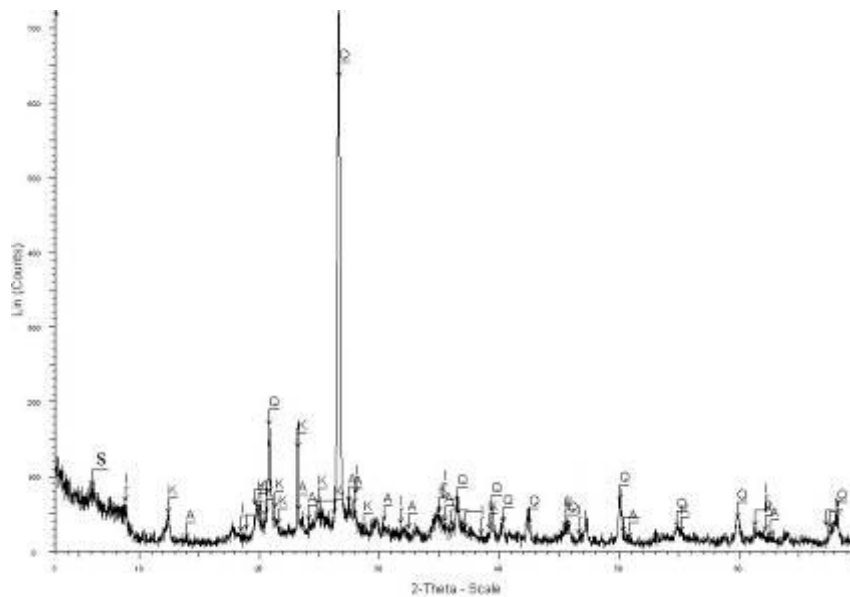


Figure 3.36 XRD traces (CuK α) of acid insoluble part of Nemrut Dağ Limestone, glycolated state, Q: Quartz, K: Kaolinite, I: Illite, A: Albite, S: Smectite group.

XRD Results of samples scraped from crack surfaces of limestones taken from east and west terraces and the west quarry after acid treatment

The XRD trace of acid insoluble crack surface material in oriented and ethylene glycolated and heated states revealed that clay components were kaolinite, illite and smectite group clays together with quartz, albite and goethite minerals (Fig. 3.37). In XRD traces of ethylene glycolated sample, clay minerals were seen more clearly.

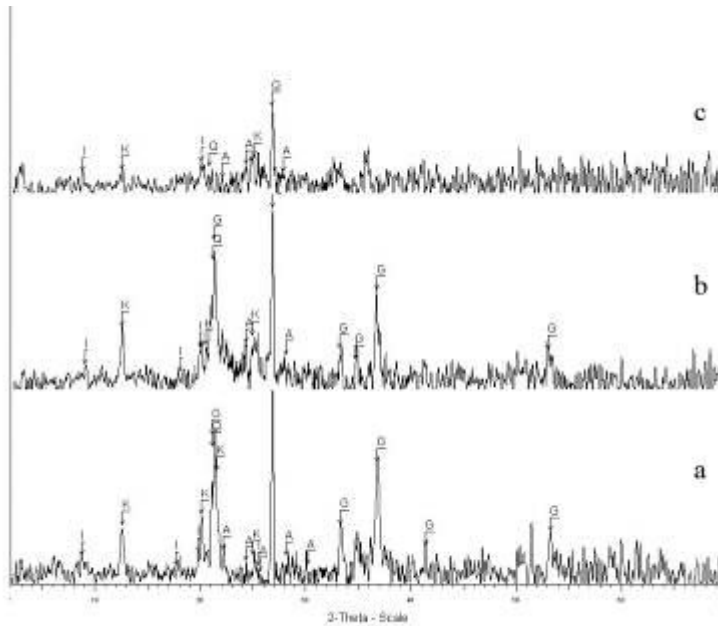


Figure 3.37 XRD traces (CuK α) of crack surface of sample NE13 after acid treatment, (a: oriented, b: glycolated, c: heated to 350°C). C: Calcite, Q: Quartz, K: Kaolinite, I: Illite, A: Albite, S: Smectite group, G: Goethite.

Goethite was detected in most of crack surfaces (Figs. 3.37, 3.38, 3.41, 3.42). However, some crack surfaces were free of goethite (Figs. 3.39- 3.40).

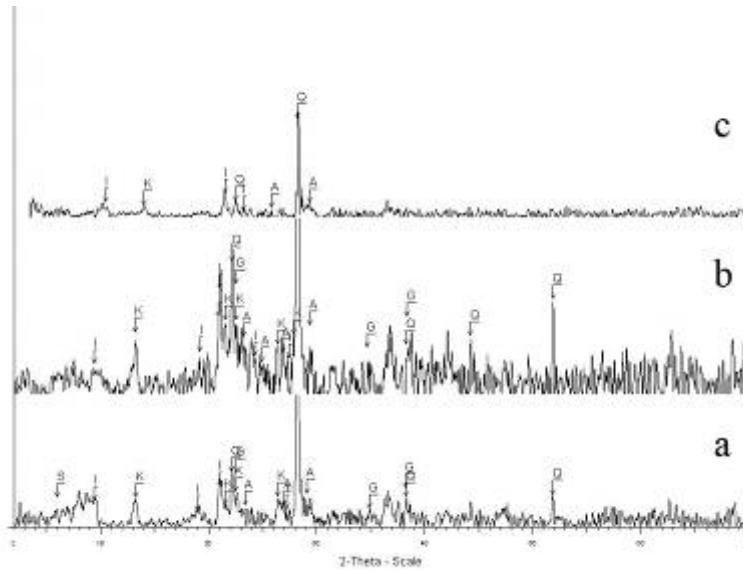


Figure 3.38 XRD traces ($\text{CuK}\alpha$) of crack surface of sample NE17 after acid treatment, (a: oriented, b: glycolated, c: heated to 350°C). C: Calcite, Q: Quartz, K: Kaolinite, I: Illite, A: Albite, S: Smectite group, G: Goethite.

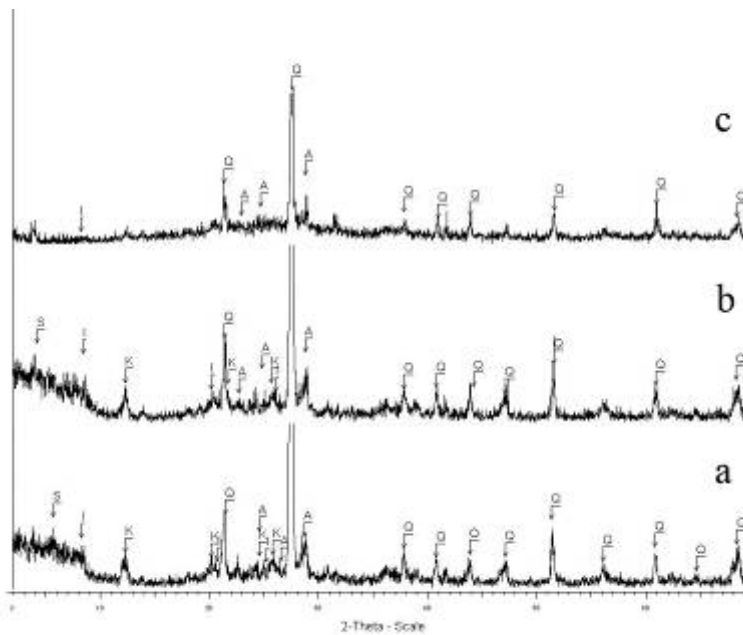


Figure 3.39 XRD traces ($\text{CuK}\alpha$) of crack surface of sample NE21 after acid treatment, (a: oriented, b: glycolated, c: heated to 550°C). C: Calcite, Q: Quartz, K: Kaolinite, I: Illite, A: Albite, S: Smectite group.

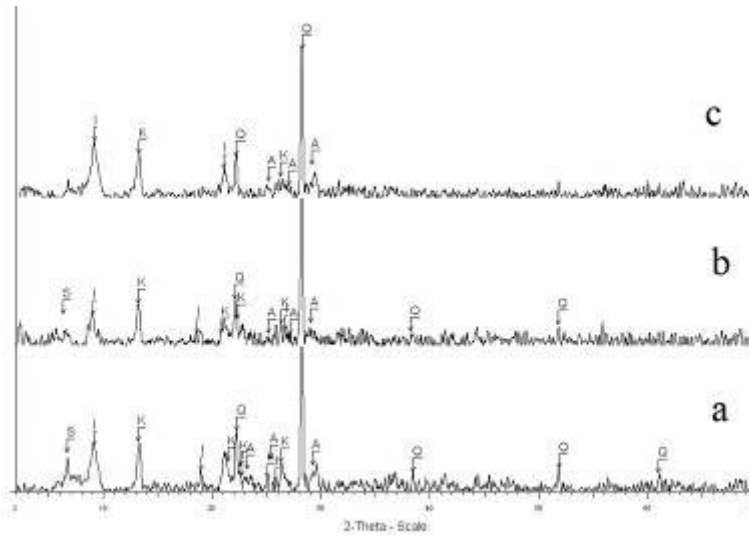


Figure 3.40 XRD traces (CuK α) of crack surface of sample NW7 after acid treatment, (a: oriented, b: glycolated, c: heated to 350°C). C: Calcite, Q: Quartz, K: Kaolinite, I: Illite, A: Albite, S: Smectite group.

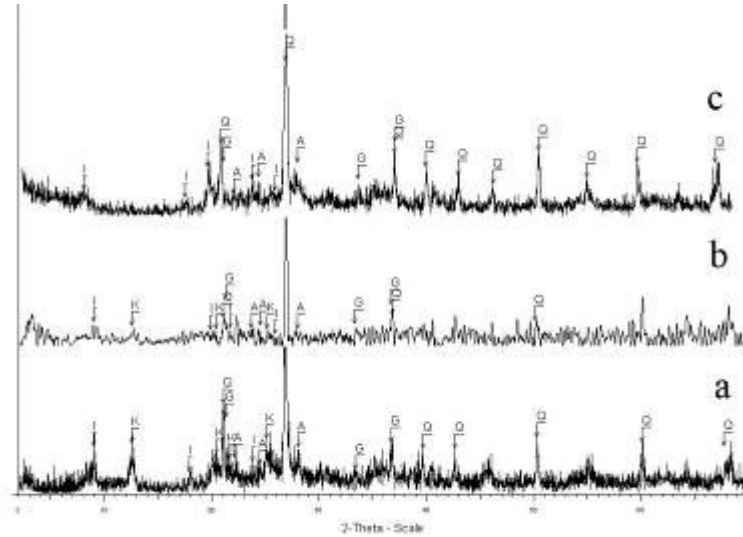


Figure 3.41 XRD traces (CuK α) of crack surface of sample NWQ6 after acid treatment, (a: oriented, b: glycolated, c: heated to 550°C). C: Calcite, Q: Quartz, K: Kaolinite, I: Illite, A: Albite, S: Smectite group.

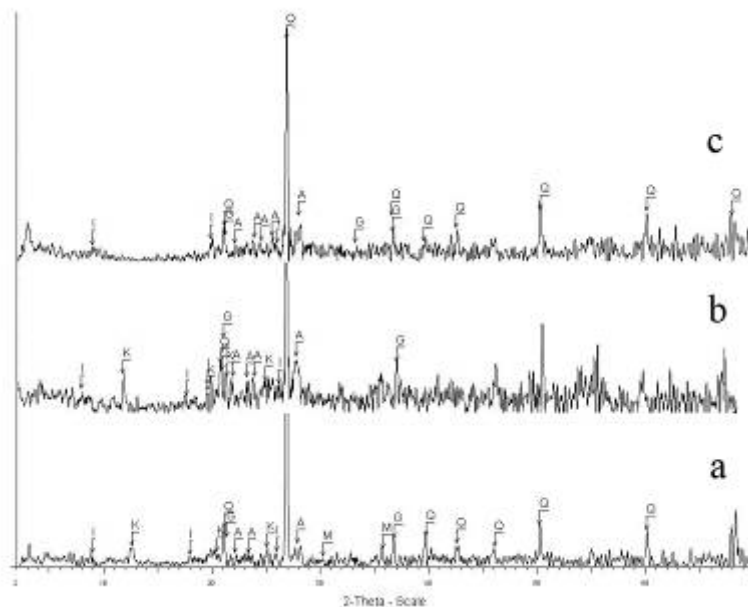


Figure 3.42 XRD traces (CuK α) of surface soil around the monument after acid treatment, (a: oriented, b: glycolated, c: heated to 550°C). C: Calcite, Q: Quartz, K: Kaolinite, I: Illite, A: Albite, S: Smectite group, G: Goethite, M: Maghemite.

The surface soil around the monument was also analyzed for its clay content and iron oxide. The surface soil was treated with 2% HCl, washed, air dried and analyzed by XRD (Fig. 3.42).

Quartz, kaolinite, illite, albite and goethite minerals were detected by XRD analysis of surface soil around the monument (Fig. 3.42).

To determine the iron oxide minerals more clearly, iron oxides were separated magnetically from the surface soil. Maghemite was detected in the XRD traces. No goethite was found in magnetically separated part of the soil (Fig. 3.43).

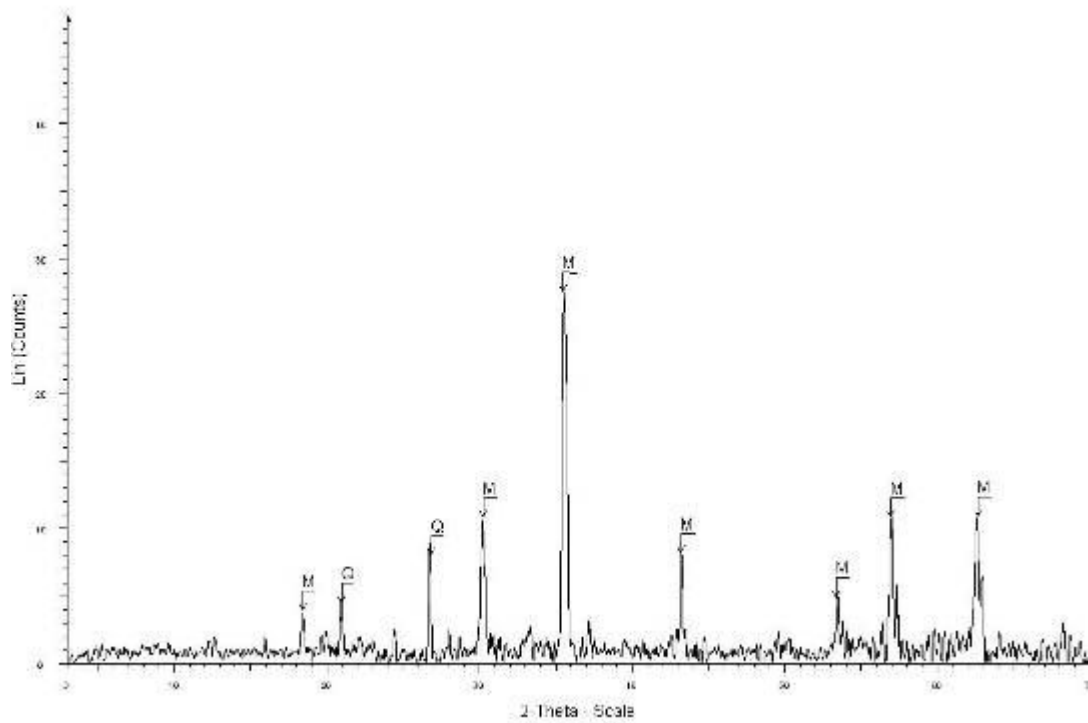


Figure 3.43 XRD traces (CuK α) of magnetically separated part of the surface soil around the monument , M: Maghemite, Q: Quartz.

3.5. FTIR Analyses of Weathered Zones and Clays

Some samples that were examined by XRD were also examined with FTIR. The FTIR spectra of surface soil around the statues and the weathered limestone samples scraped from the surface of the crack were taken before and after 2% HCl treatment. Presence of kaolinite were detected in all samples by means of the presence peaks in 3697cm^{-1} and 3620cm^{-1} . Although FTIR was good to reveal the kaolinite peaks clearly in samples before and after acid treatment, it was not so good to identify the other types of clay minerals (Fig. 3.44).

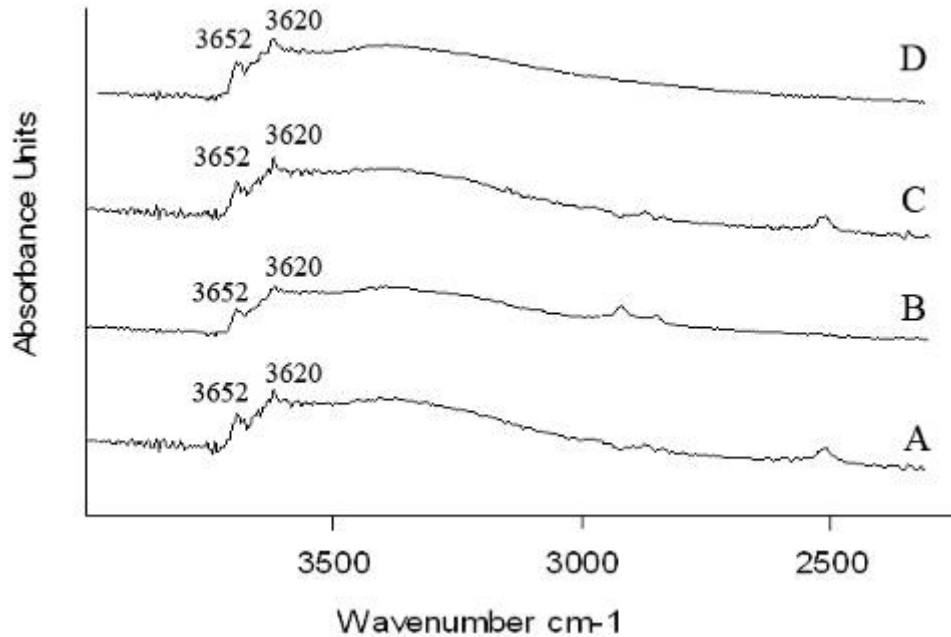


Figure 3.44 Infrared spectra of the sample scraped from the surface of the crack (B) and surface soil around the monument (C) after 2% HCl treatment.

A: surface soil around the monument before acid treatment

B: surface soil around the monument after acid treatment

C: sample scraped from the surface of the crack before acid treatment

D: sample scraped from the surface of the crack after acid treatment

3.6. Scanning Electron Microscope-EDX Results

SEM analyses of Nemrut limestones were done at the relatively unweathered interior parts of limestones and at their weathering zones such as interior cracks and exposed surfaces.

Cross sections were examined to follow the morphological changes at the exposed surfaces and in the cracks surfaces. EDX analyses of the same cross sections and their elemental maps were performed to see the compositional changes and the distribution of clay minerals and iron oxides in the microstructure (Figs. 3.45-3.47).

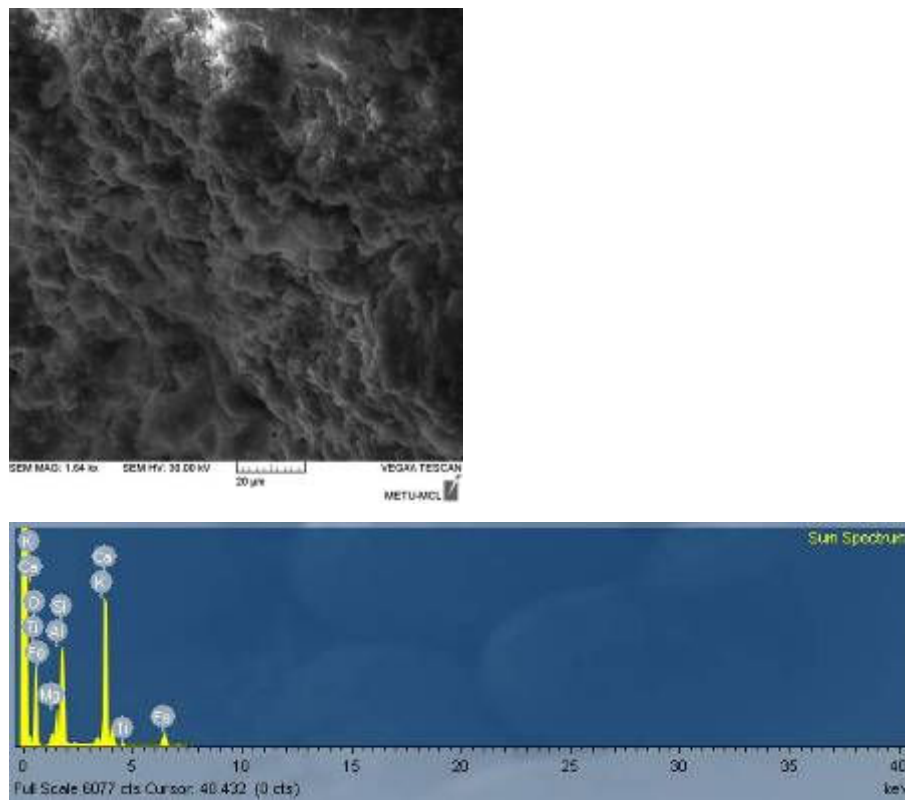


Figure 3.45 SEM view (scale: 20μ) and EDX spectrum of a crack surface of Nemrut Quarry sample.

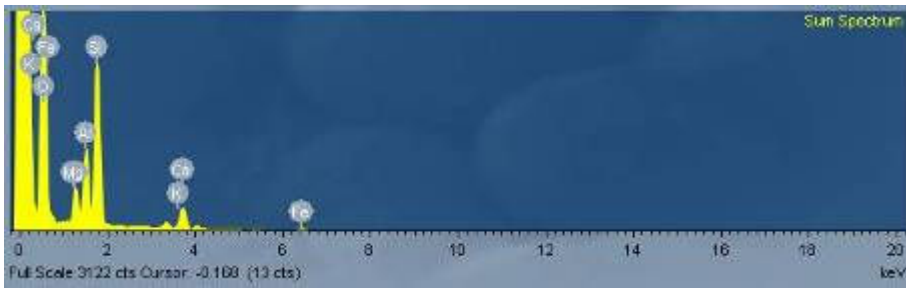
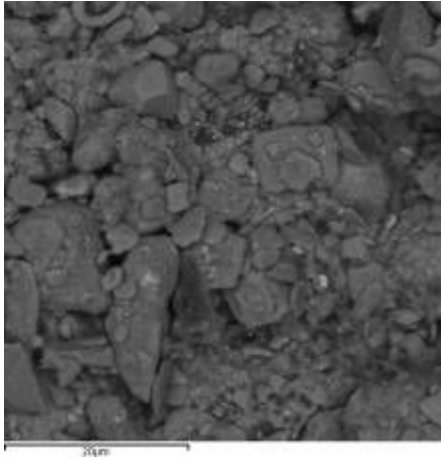


Figure 3.46 SEM image of a crack surface covered with clay minerals and EDX spectrum

EDX analysis of a crack surface from Nemrut quarry sample have indicated the presence of calcite (Ca), iron oxides (Fe) and clay minerals (Si, Al, Mg) at the surface (Figs.3.45-46).

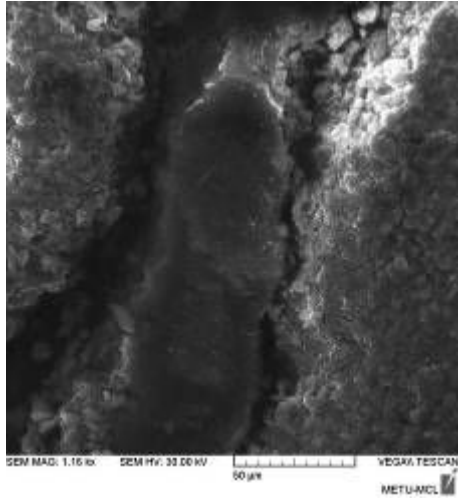


Figure 3.47 SEM view of a karstic vein of Nemrut Quarry limestone (scale: 50 μ).

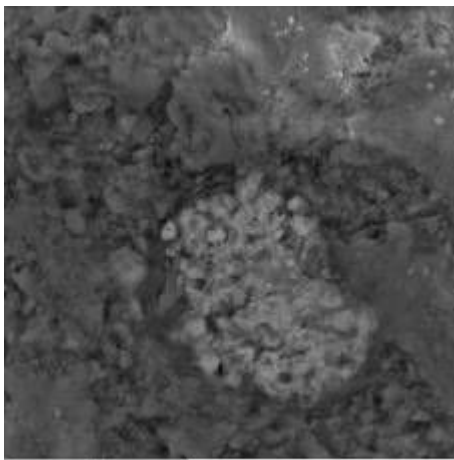


Figure 3.48 A SEM view from iron rich region at the exterior surface of the Nemrut Quarry limestone (scale:40 μ)

SEM view of a karstic vein showed the thickness and separation of karstic infill from the rest of the limestone. Presence of areas rich in iron oxides that were composed of fine grains were detected on the exposed surfaces of limestone (Fig. 3.48).

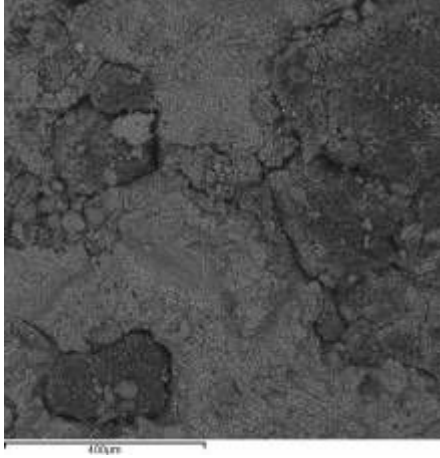


Figure 3.49 SEM image of pits at the exposed surfaces have shown the presence of biological growth in those pits and their separation from the rest of the stone by fine cracks.

3.6. EDX Analyses of Clays and Iron Oxides

The crack zones of Nemrut Quarry limestone samples were analyzed by SEM-EDX. The views of those cracks were observed in thin sections by optical microscope have shown the presence of opaque minerals and yellow brown iron oxides in those cracks (Fig. 3.50).

SEM EDX analyses, elemental mapping of those cracks have verified the presence of clay minerals in those cracks together with iron oxides (Figs. 3.51-52).

Distribution of silicium and aluminum has clearly revealed the distribution of clay minerals in the crack. Iron distribution coincided with clay minerals distribution verifying the copresence of iron oxides in the crack.

The elemental distribution maps of Fe, Ca, Si and Al indicated that the clay minerals and iron oxides were mostly located in the crack zones (Figure 3.51-52).

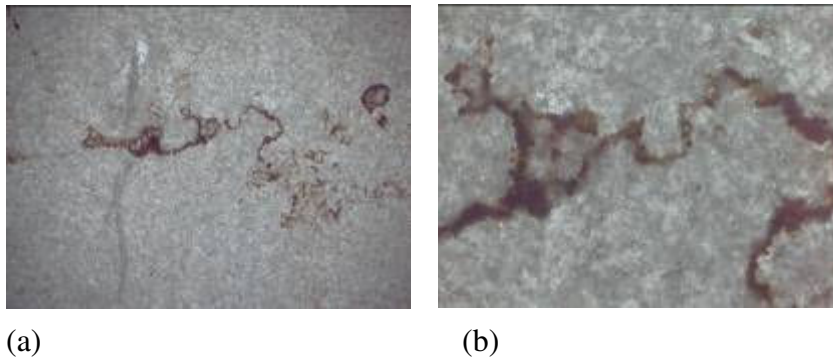


Figure 3.50 Nemrut Quarry Limestone: A view of thin section in optical microscope (a) 2,5X cross nicols, (b) 10X cross nicols

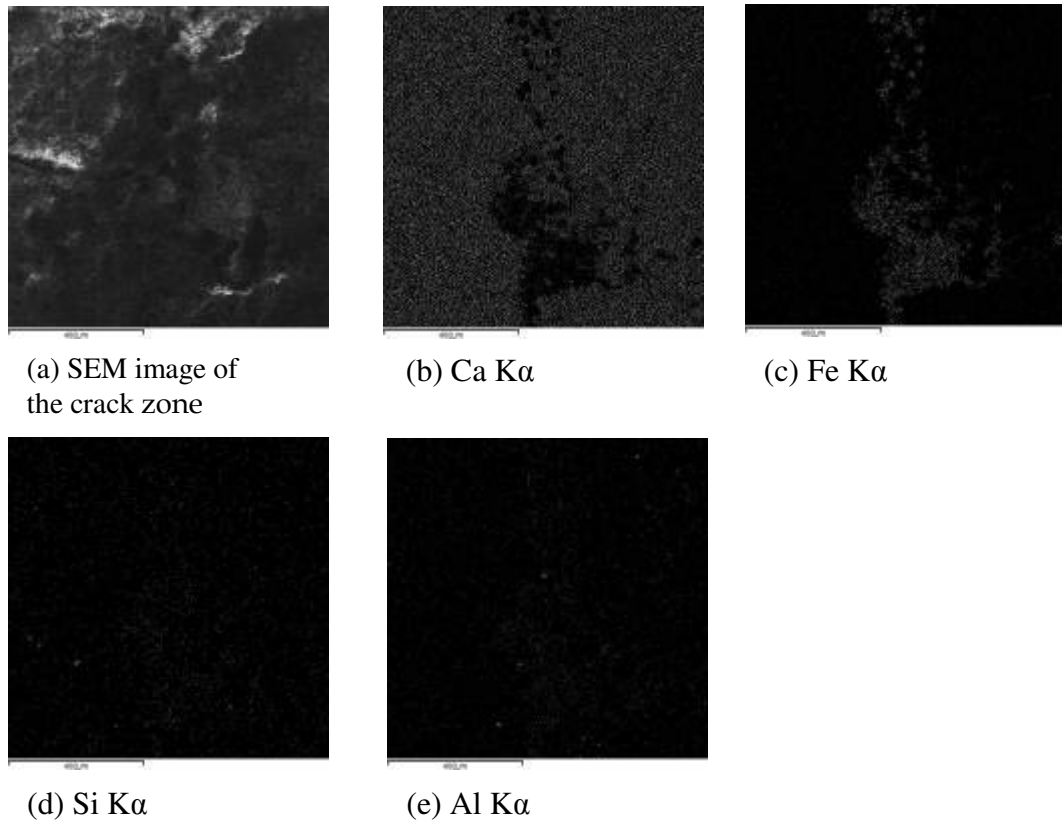


Figure 3.51 Nemrut Quarry Limestone: View of a crack the crack detail of Fig.3.51 (a) and distribution of Fe, Ca, Si and Al in the same region (scale: 400 microns)

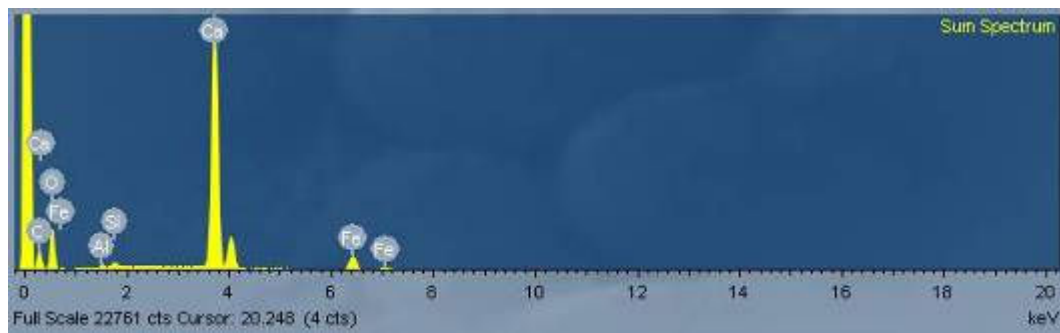


Figure 3.52 EDX spectrum of the whole area shown in Fig. 3.51 (a).

3.7. Experiments on the Preparation of Nanodispersive Calcium Hydroxide Solution for the Conservation Treatments

In this study several types of calcium hydroxide nanodispersive solutions were prepared and the concentrations of dispersed particles were determined by the EDTA titration before the success with an efficient one. The most efficient nanodispersive solution was prepared by putting 50 gr CaO in 25 water and 975 ml ethanol by magnetic stirring for 24 hours and 3 hours ultrasonic vibration of the solution. Aldrich calcium oxide nanopowder <160nm (BET) of %98 purity was used. 31 gr of Ca(OH)₂ nano particles remained suspended after 16 hours (Fig.3.53).

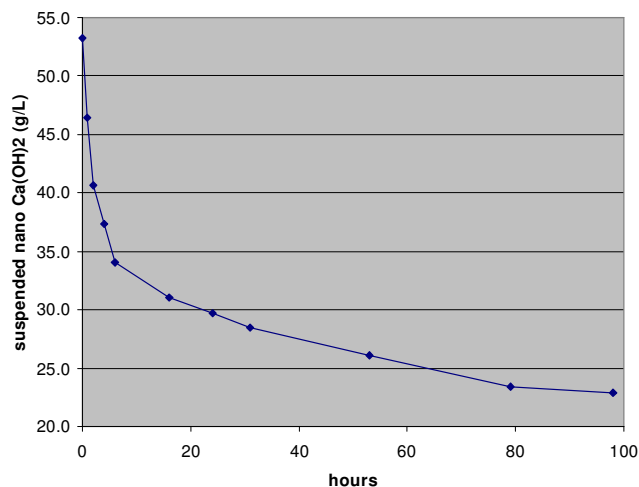


Figure 3.53 Stability of nanodispersive Ca(OH)₂ solution in time.

The particle sizes of the nanodispersed particles were measured by Malvern Nano ZS90 instrument. The average particle size was found to be in the range of 350-600nm (Fig. 3.54).

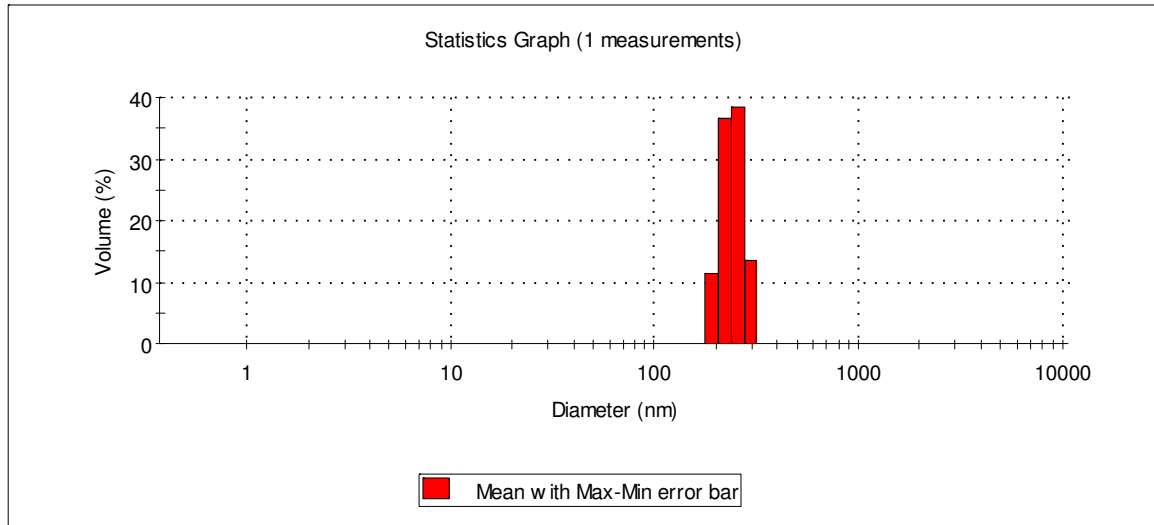


Figure 3.54 The particle size distribution of nanodispersive $\text{Ca}(\text{OH})_2$ solution.

3.8. Treatments of limestones with nanodispersive $\text{Ca}(\text{OH})_2$ solution

3.8.1. Treatment of limestone cracks and deteriorated surfaces with nanodispersive $\text{Ca}(\text{OH})_2$ solution

For detection of the penetration of the solution into the cracks of deteriorated limestone, a small concentration of Calceine which made the $\text{Ca}(\text{OH})_2$ fluorescent under ultraviolet light was added to the nanodispersive solution before the application. In that way, it was possible to follow the depth of impregnation of the nanodispersive solution and the locations of the newly formed calcite. The nanodispersive $\text{Ca}(\text{OH})_2$ solution was applied by dropping solution to the cracks and to the surface of the sample. Sections of samples were examined under the optical microscope with ultraviolet light. The thin section analyses revealed that nanodispersive solution went to the pores of the stone and distributed on the crack surface (Figs.3.58-3.63).

Deteriorated limestone samples from Nemrut Dağ monument and Pessinus marbles were treated in the laboratory and at several locations at the site with

nanodispersive Ca(OH)_2 solutions prepared in the laboratory. There was considerable increase in the Ultrasonic velocity of the samples after treatments. That showed the efficiency of the treatment indicating an increase in physicomechanical properties of limestone (Figs.3.55, 3.56, 3.57).



Figure 3.55 View of Nemrut limestone treated with nanodispersive Ca(OH)_2 solution

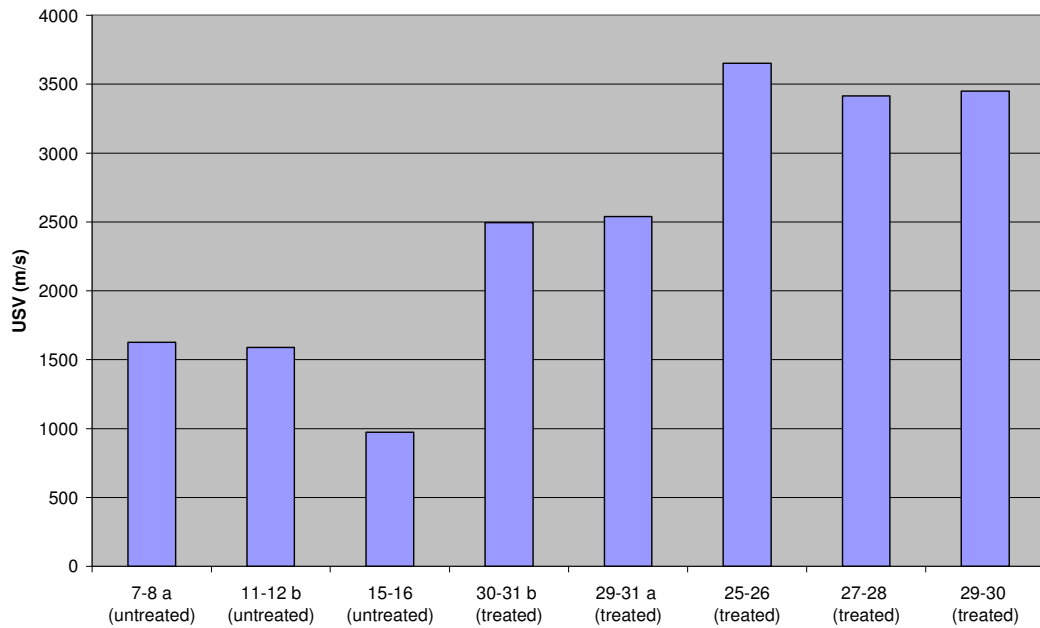


Figure 3.56 Ultrasonic velocity values of Nemrut Dağ limestone before and after treatment with nanodispersive Ca(OH)_2 solutions in the site.

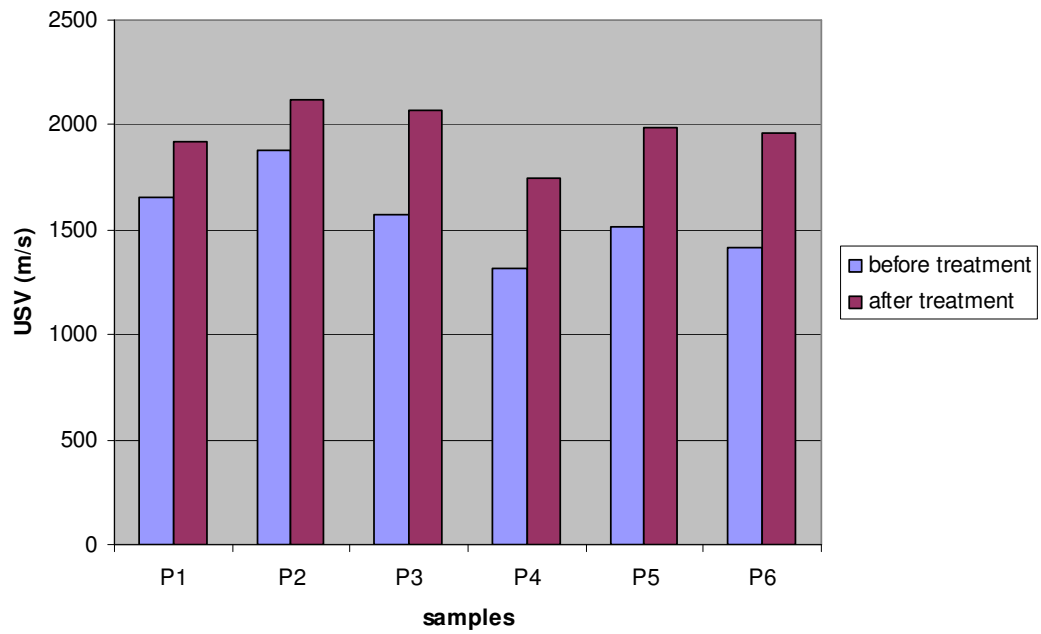


Figure 3.57 Ultrasonic velocity values of Pessinus marble samples before and after treatment with nanodispersive Ca(OH)_2 solutions in the laboratory

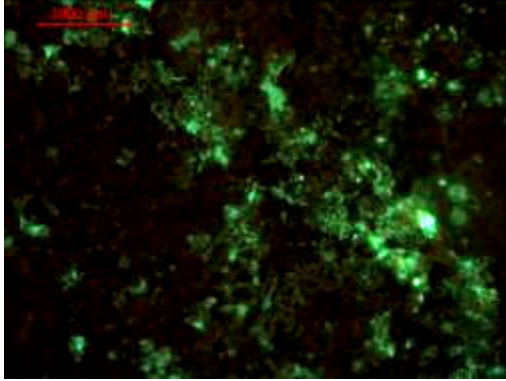


Figure 3.58 Crack surface of a Nemrut Quarry sample after treatment with fluorescent nanodispersive calcium hydroxide solution showing the distribution of the nanodispersive calcium hydroxide solution in the crack.

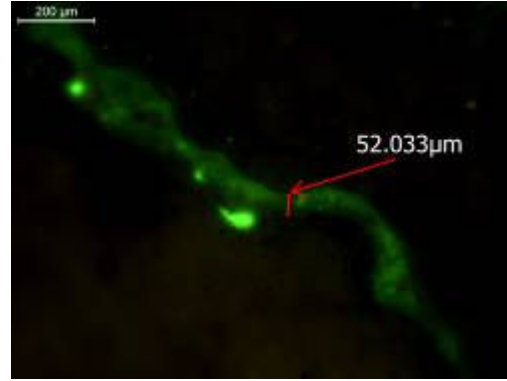


Figure 3.59 Cross section of a crack in Nemrut Quarry limestone showing penetration of nanodispersive solution of calcium hydroxide solution through crack.

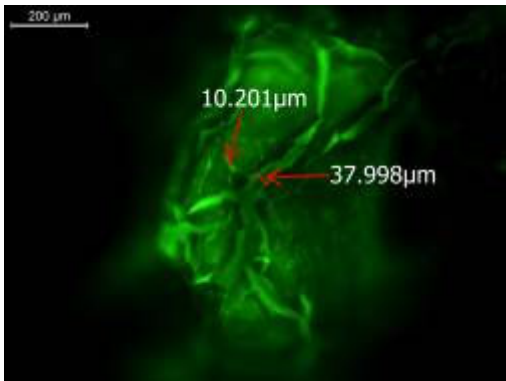


Figure 3.60 Crack surface of a Pessinus ancient quarry sample treated with fluorescent nanodispersive calcium hydroxide solution showing the distribution of the nanodispersive calcium hydroxide solution in the crack.

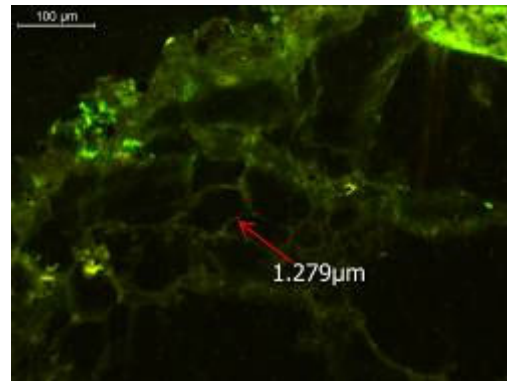


Figure 3.61 Thin section view of Pessinus ancient quarry showing penetration of nanodispersive solution of calcium hydroxide solution through the fine intergranular cracks.

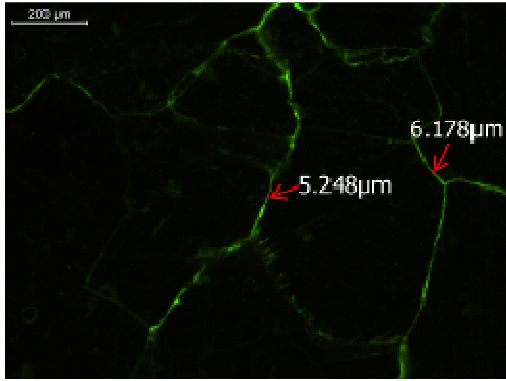


Figure 3.62 Thin section view of a Pessinus ancient quarry marble sample treated with fluorescent nanodispersive calcium hydroxide solution showing its distribution through the fine cracks.

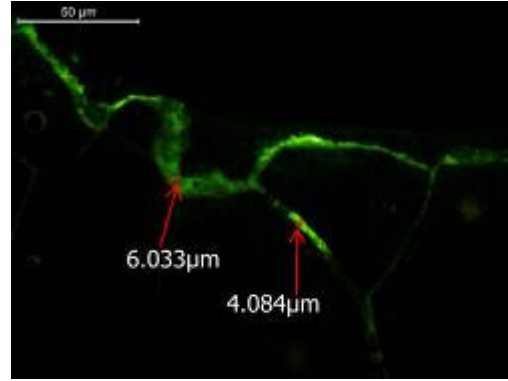


Figure 3.63 Thin section view of a crack of a Nemrut limestone showing penetration of nanodispersive solution of calcium hydroxide solution through the fine cracks.

3.8.2. Treatment of acid insoluble constituents of limestones containing clay minerals

In this study, it was aimed to measure the swelling property of clay minerals in the cracks of limestone and their reduction by treatment nanodispersive calcium hydroxide solution. For that purpose, crack surfaces of weathered limestones were scraped off and treated with 2% HCl to dissolve calcite. Insoluble parts were washed free of HCl. CEC of those insoluble parts were measured with methylene blue test before and after treatment with nanodispersive calcium hydroxide solution.

Methylene blue tests showed that the methylene blue absorption of the acid insoluble parts of Nemrut Dağ limestone samples decreased with treatment of nanodispersive calcium hydroxide (Table 3.4). Decrease in the methylene blue absorption was due to the decrease in the cation exchange capacity of clays which also imply that swelling ability of clays were considerable reduced.

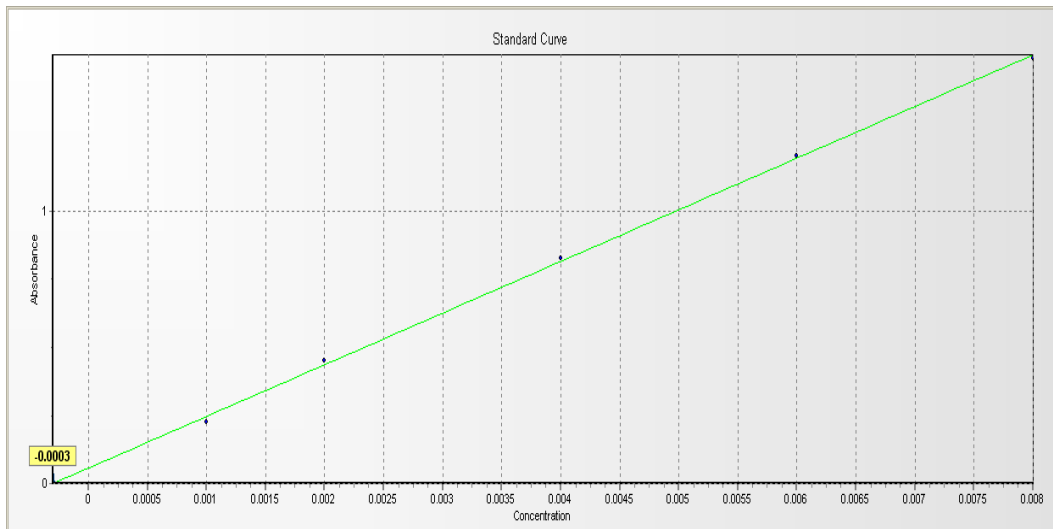


Figure 3.64 Calibration curve of methylene blue for the concentration range of 1mg/L to 8mg/L.

Table 3.4 Decrease of methylene blue absorption in acid insoluble constituents of interior cracks with treatment of nanodispersive calcium hydroxide solution

Sample Name	Wavelength (nm)	Concentration (mg/ml)	CEC (meq/100 g)
Blank	663	0,000	-
Methylene Blue Solution	663	0,008	-
NA untreated	663	0,003	5,35
NA treated	663	0,005	3,21
NE16 untreated	663	0,002	2,04
NE16 treated	663	0,005	1,07
NW5 untreated	663	0,003	0,93
NW5 treated	663	0,007	0,19

3.9. Carbonation of nanodispersive Ca(OH)₂ solution

It was necessary to increase the carbonation efficiency of nanodispersive Ca(OH)₂ solution in treated limestones.

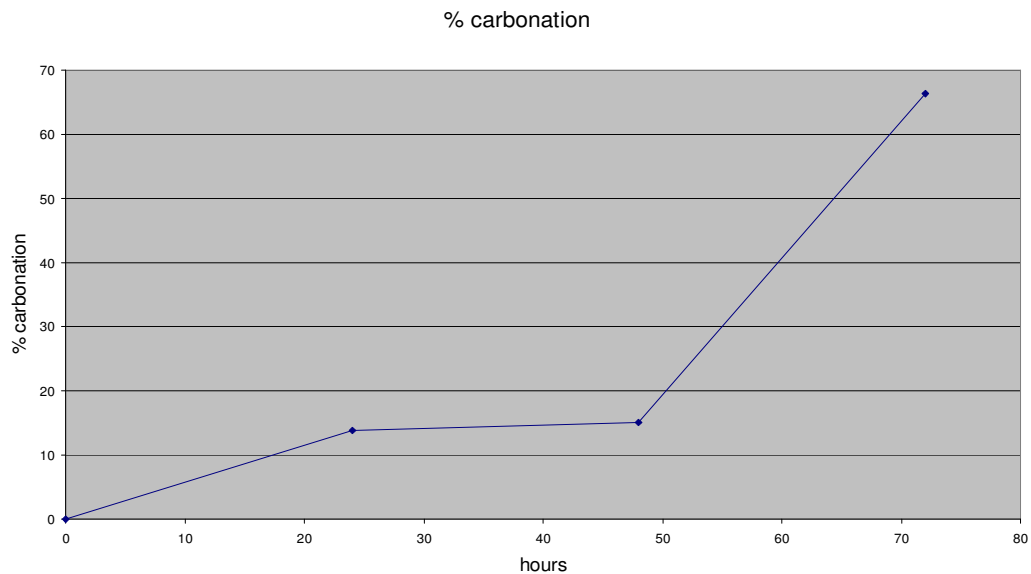


Figure 3.65 Carbonation of Nanodispersive Ca(OH)₂ solution

Carbonation of Nanodispersive Ca(OH)₂ solution in an atmosphere enriched with CO₂ (5%) and at high relative humidity was found to be about 66% at the end of the 72 hours (Fig. 3.65). High relative humidity conditions and an atmosphere

enriched with CO₂ were necessary during the treatments of deteriorated limestones to obtain its efficient carbonation to calcite.

Carbonation percent was followed by EDTA titration as described in section 2.4.8.

Use of sodium stearate in nanodispersive Ca(OH)₂ solution

For good consolidation action of carbonation, it was necessary to have good contact with the substrate limestone and the newly formed calcite grains. That aspect of the carbonation was studied in more detail by using additive sodium stearate in the nanodispersive Ca(OH)₂ solution and under an atmosphere rich in CO₂ (5-20%) and RH being 75-80% (Ukrainczyk et. al., 2009). 0.025 g of sodium stearate was added to 1000 ml nanodispersive calcium hydroxide solution to investigate its effect on calcite formation. The formation of calcite crystals with and without sodium stearate and their texture were investigated by SEM-EDX.

The addition of sodium stearate did not change the shape of calcite crystals but the sizes of the precipitated calcite crystals were increased (Fig.3.67-68) and facilitated good bonding in cracks. Increase of calcite crystal size with the addition of sodium stearate was in agreement with the studies of Ukrainczyk et. al. (2009).

Addition of sodium stearate in low concentrations (0.025 g/l) to the nanodispersive calcium hydroxide solution did not affect the stability of nanodispersive solution as seen in Fig.3.66.

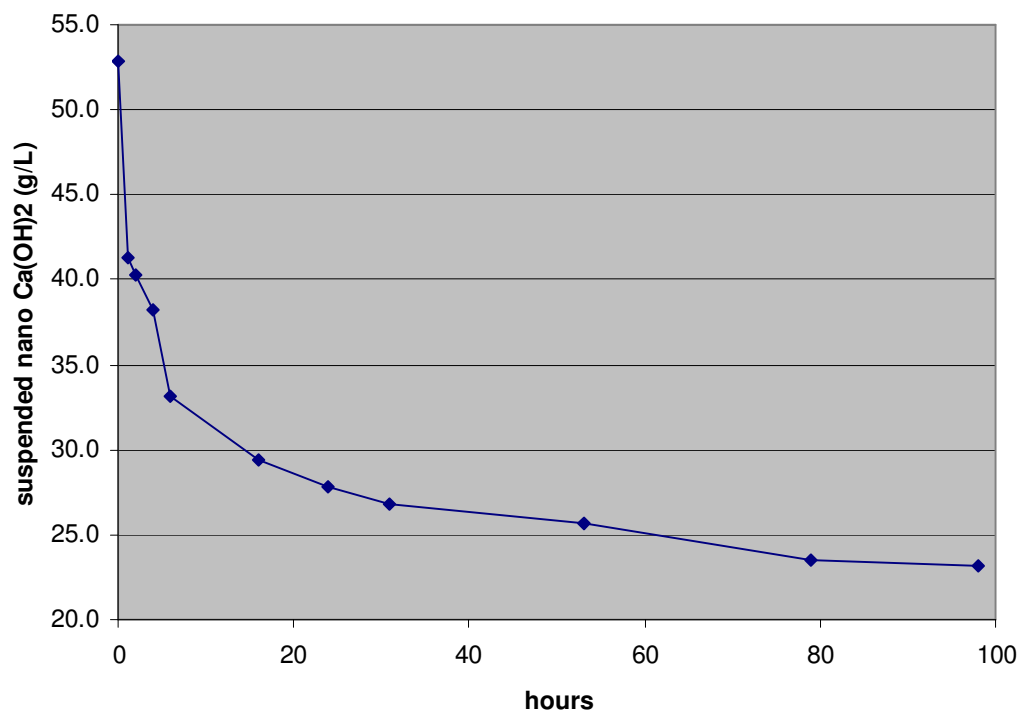


Figure 3.66 Suspended nano Ca(OH)_2 particles (g/L) in time in the sodium stearate added nano calcium hydroxide solution.

It was observed that addition of sodium stearate did not affect the concentration of suspended calcium hydroxide nano particles during the 98 hours of follow up (Fig. 3.66).

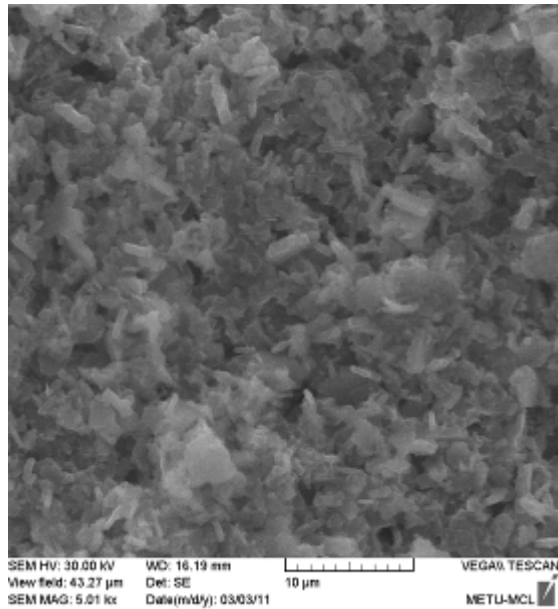


Figure 3.67 SEM view of crystals carbonated from nanodispersive calcium hydroxide solution without any additives.

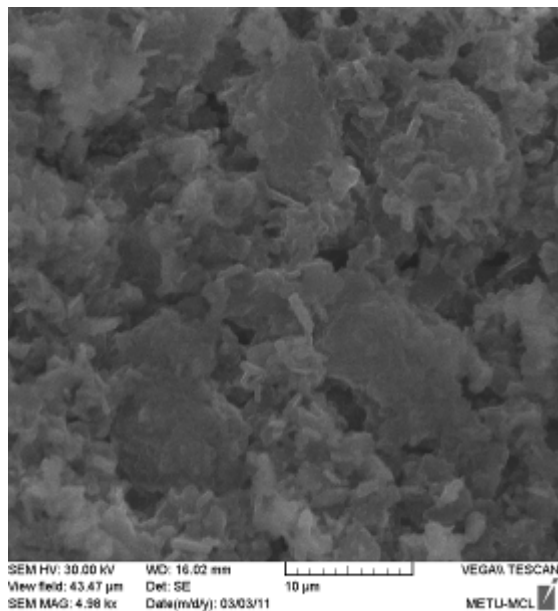


Figure 3.68 SEM view of bigger size crystal agglomerates carbonated from nanodispersive calcium hydroxide solution with sodium stearate (0.025 g/L).

CHAPTER 4

DISCUSSIONS AND CONCLUSIONS

This study has attempted to make a contribution to historic limestone conservation in two main fields. Firstly, by determination of the important weathering mechanisms of limestone and secondly by the development of its conservation treatments using nanodispersive calcium hydroxide solutions. Limestone samples of Nemrut Dağ Monument were used during those studies, since they exhibited advanced state of limestone deterioration that has developed in 2000 years.

Experimental results were evaluated and discussed in the following section under the titles of weathering of limestones and conservation of limestones with nanodispersive $\text{Ca}(\text{OH})_2$ solutions.

4.1. Weathering of Limestone

Weathering of limestone involves important dissolution and precipitation reactions of calcium carbonate together with the roles of clay minerals, iron oxides and biological activity affecting them.

Weathering Forms

Abundant decay forms at the Nemrut Dağ Monument were color change and biological depositions, material loss by fragmental disintegration through the karstic zones and/or the cracks, as well as the detachments with fragmental

disintegration. Other decay forms that were often seen were pitting and dissolution of limestone through the karstic veins (see section 3.1).

Dissolution and precipitation reactions of calcite

The petrographical analysis of limestones indicated that the limestones had micritic and microsparitic particles and they were bonded with sparitic calcite crystals. Karstic veins of limestones contained sparitic calcite crystals and often larger ones. The preferential dissolution through karstic veins that reached the exterior surface was common in limestones (Figs. 3.14-3.26). Normally, dissolution of micritic calcite in limestone matrix was expected to start instead of dissolution in bigger calcite grains in the karstic veins. However preferential dissolution of bigger crystals of calcite in the karstic veins in comparison to the micritic calcite and microsparitic calcite of the limestone matrix was observed. That must be due to the large amounts of surface dislocations (kinks, pits, holes etc.) of those calcite crystals in karstic veins (Morse and Arvidson, 2002).

The dissolution and precipitation reactions of calcite were considered to proceed through surface reaction controlled kinetics at a large pH range being 4-14. Precipitation of calcite, sometimes aragonite (Fig.3.29) and biominerals of weddellite and whewellite were another phenomena observed at the crack surfaces (Fig.3.27). Weddellite and whewellite were also found at exposed surfaces of limestone. Lichens as well as clay minerals must have contributed to the precipitation of calcite, aragonite and biominerals of weddellite and whewellite. Clay minerals must be acting as sites of nucleation and crystal growth during wetting and drying cycles of weathering (see section 1.4). Precipitation of biominerals along with calcite dissolution and precipitation has proved the existence of biological activity in decay zones such as exposed surfaces and interior crack surfaces.

Role of clay minerals

It was observed that Nemrut Dağ limestones decayed through some karstic veins and cracks in the form of fragmental disintegration where the veins were found to have the clay minerals, iron oxides and biological activity. Identification of clay minerals were done by combined analyses with XRD and SEM-EDX. Their cation exchange capacities were determined by methylene blue test.

XRD analyses of acid insoluble constituents of the Nemrut Dağ quarry limestones and soil on the terraces around the statues showed the presence of clay minerals kaolinite, illite and smectite. Quartz and albite were also found together with those clay minerals (Figs. 3.30-3.41). Those acid insoluble constituents of Nemrut Dağ limestones were mostly concentrated in some of their karstic veins. The presence of clay minerals in the karstic veins together with iron oxides were also verified by following their distribution in SEM images with EDX analyses (Figs. 3.51- 3.52).

Weathered limestone samples separated by fragmental disintegration were also studied the by XRD, by taking the XRD traces of scraped powder samples as well as by direct measurements at the exposed surfaces and interior crack surfaces of the samples. It was observed that smectite group clay minerals were the abundant clay minerals in the decay zones as well as kaolinite and illite (See section 3.4). CEC values of clay constituents in interior cracks of Nemrut limestones were shown in Table 3.3. They indicated swelling ability of the clays in the decay zones of stone.

The swelling characteristics of kaolinite and illite were expected to be very small in comparison to smectite. The clay minerals take part in the deterioration processes by several other mechanisms as well. The mobility of clay minerals in the aqueous media causing their transportation to the fine capillaries of the stone was stated by some researchers (Jimenez-Gonzales et. al, 2008). The role of clay minerals in deterioration by mechanisms such as ion exchange capacity, acting as reservoirs for nucleation of new crystals etc. were thought to be important in the growth of

cracks. Increase in the swelling of clay minerals by weathering were also mentioned by some studies (Wangler, and Scherer, 2008).

The presence of clay minerals detected in the cracks of limestone were concluded to be the cause of separation through the cracks and losses by fragmental disintegration. Fragmental disintegration was the main deterioration process of limestones of Nemrut Dağ Monument where clay minerals played important roles during wetting and drying cycles experienced by the stone.

Role of Iron Oxides

Presence of iron oxides in the microstructure of limestones was observed especially in the cracks and karstic zones through the analyses by XRD, SEM-EDX and thin sections examinations by optical microscopy (Figs. 3.37, 3.38, 3.41, 3.42, 3.51, 3.52, 3.15, 3.17). Presence of magnetite/maghemite and goethite in the decay zones along with clay minerals was interpreted as goethite being the main weathering product of iron oxides in the decay zones of limestones (see section 3.4). Their contribution to the decay mechanisms must be studied in more detail in the light of recent studies in the literature, since phase changes in iron oxides have resulted in volume changes as well as their migration (Saheb et al., 2007; Monnier, 2008; Dillmann, 2008; Hanesch, 2009).

On the other hand, it has been experimentally proved that applied magnetic field has encouraged the nucleation and precipitation of calcium carbonate in hard water (Wang et al. 1997; Alimi et al. 2007). Presence of maghemite/magnetite in cracks of limestone that was proved by XRD and thin section analyses of this study, indicated their possible influence in precipitation reactions of calcium carbonate. Precipitation of calcium carbonate must be encouraged in the crack zones due to the presence of those iron oxides when water penetration occurred through the cracks of limestone. Treatments with nanodispersive solutions of Ca(OH)_2 were also expected to be influenced from those iron oxides in the crack zones by their encouragement for nucleation and precipitation of calcium carbonate.

4.2. Conservation treatments with nanodispersive calcium hydroxide solutions

Before the conservation treatments, a study on the mechanisms and the progress of deterioration in the stone was required. It was necessary to know the differences between the healthy and decayed limestone, so that expected roles from the treatments could be defined and the success of the treatments could be tested. It was found that limestones mainly deteriorated by fragmental disintegration through their karstic veins where the swelling of clays occurred by cyclic wetting and drying conditions. Dissolution and recrystallization of calcite, precipitation of biominerals such as weddellite and whewellite and phase changes of iron oxides have also occurred in those cracks during cyclic wetting and drying.

It was necessary to decrease the CEC of clay minerals in order to control their swelling ability and it was also necessary to fill those cracks by reincorporating similar type of structure with the limestone and improve the adhesion in those growing cracks. Therefore, the use of nanodispersive calcium hydroxide solution seemed to be suitable for those two main purposes of i) decreasing the CEC of clay minerals in the cracks and ii) crystallization of calcite in opened cracks.

First of all, there was a need to prepare stable and concentrated solutions of nanodispersive calcium hydroxide solutions. In this study, preparation of nanodispersive solutions with improved concentrations was achieved in comparison to the ones in the literature and in commercially produced nanodispersive solutions (Ambrossi et al., 2001; Tiano et al., 2006; Giorgi et al., 2000; Dei and Salvadori, 2006; Lopez-Arce et al., 2010). In this study, the concentration of suspended nanodispersive $\text{Ca}(\text{OH})_2$ in ethyl alcohol was about 31g/l after 16 hours of its preparation, whereas a recent study mentioned that a commercial product named as Nanorestore® developed at the University of Florence had a concentration of 5gr/l suspended nano particles in isopropyl alcohol (Lopez-Arce et al., 2010).

During the treatments, it was important that the re-crystallized calcium carbonate in limestone capillaries and pores should bond chemically to the internal surface of the

pores and capillaries. Otherwise, newly formed calcium carbonate in the stone would not give substantial reinforcement.

Efficiency of the nanodispersive solution in filling the fine cracks by the formation of calcite was better achieved under an atmosphere rich in CO₂ (5-20%) and RH being 75-80%. At the end of three days in those conditions carbonation was substantial but not yet complete (See section 3.8). For an effective consolidation action of carbonation, it was necessary for the newly formed calcite grains to have good contact with the substrate limestone. That aspect of the carbonation was studied in more detail by using additive sodium stearate in the nanodispersive Ca(OH)₂ solution (Ukrainczyk et. al., 2009). The addition of sodium stearate to nanodispersive calcium hydroxide solution have increased the size of calcite particles formed and facilitated effective bonding in the cracks of limestones (See Section 3.8).

Swelling property of clay minerals in limestones and its reduction by treatments with nanodispersive calcium hydroxide solutions were determined by CEC measurements using methylene blue solution (see section 3.8). After the treatments with nanodispersive solutions, CEC values of clay constituents of Nemrut Limestones have decreased considerably. That showed the efficiency of the nanodispersive calcium hydroxide solution for controlling the swelling properties of clay minerals. That was an advantage to control the crack formation and to prevent fragmental disintegration in limestones.

4.3. Conclusions

Although a number of decay forms such as color change, biological depositions, pitting and dissolution of limestone through the karstic veins and fragmental disintegration were observed, the most important decay forms at the Nemrut Dağ Monument were material loss and detachments by fragmental disintegration,

Clay minerals having high swelling potential caused separation through the cracks and losses by fragmental disintegration. That was thought to be the main deterioration process of limestones of Nemrut Dağ Monument.

In this study, nanodispersive calcium hydroxide solutions in ethyl alcohol with improved concentrations were successfully prepared.

Efficiency of the nanodispersive calcium hydroxide solutions in filling the fine cracks by the formation of calcite was better achieved under an atmosphere rich in CO₂ (5-20%) and RH being 75-80%.

Nanodispersive calcium hydroxide solution was successful to control the swelling properties of clay minerals for controlling the crack formation and to prevent fragmental disintegration of limestones.

The addition of sodium stearate to nanodispersive calcium hydroxide solution have increased the size of calcite particles formed and facilitated efficient bonding in the cracks of limestone.

Presence of magnetite/maghemite and goethite in the decay zones along with clay minerals was interpreted as goethite being the main weathering product of iron oxides in those limestones. Their importance in decay need to be further studied.

4.4. Further Studies

The long term durability of nanodispersive calcium hydroxide solution has to be further studied by dilatation measurements and cyclic durability tests, along with microstructural analyses similar to the ones performed in this study.

The effect of the nanodispersive Ca(OH)₂ solutions on the biologic activity on limestones need to be further studied.

The transformation of clay minerals and iron oxides in the cracks as a result of deterioration has to be investigated.

Use of various additives with nanodispersive $\text{Ca}(\text{OH})_2$ solutions that may improve the bonding of newly formed calcite with the substrate limestone in the cracks, need to be studied.

Studies to further increase the concentration of suspended nano $\text{Ca}(\text{OH})_2$ particles in ethyl alcohol should be continued.

The efficiency of nanodispersive $\text{Ca}(\text{OH})_2$ solutions on the consolidation of different stones such as marble, travertine, tuff etc. has to be investigated.

REFERENCES

Alimi, F., Tlili, M., Ben Amor, M., Gabrielli, C., Maurin, G., 2007., Influence of Magnetic Field on Calcium Carbonate Precipitation, *Desalination*, 206, 163-168.

Al-Rawas, A. A., Hagoa, A.W., Al-Sarmi, H., 2005., Effect of lime, cement and Sarooj (artificial pozzolan) on the swelling potential of an expansive soil from Oman., *Building and Environment*, 40, 681–687.

Ambrossi, M., Dei, L., Giorgi, R., Neto, C., Baglioni, P., 2001, Colloidal Particles of $\text{Ca}(\text{OH})_2$ Properties and Applications to Restoration of Frescoes, *Langmuir*, 17, 4251-4255.

Angwal, K., 1983, *Elementary Crystal Growth*, Saan Publ., Lublin, 83-176

Arandigoyen, M., Bicer-Simsir, B., Alvarez, J.I., Lange, D.A., 2006, Variation of microstructure with carbonation in lime and blended pastes, *Applied Surface Science*, Vol. 252, Issue 20, 7562-7571

ASTM D 2845-90, 1990, Standard Test Method for Laboratory Determination of Pulse Velocities and Ultrasonic Elastic Constants for Rock, *American Society for Testing and Materials*.

Avsar, E., Ulusay, R., Sonmez, H., 2009, Assessments of swelling anisotropy of Ankara clay, *Engineering Geology* 105, 24-31.

Bellot-Gurlet L., Neff, D., Réguer, S., Monnier, J., Saheb, M., Dillmann, P., 2009, Raman studies of corrosion layers formed on archaeological irons in various media., *Journal of Nano Research* 8 (2009) 147-156.

Berner, R.A., 1976, The solubility of calcite and aragonite in sea water at atmospheric pressure and 34.5% salinity, *Am. Jour. Sci.*, 276, 713-730

Berner, R.A., Morse, J.W., 1974, Dissolution kinetics of Calcium Carbonate in Sea Water IV. Theory of Calcite Dissolution, *Am. Jour. Sci.*, 274, 108-134

Bhatnagara, A, Choia, YH., Yoona, YJ., Shinb, Y, Jeona, B-H, Kanga, J-W., 2009., Bromate removal from water by granular ferric hydroxide (GFH)., *Journal of Hazardous Materials* 170 (2009) 134–140

Bishoff, J. L., Fyfe, W. S., 1968, Catalyses, inhibition and the calcite-aragonite problem, Part.1, The aragonite- calcite transformation, *Am. Jour. Sci.*, 266, 65-79.

Black, C.A., 1965, *Methods of Soil Analysis, Part 2*, American Society of Agronomy, inc. Publisher, Madison, Wisconsin, U.S.A., 999-1010

Busenberg., E. and Plummer, L.N., 1986, A comparative Study of the dissolution and crystal growth kinetics of calcite and aragonite. In: Mumpton, F.A. Ed., *Studies Diagenesis*, U.S.G.S. Bull., vol.1578, U.S. Department of the Interior, Reston, 139-168.

Caner, E., Caner-Saltık, E.N., Oriol, G., Mertz, J.D., Deterioration Mechanisms of Historic Limestone and Development of Its Conservation Treatments with Nanodispersive $\text{Ca}(\text{OH})_2$ Solutions, 8th International Symposium on the Conservation of Monuments in the Mediterranean Basin, Book of Abstracts, Ed. M. Kouli, F. Zezza, National Technical University of Athens, p.183, 2010

Caner, E.N, 1978, Factors Affecting the Deterioration of Limestones from Historic Monuments in Anatolia, University of London, Faculty of Arts, Ph.D. Thesis, London, p.131

Caner, E.N., Seeley, N.J., (1978), "The clay Minerals and Decay of Limestone Monuments", International Symposium, UNESCO-Rilem, Paris, 5.3. 34p.

Caner, E.N., Seeley, N.J., (1979), "Dissolution and Precipitation of Limestone", Deterioramento e Conservazione della Pietra, Fondazione Giorgio Cini, Venezia, 107-129.

Caner-Saltık E.N., 2011, Materials research, final report, METU-CNCDP (Commagene Nemrut Conservation and Development Project), 192 p. unpublished report.

Caner Saltık E. N., Güney B. A., Akoğlu K. G., Caner E., Ergenç D., Dincer A. Ş., 2011, Development of Repair Mortars for the Ruined Stone Towers in Perge Archaeological Park Site, Conservation of stone in Parks, Gardens and Cemeteries, Paris, 22-24 June 2011

Carroll, D., 1970a, Rock Weathering, Ed. R.W. Fairbridge, Plenum Press, New York-London, 203 p.

Carroll, D., 1970b, Clay Minerals: A guide to their X-ray identification, Special paper 126, The Geological Society of America, Colorado, USA. 80p.

Charola, A.E., 1993, General report on prevention and treatment: Cleaning, biocides and mortars, Congres International sur la Conservation de la Pierre et autres Materiaux, ACTES, UNESCO Paris, 65-68.

Cheng, B., Lei, M., Yu, J., Zhao, X., 2004, Preparation of monodispersed cubic calcium carbonate particles via precipitation reaction, *J. Materials Letters*, 58, 1565-1570.

Christ, C. L., Hostetler, P. B., Siebert, R. M., 1974, Stability of calcite and aragonite, *J. Res. U.S. Geol. Surv.*, 2, 175-184.

Clarke, B.L. and Ashurst, J., 1972, Stone Preservation Experiments, Building Research Establishment, 78 p.

Claudia, M., 2000. Predicting swelling/shrinkage potential using the blue methylene method: some examples in Italian clayey soils. *GeoEng 2000*, An International Conference on Geotechnical and Geological Engineering, Melbourne, Australia.

Cölfen, H., 2003, Precipitation of carbonates: recent progress in controlled production of complex shapes, *Current Opinion in Colloid and Interface Science*, 8, 23-31.

Compton, R.G. and Unwin, P.R., 1990, the dissolution of calcite in aqueous solution at $\text{pH} > 4$: kinetics and mechanism. *Philos. Trans. R. Soc. Lond.*, A 330, 1-45.

Cubillas, P., Köhler, S., Prieto, M., Chairat, C., Oelkers, E.H., 2004, Experimental determination of the Dissolution Rates of Calcite, Aragonite and Bivalves, *Chemical Geology* 216, 59-77.

Cultrone G., Sebastián E., Ortega Huertas M., 2005, Forced and natural carbonation of lime-based mortars with and without additives: Mineralogical and textural changes Original Research Article *Cement and Concrete Research*, Volume 35, Issue 12, Pages 2278-2289

De Leeuw N.H., 2002, Molecular dynamics simulations of the growth inhibiting effect of Fe^{2+} , Mg^{2+} , Cd^{2+} , and Sr^{2+} on calcite crystal growth, *Journal of Physical Chemistry B* 106

De Witte, E., Charola, A. E., Sherryl, R. P., 1985, "Preliminary Tests on Commercial Stone Consolidants", in: V^e Congrès International sur L'Altération et La Conservation de La Pierre - Vth International Congress on Deterioration and Conservation of Stone, Volume 2, 25-27, 9, 1985, Lausanne, Suisse, 709-719

Dei, L., and Salvadori, B., 2006, Nanotechnology in cultural heritage conservation: nanometric slaked lime saves architectonic and artistic surfaces from decay, *Journal of Cultural Heritage*, 7, 110-115.

Dheilly, R.M., Tudo, J., Sebaibi, Y., Queneudec, M., 2002, Influence of Storage Conditions on the Carbonation of Powdered $\text{Ca}(\text{OH})_2$, *Construction and Building Materials*, 16, 155-161.

Dove, P. M., Hochella, M. F. Jr., 1993, Calcite precipitation mechanisms and inhibition by orthophosphate: In situ observations by Scanning Force Microscopy, *Geochimica et Cosmochimica Acta*, Vol. 57, No. 3, 705-714

Dunn, J.R. and Hudec, P.P., 1966, Water, clay and rock soundness, *Ohio J. Sci.*, 66, 153-168.

Dupuy, P., Trotet, G., Grossin, F., 1976, Centro per la Conservazione delle Sculture all'Aperto, *The Conservation of Stone (I)*, Bologna, 205-219.

El Sabrouti, M.A., Sokkary, A..A.,1982., "Distribution of clay minerals and their diagenesis in the sediments of Lake Edku" *Marine Geology*, Volume 45, M15-M21.

Ergüler, Z.A. and Ulusay, R., 2003, A simple test and predictive models for assessing swell potential of Ankara (Turkey) clay, *Engineering Geology* 67, 331-352.

Falini, G., Fermani, S., Ripamonti, A., 2002, Crystallization of calcium carbonate salts into beta-chitin scaffold, *Journal of Inorganic Chemistry*, 91, 475-480.

Fattuhi N.I, 1988, Concrete carbonation as influenced by curing regime, *Cement and Concrete Research*, Volume 18, Issue 3, Pages 426-430

Feng, B., Yong, K.A., An, H., 2007, Effect of various factors on the particle size of calcium carbonate formed in a precipitation process, *Material Science and Engineering*, A 445-446, 170-179.

Fernandez Bertos, M., Simons, S.J.R., Hills, C.D., Carey, P.J., 2004, A review of accelerated carbonation technology in the treatment of cement-based materials and sequestration of CO₂, *Journal of Hazardous Materials*, Volume 112, Issue 3, 193-205

Fitzner, B., Heinrichs, K., Kownatzki, R., 1995, „Weathering Forms-Classification and Mapping“, in: *Verwitterungsformen-Klassifizierung und Kartierung-Denkmalpflege und Naturwissenschaft, Natursteinkonservierung I, Förderprojekt des Bundesministeriums für Bildung, Wissenschaft, Forschung und Technologie*, Verlag Ernst & Sohn, Berlin, 41-88

Fogg, G.E., 1973, *Physiology and Ecology of Marine Blue-Green Algae*, The Biology of Blue-Green Algae, Botanical monographs, Ed. N.G. Carr and B.E. Whitton, University of California Press, Vol. 9, 368-378.

Fyfe, W.S. and Bischoff, J.L., 1965, The calcite-aragonite problem, *Soc. Econ. Paleontologists*, Special Publication No 13, 3.

Gebelein, C.D. and Hoffman, P., 1973, Algal origin of dolomite laminations in stromatolitic limestone, *Jour. Sed. Petrology*, 43, 603-613.

Giorgi, R., Dei, L., Baglioni, P., 2000, A new method for consolidating wall paintings based on dispersion, of lime in alcohol, *Studies in Conservation*, 45, 154-161.

Giresse P, Wiewiora A., 2001., Stratigraphic condensed deposition and diagenetic evolution of green clay minerals in deep water sediments on the Ivory Coast-Ghana Ridge , Volume 179, Number 1, , 51-70.

Grandet, B., 1975, Physico-chemical mechanisms of the bond between clay and cement., *Proc., 3rd Int. Brick and Block Masonry Conf.*, H. Glitza and K. Göbel, eds., Bonn, Germany, 217–221.

Grim, R.E., 1968, *Clay Minerology*, McGraw-Hill International Series in the Earth and Planetary Sciences, New York, USA, 596 p..

Gürses, A., Doğar, Ç., Yalçın, M., Açıkyıldız, M., Bayrak, R., Karaca, S., 2006., The adsorption kinetics of the cationic dye, methylene blue onto clay, *Journal of Hazardous Materials B131*, 217-228.

Hale, M.E., 1974, *The Biology of Lichens*, 2nd ed., Edward Arnold Ltd., London.

Hanesch, M. 2009, Raman Spectroscopy of iron oxides and (oxy)hydroxides at low laser power and possible applications in environmental magnetic studies, *Geophys. J. Int.* ;177, 941-948.

Hausner, D.B., Reeder, R.J., Strongin, D.R., 2007, Humidity-induced restructuring of the calcite surface and the effect of divalent heavy metals, *Journal of Colloid and Interface Science* 305 101–110

Hausner, D B., Bhandari, N., Pierre-Louis A-M., Kubicki J. D., Strongin, D. R., 2009., Ferrihydrite reactivity toward carbon dioxide., *Journal of Colloid and Interface Science* 337 (2009) 492–500

Jacobson, R. L., Langmuir, D., 1974., Dissociation constants of calcite and CaHCO_3^+ from 0 to 50⁰C, *Geochim. et Cosmochim. Acta*, 38, 301-318.

Jimenez-Gonzales, I., Rodriguez-Navarro, C. and Scherer, W.G., 2008, Role of clay minerals in the physicochemical deterioration of sandstone, *Journal of Geophysical Research*, Vol.113, F02021

Jimenez-Gonzalez, I. and Scherer, G.W., 2004, Effect of swelling inhibitors on the swelling and stress relaxation of clay bearing stones, *Environ. Geol.*, 46, 364-377.

Kamiya K, Kagi, H., Tsunomori, F., Tsuno, H., Notsu, K., 2004, Effect of trace lanthanum ion on dissolution and crystal growth of calcium carbonate, *Journal of Crystal Growth*, Volume 267, Issues 3-4, 1 July 2004, 635-645

Kanellopoulou, D.G., Kontoyannis, C.G., Koutsoukos, P.G., 2001, Marble weathering: The chemical dissolution aspect, *Proceedings of the 11th Workshop, Eurocare Euromarble EU 496*, 5-7 October, Vienna, 43-52.

Kirchgessner, D.A. and Lorrain, J.M., 1987, *Ind. Eng. Chem. Res.*, 36, 2397-2400.

Kitano, Y. and Hood, D.W., 1965, the influence of organic material on the polymorphic crystallization of calcium carbonate, *Geochim. et Cosmochim. Acta*, 29, 29-41.

KNCDP, 2001, Kommagene Nemrut Conservation and Development Program Project, Project Report, METU.

Koutsoukos, P.G., Orkoula, M., Kanellopoulou, D., Kontoyannis, C.G., 2001, Understanding Marble Deterioration at a Microscopic Level, Proceedings of Eurocare Euromarble, Vienna, 75-88.

Lea, A.S., Amonette, J.E., Baer, D.R., Liang, Y., Colton, N.G., 2001, Microscopic Effects of Carbonate, Manganese and Strontium Ions on Calcite Dissolution, Geochim., Cosmochim. Acta 65, 369-379.

Lewin, S.Z., 1966, The Preservation of Natural Stone, Art and Archaeology Technical Abstracts, Vol.6, Number 1, 185-188.

Lipmann, F., 1973., Sedimentary Carbonate Minerals, Springer Verlag, Berlin.

Lopez-Acre, P., Gomez-Villalba, L.S., Pinhp, L., Fernandez-Valle, M.E., Alvarez de Buergo, M., Fort, R., 2010, Influence of porosity and relative humidity on consolidation of dolostone with calcium hydroxide nanoparticles: Effectiveness assessment with non-destructive techniques, Material Characterization 61, 168-184.

Manoli, E., Kanakis, J., Malkaj, P., Dalas, E., 2002, The effect of aminoacids on the crystal growth of calcium carbonate, Journal of Crystal Growth, 236, 363-370.

Manoli, F. and Dalas.E., 2001, Calcium carbonate crystallization in the presence of glutamic acid, Journal of Crystal Growth, 222, 293-297.

Mertz J.D., 2006, L'équilibre calco-carbonique des solutions sur les parois, In Dossier Les Grottes Ornées, Monumental 2006, 2^{ème} semestre, Monum, Ed. du Patrimoine, p.85

Monnier, J., Legrand, L., Bellot-Gurlet, L., Foy, E., Reguer, S., Rocca, E., Dillmann, D., Neff, D., Mirambet, F., Perrin, S., Guillot, I., 2008, Study of

archaeological artefacts to refine the model of iron long-term indoor atmospheric corrosion, *Journal of Nuclear Materials*, 105-111.

Morehead, D.R., 1986, Cementation of hydrated lime, cement and Concrete Research, Vol.16, 700-708.

Moore, D.M. and Reynolds, R.C., 1997, X-Ray Diffraction and the Identification and Analysis of Clay Minerals, Second Edition, Oxford University Press, New York, p.378.

Morse, J. W., and Arvidson, R. S., 2002, The dissolution kinetics of major sedimentary carbonate minerals, *Earth Science Reviews*, 58, 51-84.

Nestaas, I., Terjesen, S. G., 1969, The inhibiting effect of scandium ions upon the dissolution of calcium carbonate, *Acta Chemica Scandinavia*, 23, 2519-2531.

Northwood, D.O. and Lewis, d., 1968, Transformation of vaterite to calcite during grinding, *Am. Mineralogist*, 53, 2089-92.

Northwood, D.O. and Lewis, d., 1968, Transformation of vaterite to calcite during grinding, *Am. Mineralogist*, 53, 2089-92.

Plummer, L.N., Wigley, T.M.L., 1976, The Dissolution of Calcite in CO₂-Saturated Solutions at 25°C and One Atmosphere total Pressure, *Geochim. et Cosmochim. Acta*, 40, 191-202.

Price, C. A., 1996., *Stone Conservation: An Overview of Current Research.*, Getty conservation Institute., 73p. A

Price, C.A., 1978, The use of the sodium sulphate crystallization test for determining the weathering resistance of untreated stone, Proc. Int. Symp. On the Deterioration and Protection of Stone Monuments, Paris, 3.6, 23p.

Ramasamy, V. and Anandalakshmi, K., 2008, The Determination of Kaolinite Clay Content in Limestones of Western Tamil Nadu by Methylene Blue Adsorption Using UV-vis Spectroscopy, Spectrochimica Acta Part A: Molecular and Biomolecular Spectroscopy, Vol. 70, No. 1, 25-29

Raz, S., Weiner, S., Addati, L., 2000, Formation of high magnesian calcites via an amorphous precursor phase: possible biological implications, J. Adv. Matter, 12, 38-42.

RILEM, 1980, Tentative Recommendations, Commission-25-PEM, Recommended Tests to Measure the Deterioration of Stone and to Assess the Effectiveness of Treatment Methods, Materiaux and Construction, Vol.13, No.73, 173-253.

Rodriguez Navarro, C., Sebastian, E., Dohene, E., Ginell, W.S., 1998, The role of sepiolite-palygorskite in the decay of ancient Egyptian limestone sculptures, Clays Clay Miner., 46, 414-422.

Rossini, F.D., Wagman, D.D., Evans, W.H., Levine, S., Jaffe, I., 1952, Selected Values of Chemical Thermodynamic Properties, Nat.Bur.Standarts Circ. 500, U.S. Dept. Commerce.

Sabrouti, M.A. El and Sökkary, A.A., 1982, Distribution of Clay Minerals and Their Diagenesis in The Sediments of Lake Edku, Marine Geology, Vol. 45, Nos 1-2, M15-M21

Saheb, M., Neff, D., Dillman, P., Matthiesen, H., 2007, "Long Term Corrosion Behaviour of Low Carbon Steel in Anoxic Soils", in: 2nd Innovative Investigation

of Metal Artefacts, METAL '07, Interim Meeting of the ICOM-CC metal WG, Amsterdam, 17-20 September 2007, Eds: C. Degryny, R. van Langh, I. Joosten, B. Aknersmith, 69-75

Sasse, H.R., 1993, Care of monuments and quality assurance system : Incompatible or indispensable, *Congres International sur la Conservation de la Pierre et autres Materiaux*, ACTES, UNESCO Paris, 59-64.

Sasse, H.R. and Snethlage, R., 1997, Methods for the Evaluation of Stone Conservation Treatments, *Saving our Architectural Heritage*, ed. by N.R. Baer and R. Snethlage, John Wiley&Sons, Berlin, 223-243.

Simon, S. and Herm, C., 1996, Conservation of marble and limestone traditional new treatment methods in comparison, *Proceedings of Eurocare Euromarble*, Patras, .46.

Simon, S., Snethlage, R., 1992, The First Stages of Marble Weathering, Preliminary Results After Short-Term Exposure of Nine Months, *Proceedings of Eurocare-Euromarble*, Göteborg, 37-44.

Sjöberg, E.L., 1976, A fundamental equation for calcite dissolution kinetics, *Geochim. et Cosmochim. Acta*, 40, 441-447.

Sjöberg, E.L., 1978, Kinetics and mechanism of calcite dissolution in aqueous solutions at low temperatures, *Stockholm, Contrib. Geol.*32, 1-92.

Sjöberg, E.L., 1983, Mixed kinetic control of calcite dissolution. *Sci.Geol., Mem.* 71, 119-126.

Smith, L.B., Paloczi, G.T., Hansma, K.P., Levine, P.R., 2000, Discerning nature's mechanisms for making complex biocomposite crystals, *Journal of Crystal Growth*, 211, 116-121.

Spanos, N. and Koutsoukos, P.G., 1998, The transformation of vaterite to calcite: effect of the conditions of the solutions in contact with the mineral phase, *Journal Crystal Growth*, 191, 783.

Şahin-Güçhan, N., 2011, The Commagene Nemrut Conservation and Development Program: An Approach to the Conservation Problem of Nemrut Dağ Tumulus, in E. Winter (ed.), *Von Kummuh Nach Telouch. Archäologische und Historische Untersuchungen in Kommagene. Dolicener und Kommagenische Forschungen IV. Asio Minor Studien 64*, Bonn 2011, 309-339.

Tabasso, L. M., 1988, "Conservation Treatment of Stone", in: *The Deterioration and Conservation of Stone*, Eds: L. Lazzarini, R. Pieper, *Studies and Documents on the Cultural Heritage 16, CC/88/WS.8, UNESCO*, 271-290

Tabasso, L. M., 1993, *Materials for stone conservation*, *Congres International sur la Conservation de la Pierre et autres Materiaux, ACTES, UNESCO Paris*, 54-58.

Tai C.Y. and Chen, P.C., 1995, Nucleation, agglomeration and crystal morphology of calcium carbonate, *AIChE J.*, 41, 68-77.

Tavukçuoğlu, A. Caner-Saltık E. N., Akoğlu K. G., Caner E., Işıkloğlu M., 2011, *In situ Examination of Nemrut Dağ Sandstone and Limestone Statues by NDT Methods*, *Conservation of stone in Parks, Gardens and Cemeteries, Paris*, 22-24 June 2011

Tennent, N. H., 1994., *The Role of the Conservation Scientist in Enhancing the Practice of Preventive Conservation and the Conservation Treatment of Artifacts.*,

in: “Durability and Change: The Science, Responsibility and Cost of Sustaining Cultural heritage” eds. W. E. Krumbein., P. Brimbelcombe, D. E. Cosgrove., S. Staniforth., John Wiley & Sons Ltd., 165-172.

Teutonico, J.M, McCaig, I., Burns, C., Ashurst, J., 1994, the Smeaton Project: factors affecting the properties of lime-based mortars, *Lime News*, 2:2, 7-13.

Teutonico, J.M. (rapporteur), Charola, A.E., De Witte, E., Grassegger, G., Koestler, R.J., Tabasso, M.L., Sasse, H.R., Snethlage, R., 1997, Group Report: How can we ensure the responsible and effective use of treatments (cleaning, consolidation, protection)? in N.S. Baer and R. Snethlage (eds), *Saving Our Architectural Heritage: The Conservation of Historic Stone Structures*, Dahlem Workshop Report ES20, Chichester, Wiley, New York, 293–313.

Thiel, M.J. (Ed), 1993, *International Congress on the Conservation of Stone and Other Materials*, Acts, Unesco-Rilem, Paris, 160 p.

Tiano, P., Cantisani, E., Sutherland, I., Paget, J.M., 2006, Biomediated reinforcement of weathered calcareous stones, *Journal of Cultural Heritage*, 7, 49-55.

Timoshenko, S., 1970, *Strength of Materials*, in Chapter II, Analysis of Stress and Strain, Van Nostrand Reinhold Company, Holland, p.53.

Tong, H., Ma, W., Wang, L., Wan, P., Hu, J., Cao, L., 2004, Control over the crystal phase, shape, size and aggregation of calcium carbonate via a L-aspartic acid inducing process, *J. Biominerals*, 25, 3923-3929

Torraca, G., 1976, *Treatments of Stone in Monuments : A review of principles and processes*, in: *The Conservation of Stone*, Proceedings of the International Symposium, Bologna, Ed.R. Rossi-Manaresi, 217-316.

Torraca, G., 1982, *Porous Building Materials*, Rome, p.145.

Tran, H. V., Tran, L. D., Vu, H. D., Thai, H., 2010, Facile surface modification of nanoprecipitated calcium carbonate by adsorption of sodium stearate in aqueous solution, *Colloids and Surfaces A: Physicochem. Eng. Aspects* 366, 95-103.

Ukrainczyk, M., Kontrec, J., Kralj, D., 2009., "Precipitation of different calcite crystal morphologies in the presence of sodium stearate", *Journal of Colloid and Interface Science*, 329, 89-96.

Uskov, M. N., 1978., "Clay minerals in Pleistocene Permafrost and contemporaneous bottom deposits of central Yakutia (an X-Ray study)" 210-212., in Eds. F. J. Sanger, P. J. Hyde., "Permafrost, Second International Conference –USSR contribution-, National Academy of Sciences, Washington D.C. 866p.

V. Tarasov, 2001, I. New colloid silicate solutions for restoration and conservation of stone facades, *Russ. J. Appl. Chem.* 74 (12) 1985–1989.

Veniale, F., Setti, M., Rodriguez Navarro, C., Lodola, S., 2001, Role of clay constituents in stone decay processes, *Mater. Constr.*, 51, 163-182.

Walton, J.C., Bin-Shafique, S., Smith, R.W., Gutierrez N., Tarquin, A., 1997, The role of carbonation in transient leaching of cementitious waste forms, *Environ. Sci. Technol.* 31, 2345-2349.

Wang, Y., Babchin, A. J., Chernyi, L.T., Chow, R. S., Sawatzky, R. P., 1997., Rapid onset of calcium carbonate crystallization under the influence of magnetic field., *Wat. Res.* Vol. 31, No.2., 346-350.

Wangler, T. and Scherer, G.W., 2008, Clay swelling mechanism in clay-bearing sandstones, *Journal of Environ Geol*, 56:529-534.

Wei, S.H., Mahuli, S.K., Agnihotri, R., 1997, *Ind. Eng. Chem. Res.*, 36, 2141-2148.

Wendler, E., 1997, *New materials and Approaches for the conservation of stone, Saving Our Cultural Heritage*, Ed. By Baer and Snethlage, Berlin, 181-196.

Williams, R. and Robinson, D., 1989, *Origin and distribution of polygonal cracking of rock surfaces*, *Geogr. Ann. Ser. A*, 71, 145-151.

Wüst, R.A.J. and McLane, J., 2000, *Rock deterioration in the royal tomb of Seti I, Valley of Kings, Luxor, Egypt*, *Eng. Geol.*, 58, 163-190.

Xiang, L., Xiang, Y., Wang, Z.G., Jin, Y., 2002, *Influence of chemical additives on the formation of super-fine calcium carbonate*, *J. Powder Technology*, 126, 129-133.

Xiang, L., Xiang, Y., Wen, F., Wei, F., 2004, *Formation of CaCO₃ nanoparticles in the presence of terpineol*, *J. Materials Letters*, 58, 959-965.

Xie, A., Shen, Y., Zhang, C., Yuan, Z., Zhu, X., Yang, Y., 2005, *Crystal growth of calcium carbonate with various morphologies in different amino acid systems*, *Journal of Crystal Growth*, 285, 436-443.

Yu, J., Lei, M., Cheng, B., Zhao, X., 2004, *Facile preparation of calcium carbonate particles with unusual morphologies by precipitation reaction*, *Journal of Crystal Growth*, 261, 566-570.

Yukselen, Y. and Kaya, A., 2008, *Suitability of the methylene blue test for surface area, anion exchange capacity and swell potential determination of clayey soils*, *Engineering Geology* 102, 38-45.

Zagari, M., Antonelli, C., Urzi, C., 2000, Biological patinas on the limestones of the loches romanic tower (Touraine, France) Proceedings of the 9th International Congress on Deterioration and Conservation of Stone, 2000, 445-451

APPENDIX A

BASIC PHYSICAL PROPERTIES OF LIMESTONE SAMPLES TAKEN FROM NEMRUT DAĞ MONUMENT

Table A.1. Density and porosity of limestone samples taken from Nemrut Dağ Monument

sample	M dry (g)	M sat (g)	M arch (g)	d (g/cm ³)	avg d (g/cm ³)	std. dev.	porosity (%)	avg porosity (%)	std. dev.
NE1	14.66	14.70	9.23	2.68	2.69	0.01	0.73	0.55	0.26
	14.66	14.68	9.24	2.69			0.37		
NE2	25.81	25.95	16.27	2.67	2.66	0.01	1.45	1.44	0.00
	25.78	25.92	16.21	2.65			1.44		
NE3	21.06	21.11	13.27	2.69	2.68	0.00	0.64	0.70	0.09
	21.06	21.12	13.26	2.68			0.76		
NE4	30.17	30.29	19.02	2.68	2.68	0.00	1.06	1.20	0.19
	30.16	30.31	19.05	2.68			1.33		
NE5	64.95	65.01	40.96	2.70	2.70	0.00	0.25	0.27	0.03
	64.94	65.01	41.00	2.70			0.29		
NE6	3.76	3.78	2.38	2.68	2.68	0.00	1.61	1.49	0.17
	3.91	3.93	2.47	2.68			1.36		
NE7	8.93	9.02	5.64	2.64	2.64	0.00	2.81	2.66	0.22
	7.34	7.41	4.63	2.64			2.51		
NE8	7.30	7.39	4.60	2.62	2.64	0.02	3.17	2.82	0.49
	8.23	8.30	5.20	2.65			2.47		
NE9	0.46	0.48	0.29	2.45	2.54	0.12	7.57	5.28	3.24
	0.94	0.95	0.59	2.62			2.99		
NE10	18.45	18.58	11.65	2.67	2.66	0.01	1.80	2.17	0.51
	10.57	10.67	6.68	2.65			2.53		
NE11	10.44	10.55	6.58	2.66	2.65	0.02	2.14	2.42	0.39
	9.14	9.21	5.77	2.63			2.69		
NE12	4.18	4.28	2.62	2.52	2.54	0.04	6.04	5.25	1.12
	6.14	6.24	3.86	2.57			4.45		

Table A.1 continued

NE13	7.94	8.05	5.02	2.62	2.61	0.01	3.70	3.68	0.02
	4.69	4.76	2.96	2.61			3.67		
NE14	6.04	6.14	3.80	2.58	2.56	0.03	4.22	4.89	0.95
	8.71	8.90	5.46	2.53			5.55		
NE15	5.94	5.97	3.75	2.68	2.67	0.01	1.35	1.57	0.31
	12.06	12.14	7.61	2.66			1.79		
NE16	6.72	6.76	4.25	2.68	2.69	0.01	1.22	1.01	0.31
	13.11	13.15	8.28	2.70			0.79		
NE17	5.13	5.17	3.25	2.67	2.66	0.02	1.86	2.07	0.29
	13.89	14.01	8.76	2.65			2.28		
NE18	11.29	11.43	7.12	2.62	2.54	0.11	3.06	5.84	3.93
	2.18	2.25	1.37	2.46			8.62		
NE19	9.39	9.58	5.92	2.57	2.60	0.05	5.29	4.09	1.71
	15.02	15.19	9.49	2.64			2.88		
NE20	2.20	2.29	1.36	2.37	2.40	0.03	9.95	9.11	1.18
	3.66	3.79	2.27	2.42			8.28		
NW1	4.00	4.08	2.51	2.55	2.44	0.16	5.19	8.46	4.61
	2.19	2.30	1.36	2.32			11.72		
NW2	4.95	5.03	3.12	2.58	2.54	0.06	4.26	5.44	1.68
	2.95	3.03	1.85	2.49			6.63		
NW3	1.44	1.47	0.91	2.58	2.62	0.06	4.19	2.86	1.88
	4.03	4.06	2.54	2.67			1.53		
NW4	1.73	1.83	1.09	2.33	2.33	0.00	13.17	13.17	0.00
	1.73	1.83	1.09	2.33			13.17		
NW5	11.05	11.16	6.96	2.63	2.58	0.07	2.50	3.92	2.01
	12.36	12.62	7.75	2.54			5.34		
NW6	2.57	2.58	1.62	2.67	2.68	0.00	1.30	1.25	0.07
	4.32	4.34	2.73	2.68			1.20		
NW7	14.08	14.17	8.89	2.67	2.65	0.02	1.62	2.15	0.74
	3.10	3.13	1.96	2.63			2.67		
NW8	2.56	2.58	1.61	2.62	2.63	0.01	2.87	2.65	0.32
	2.54	2.56	1.60	2.64			2.42		
NW9	7.00	7.05	4.43	2.68	2.66	0.03	1.75	2.19	0.63
	18.71	18.90	11.80	2.64			2.64		
NW10	2.79	2.83	1.76	2.61	2.62	0.02	3.67	3.28	0.55
	2.32	2.34	1.46	2.64			2.89		
NW11	3.45	3.47	2.18	2.67	2.52	0.20	1.64	5.86	5.97
	1.99	2.07	1.24	2.38			10.08		
NWQ1	15.70	15.75	9.92	2.69	2.68	0.02	0.87	1.57	1.00
	4.65	4.69	2.94	2.66			2.28		
NWQ2	8.21	8.29	5.17	2.63	2.61	0.03	2.56	3.41	1.19
	17.52	17.81	11.04	2.59			4.25		
NWQ3	6.13	6.16	3.86	2.67	2.68	0.01	1.31	1.08	0.33
	13.17	13.21	8.32	2.69			0.84		

Table A.1 continued

NWQ4	2.97	2.99	1.87	2.64	2.64	0.00	2.26	2.32	0.09
	4.47	4.51	2.81	2.63			2.38		
NWQ5	19.80	20.27	12.46	2.53	2.57	0.06	6.05	4.65	1.98
	9.45	9.57	5.95	2.62			3.25		
NWQ6	13.18	13.40	8.30	2.58	2.62	0.04	4.33	3.29	1.47
	7.57	7.64	4.78	2.65			2.25		
NWQ7	9.53	9.62	6.01	2.64	2.65	0.01	2.35	2.41	0.08
	3.48	3.51	2.20	2.65			2.46		

APPENDIX B

BASIC PHYSICAL AND PHYSICOMECHANICAL PROPERTIES OF ARTIFICIALLY WEATHERED LIMESTONE SAMPLES

Table B.1 Density, porosity, ultrasonic pulse velocity measurements and modulus of elasticity of artificially weathered limestone samples at different cycles.

cycle	sample	velocity (m/s)	density (g/cm ³)	porosity (%)	E _{mod} (MPa)
cycle 15	2	3264	2.67	0.61	19199
	3	3807	2.69	0.41	26313
	4	3274	2.68	0.45	19389
	5	1953	2.66	1.02	6848
	6	3674	2.69	0.33	24507
	7	2478	2.68	0.67	11107
	8	2401	2.66	0.87	10350
	9	3087	2.68	0.46	17237
cycle 20	10	3088	2.69	0.46	17313
	11	3402	2.69	0.38	21012
	12	3173	2.69	0.29	18279
	13	3631	2.70	0.32	24025
	14	3255	2.68	0.74	19164
	15	3440	2.70	0.22	21564
	16	3819	2.69	0.27	26479
	17	2902	2.67	1.08	15176

Table B.1 continued

cycle 25	18	3196	2.69	0.92	18545
	19	3396	2.68	0.64	20861
	20	3275	2.67	0.81	19328
	21	3355	2.69	0.36	20436
	22	3466	2.69	0.27	21810
	23	2693	2.69	0.52	13167
	24	2741	2.68	0.59	13590
	25	3875	2.69	0.20	27262
cycle 30	26	1981	2.69	0.19	7125
	27	2498	2.69	0.29	11329
	28	2022	2.7	0.24	7450
	29	1992	2.68	0.37	7177
	30	1683	2.65	0.99	5066
	31	2107	2.69	0.31	8060
	32	1790	2.69	0.38	5817
	33	2132	2.69	0.22	8252
cycle 35	34	2863	2.7	0.48	14937
	35	2189	2.66	1.13	8603
	36	2489	2.69	0.55	11248
	37	2304	2.68	0.58	9602
	38	1399	2.67	1.05	3527
	39	2106	2.69	0.33	8052
	40	2468	2.69	0.4	11059
	41	2333	2.69	0.32	9882
cycle 40	42	2245	2.67	0.88	9082
	43	2468	2.7	0.22	11100
	44	2427	2.69	0.45	10694
	45	2203	2.68	0.55	8778
	46	2339	2.65	1.44	9785
	47	2314	2.66	1.05	9613
	48	2842	2.67	0.66	14555
	49	2314	2.69	0.3	9722
cycle 45	50	2308	2.65	1.05	9527
	51	2456	2.7	0.26	10992
	52	2194	2.67	0.98	8674
	53	2318	2.66	0.86	9646
	54	2824	2.67	0.75	14371
	55	1869	2.67	0.78	6295
	56	1953	2.67	0.32	6873
	57	2375	2.68	0.41	10203

Table B.1 continued

cycle 50	58	2443	2.68	0.53	10795
	59	1930	2.66	0.85	6687
	60	1875	2.67	0.76	6335
	61	2437	2.67	0.89	10702
	62	2344	2.69	0.36	9975
	63	1587	2.62	1.45	4454

APPENDIX C

CONCENTRATION OF SUSPENDED NANO CALCIUM HYDROXIDE SOLUTION IN TIME

Table C.1 Suspended nano Ca(OH)₂ particles (g/L) in time

hours	Suspended Ca(OH) ₂ in 1000 ml (g)
0	53.3
1	46.5
2	40.7
4	37.3
6	34.0
16	31.0
24	29.7
31	28.5
53	26.0
79	23.5
98	22.9

Table C.2 Suspended nano $\text{Ca}(\text{OH})_2$ particles (g/L) in time with the addition of sodium stearate (0.025 g/L)

hours	suspended $\text{Ca}(\text{OH})_2$ in 1000 ml (g)
0	52.8
1	41.3
2	40.3
4	38.2
6	33.2
16	29.4
24	27.8
31	26.8
53	25.7
79	23.5
98	23.2